January 2022

Lanthanide Coordination Chemistry In Rare-Earth Element Extraction And Photocatalysis

Jessica Hovey
Wayne State University

LANTHANIDE COORDINATION CHEMISTRY IN RARE-EARTH ELEMENT EXTRACTION AND PHOTOCATALYSIS

by

JESSICA LYNN HOVEY

DISSERTATION

Submitted to the Graduate School

of Wayne State University,

Detroit, Michigan

in partial fulfillment of the requirements

for the degree of

DOCTOR OF PHILOSOPHY

2022

MAJOR: CHEMISTRY (Inorganic)

Approved by:

_____

Advisor Date

_____

_____

_____

_____

DEDICATION

To my husband, Jacob, who is my constant source of joy and inspiration. Your love and encouragement know no bounds and I dedicate my success to your endless support.

To my parents, who taught me the meaning of hard work. The years of pushing me to try my absolute best have made me into a strong, successful scientist. I love you so much!

To my sister, Katelyn, who exemplifies the ideals of an independent and successful woman. Thank you for being my constant and always loving me. To my brother-in-law, James Paval, thank you for showing me how to live life to its fullest while achieving my dreams.

To my very best friends, Kayla and Alex, we have been through so much together, and we celebrate all of our successes together. Thank you for always encouraging me and shouldering my worries.

ACKNOWLEDGEMENTS

Reaching one's goals is something to be celebrated by all who encouraged, assisted, or mentored in any way. All of my mentors and colleagues had an impact on my success, and I would like to thank them for their contributions.

I would like to give the biggest thank you to my graduate school advisor, Dr. Matthew Allen, for his constant (and patient) encouragement and advice. You have given me a strong scientific foundation that will carry me throughout my scientific career.

Thank you to my committee members, Dr. Cláudio Verani, Dr. Vladimir Chernyak, and Dr. Timothy Dittrich. I am grateful for your pedagogical and discourse-focused approach to my graduate learning.

Thank you to all of the administration and staff at Wayne State. You made every day brighter and gave us warm friendship during a time that can be very isolating.

I would like to thank the collaborators and mentors including professors and graduate students with whom I have researched during my time as a graduate student. Every moment spent discussing data or writing up results has led to this moment and I cannot thank you enough for your encouragement and assistance.

Thank you to my undergraduate advisors, Dr. Roman Dembinski and Dr. Evan Trivedi for stoking my love for chemistry and giving me the tools to flourish in graduate school. I am grateful for your mentorship in this chapter of my scientific career.

A special thank you to all of my colleagues in the Allen Lab during my time at Wayne State. I owe a special acknowledgement to my very dear friend Dr. Brooke Corbin, who has been by my side through this journey and has taught me many important chemistry and life lessons. Graduate school is not an easy time for anyone but having friends with whom to share the journey makes the time spent studying and researching much more enjoyable. I wish you all the best.

TABLE OF CONTENTS

Dedication ii

Acknowledgements iii

List of Tables vii

List of Figures viii

Chapter 1: Coordination Chemistry of Solid–Liquid Adsorption of Rare-Earth Elements 1

1.1 Permissions and Description of Author Contributions 1

1.2 Introduction 1

1.3 Solid-phase Materials 7

1.3.1 Carboxylic Acids, Alcohols, Glycolic Acids, Glycolamic Acids, and Glycolamides 7

1.3.2 Phosphoric Acids, Phosphate Esters, Phosphazenes, and Phosphoryl-containing Ligands 16

1.3.3 Hydroxamates, Polyamido Acetic Acids, Schiff Bases, Pyridine Derivatives, ... Phenanthroline, Benzotriazoles, Aza-crown Ethers, Amides, and Imines 22

1.3.4 Thiazols, Thiols, Sulfides, and Sulfoxides 28

1.4 Ion-imprinted Polymers 30

1.5 Polymers, Solid-supports, and Hydrogels 33

1.6 Conclusions and Future Outlook 34

1.7 Thesis Overview 34

Chapter 2: Sorption of Rare-Earth Elements onto a Ligand-Associated Media for pH-Dependent Extraction and Recovery of Critical Materials 37

2.1 Permissions and Description of Author Contributions 37

2.2 Introduction 37

2.3 Materials and Methods 41

2.4 Results and Discussion 49

2.5 Conclusions 57

Chapter 3: Adjusting Chain Length of Amphiphilic Ligands for the Preparation of Solid-Phase Media Designed to Enrich Rare-Earth Elements 59

3.1 Description of Author Contributions 59

3.2 Introduction 59

3.3 Materials and Methods 62

3.4 Results and Discussion 69

3.5 Conclusions 71

Chapter 4: Luminescence Differences between Two Complexes of Divalent Europium 73

4.1 Permissions and Description of Author Contributions 73

4.2 Introduction 73

4.3 Materials and Methods 75

4.4 Results and Discussion 77

4.5 Conclusions 85

Chapter 5: Summary and Future Directions 87

5.1 Summary of Thesis 87

5.2 Future Directions 89

Appendix: Permissions....91

References....148

Abstract....169

Autobiographical Statement....171

LIST OF TABLES

Table 2.1: Metal concentrations of fly ash leachate measured by ICP–MS. Reported values are the mean concentration of three replicates. 55

Table 4.1: Optimization of the functional using experimental values for **4.1**. 77

Table 4.2: Bond lengths (Å) for **4.1** from crystallographic[312] and computational structures 78

Table 4.3: Bond lengths (Å) for **4.2** from crystallographic[300] and computational structures. 79

LIST OF FIGURES

Figure 1.1: General design considerations of ligands for rare-earth element enrichment including metal charge density, donor atom polarizability, ligand denticity, and pK_a values of the ligand. Elements are listed in order of decreasing ionic radius of the +3 oxidation state. Blue circles represent heavy rare-earth elements and red circles represent light rare-earth elements. The size of the circles correlates to the trend of decreasing ionic radii across the series which also correlates to increasing charge density across the series. 4

Figure 1.2: Relation between pK_a and complex formation. The left three equilibria represent the stepwise deprotonation of a multidentate triprotic ligand (H_3L) resulting from increasing the pH. The right three equilibria represent the complexation of each deprotonated species with a solvated trivalent metal ion (S_nM^{3+}), where *n* molecules of solvent are coordinated to the metal ion. This figure is an oversimplification for the purpose of illustration. 6

Figure 1.3: Oxygen-donor ligands reported as part of solid-phase materials for enrichment of rare-earth elements since 2009: diglycolic acid on polystyrene solid-phase material (**1.1**); di-substituted diglycolamic acid solid-phase material (**1.2**); *N,N*-di(2-ethylhexyl)-diglycolamide (DEHDGA) (**1.3**); diglycolamic acid solid-phase material (**1.4**); di-substituted succinamic acid solid-phase material (**1.5**); di-substituted glutaramic acid solid-phase material (**1.6**); bis-butyl diglycolamic acid (**1.7**); bis-hexyl diglycolamic acid (**1.8**); bis-octyl diglycolamic acid (**1.9**); bis-decyl diglycolamic acid (**1.10**); mono-substituted *N*-methyl diglycolamic acid solid-phase material (**1.11**); *N,N,N′,N′*-tetraoctyldiglycolamide (TODGA) (**1.12**); *N,N′*-dimethyl-*N,N′*-dioctyldiglycolamide (DMDODGA) (**1.13**); 2,2'-oxybis(1-(3-(((2-ethylhexyl)thio)methyl)-4-methylpyrrolidin-1-yl)ethan-1-one) (DEHPDGA) (**1.14**); *N,N′*-dioctyl-diglycolic acid (DODGA) solid-phase material (**1.15**); *N*,*N*-dibutyl diglycolamic acid solid-phase material (**1.16**); and *N*,*N*-diethyl diglycolamic acid solid-phase material (**1.17**); *N,N*-diisopropyl *N′*-diglycolamide solid-phase material (**1.18**); *N,N*-diethyl *N′*-diglycolamide solid-phase material (**1.19**); *N,N*-dibutyl *N′*-diglycolamide solid-phase material (**1.20**); *N,N′*-diglycolamide solid-phase material (**1.21**); *N,N,N′,N′*-tetrakis-2-ethylhexyldiglycolamide (TEHDGA) (**1.22**); *N,N*-dioctylfuran-2,4-diamide (FDGA)-solid-phase material (**1.23**); diglycolylester (DGO) solid-phase material (**1.24**); and *N,N′*-bis-propyl diglycolamide (PDGA) solid-phase material (**1.25**); mono-substituted succinamic acid solid-phase material (**1.26**); mono-substituted *N*-methyl succinamic acid solid-phase material (**1.27**); mono-substituted glutaramic acid solid-phase material (**1.28**); mono-substituted *N*-methyl glutaramic acid solid-phase material (**1.29**); fluorinated β-diketone solid-phase material (**1.30**); Arsenazo I (**1.31**); Arsenazo III (**1.32**); tannic acid (**1.33**); maleamide-solid-phase material (**1.34**); 3,6-dioxaoctanedioic acid (DOODA)-solid-phase material (**1.35**); *N*,*N*-dioctyl-1,2-phthaloyl diamido-solid-phase material (**1.36**); *N*,*N*-dioctyl-1,2-phenylenedioxy diamido-solid-phase material (**1.37**); *N*,*N*-dioctyl-1,3-phthaloyl diamido-solid-phase material (**1.38**); *N*,*N*-dioctyl-1,3-phenylenedioxy diamido-solid-phase material (**1.39**); *N*,*N*-dioctyl-1,4-phthaloyl diamido-solid-phase material (**1.40**); *N*,*N*-dioctyl-1,4-phenylenedioxy diamido-solid-phase material (**1.41**); and diglycolic acid solid-phase material (**1.42**);. Black circles in **1.1**, **1.2**, **1.4**–**1.6, 1.11**, **1.15**–**1.21**, **1.23**–**1.30**, and **1.34**–**1.42** represent the location of attachment to solid supports. 8

Figure 1.4: Speciation of Sc^{3+} in chloride medium as a function of pH. Reprinted from Hydrometallurgy, 165 (Part 1), Van Nguyen, N.; Iizuka, A.; Shibata, E.; Nakamura, T.

Study on adsorption behavior of a new synthesized resin containing glycol amic acid group for separation of scandium from aqueous solutions, Pages 51–56, Copyright (2015), with permission from Elsevier. 12

Figure 1.5: (a) Preparation of preorganized maleamide-solid-phase material for the enrichment of mid-lanthanide ions where the grey rectangles represent the solid support, MAH is maleic anhydride, MAc is maleic acid, and MACl is maleic acid chloride, and APTES is 3-aminopropyltriethoxysilane; (b) distribution constants of metal ions using **1.34** where MSNP-OH (squares) is the pre-ATPES mesoporous silica nanoparticle, MSNP-N (circles) is post-ATPES treated mesoporous silica nanoparticle, MSNP-N-1 (triangles) is monosubstituted mesoporous silica nanoparticle, and MSNP-N-2 (upside-down triangles) is disubstituted mesoporous silica nanoparticle. Adapted with permission of Royal Society of Chemistry from Design of mesoporous silica hybrid materials as sorbents for the selective recovery of rare earth metals, Zheng, X.; Wang, C.; Dai, J.; Shi, W.; Yan, Y. Volume 3, Copyright 2015; permission conveyed through Copyright Clearance Center, Inc. 13

Figure 1.6: Solid-phase media reported in rare-earth element binding studies with ligands featuring varying bite angles: (a) KIT-6-1,2-PA (**1.36**) top right, KIT-6-1,3-PA (**1.38**) top left, KIT-6-1,3-PA (**1.40**) bottom. Media generally display a direct relationship between bite angle and preference for ions based on radius. Reprinted with permission from Hu, Y.; Drouin, E.; Larivière, D.; Kleitz, F.; Fontaine, F-G. Highly efficient and selective recovery of rare earth elements using mesoporous silica functionalized by preorganized chelating ligands. *ACS Appl. Mater. Interfaces.* **2017**, *9*, 38584. Copyright 2017 American Chemical Society. 15

Figure 1.7: Phosphorous-containing ligands reported as part of solid-phase materials for enrichment of rare-earth elements since 2009: bis(2-ethylhexyl)phosphoric acid (HDEHP, D2EHPA, TOPS 99, or P204) (**1.43**); 2-ethylhexylphosphonic acid mono-2-ethylhexyl ester (HEHEHP, D2EHPA, PC88A, or P507) (**1.44**); di-(2,4,4-trimethylpentyl) phosphinic acid (HTMPeP, Cyanex 272) (**1.45**); octyl(phenyl)-N,N-diisobutylcarbamoylmethylphosphine oxide (CMPO) (**1.46**); diprotic phosphonic acid (DPA)-solid-phase material (**1.47**); ethylene glycol phosphate diethyl ester (pEG1)-polyvinylbenzyl material (**1.48**); triethylene glycol phosphate diethyl ester (pEG3)-polyvinylbenzyl material (**1.49**); ethylene glycol monoprotic phosphate ethyl ester (pEG1M)-polyvinylbenzyl material (**1.50**); and triethylene glycol monoprotic phosphate ethyl ester (pEG3M)-polyvinylbenzyl material (**1.51**); *N*-(phosphonomethyl)iminodiacetic acid (PMIDA)-solid-phase material (**1.52**); dinonyl phenyl phosphoric acid (**1.53**); Cyanex 923 (**1.54**); 1,5-bis[2-(oxyethoxyphosphoryl)phenoxy]-3-oxapentane (**1.55**); 1,5-bis[2-(oxyethoxyphosphoryl-4-ethyl)phenoxy]-3-oxapentane (**1.56**); 1,5-bis[2-(oxyethoxyphosphoryl-4-tert-butyl)phenoxy]-3-oxapentane (**1.57**); 1,5-bis[2-(oxybutoxyphosphoryl)phenoxy]-3-oxapentane (**1.58**); 1,5-bis[2-(oxybutoxyphosphoryl-4-ethyl)phenoxy]-3-oxapentane (**1.59**); 1,5-bis[2-(butoxyoxyphosphoryl-4-tert-butyl)phenoxy]-3-oxapentane (**1.60**); 1,5-bis[2-(diethoxyphosphoryl-4-ethyl)phenoxy]-3-oxapentane (**1.61**); phosphonate diester-polyvinylbenzyl material (**1.62**); phosphorylated pentaerythritol-polyvinylbenzyl material (**1.63**); phosphinic acid-polyvinylbenzyl material (**1.64**); monoprotic phosphorylated pentaerythritol-polyvinylbenzyl material (**1.65**); monoprotic phosphorylated glycerol-polyvinylbenzyl material (**1.66**); diphosphonic acid-solid-phase material (**1.67**); acetamide phosphonic acid-solid-phase material (**1.68**); propionamide phosphonic acid-solid-phase material (**1.69**); (trimethoxysilyl)propyl diethylphosphonate-solid-phase material (**1.70**); tetraphenylmethylenediphosphine oxide (**1.71**); sodium-treated

phosphonate-solid-phase material (**1.72**); phosphoric acid-solid-phase material (T-PAR solid support) (**1.73**); phosphonate-solid-phase material (**1.74**); *n*-ethyl phosphonate-solid-phase material (**1.75**); *n*-propyl phosphonate-solid-phase material (**1.76**); *n*-butyl phosphonate-solid-phase material (**1.77**); benzene triamido-tetraphosphonic acid-solid-phase material (**1.78**); phosphonoacetic acid (**1.79**); *N*,*N*-bisphosphono(methyl)glycine (**1.80**); aminophosphonic acid-solid-phase material (**1.81**); sulfonic acid/phosphonic acid-solid-phase material (**1.82**); aminoethylphosphonic acid (**1.83**); and imino-bis-methylphosphonic acid (**1.84**). Black circles in **1.47**–**1.52**, **1.62**–**1.70**, **1.72**–**1.78**, **1.81**, and **1.82** represent the location of attachment to solid supports. 17

Figure 1.8: Affinity of rare-earth elements by solid-phase material using ligands **1.43** (diamonds), **1.44** (squares), and **1.45** (triangles) described by retention factors (log k) as a function of ionic radii. Adapted with permission from Ramzan, M.; Kifle, D.; Wibetoe, G. Comparitive study of stationary phases impregnated with acidic organophosphorous extractants for HPLC separation of rare earth elements. *Sep. Sci. Technol.* **2016**, *51*, 494. Copyright © 2016 Taylor & Francis Group. 20

Figure 1.9: Nitrogen-containing ligands reported as part of the solid-phase materials for enrichment of rare-earth elements since 2009: *N*-benzoyl-*N*-phenylhydroxylamine-solid-phase material (**1.85**); monoaza dibenzo 18-crown-6 ether-solid-phase material (**1.86**); 2,6-bis(5,6,7,8-tetrahydro-5,8,9,9-tetramethyl-5,8-methano-1,2,4-benzotriazin-3-yl)pyridine (**1.87**); *N*-propyl salicylaldimine-solid-phase material (**1.88**); ethylenediaminepropyl salicylaldimine-solid-phase material (**1.89**); ethylenediaminetetraacetic acid-solid-phase material (**1.90**); diethylenetriaminepentaacetic acid-solid-phase material (**1.91**); triethylenetetraminehexaacetic acid-solid-phase material (**1.92**); diethylenetriamine (**1.93**); tetramethylmalonamide-solid-phase material (**1.94**); urea-solid-phase material (**1.95**); *N*-aminopropylen-amidoiminodiacetic acid-solid-phase material (**1.96**); dimethoxy iminodiacetate-solid-phase material (**1.97**); iminodiacetamide-type solid-phase material (**1.98**); *N*,*N′*-bis(ethylhexylamido) diethylenetriaminetriacetic acid (**1.99**); ethyleneglycol tetraacetic acid (**1.100**); pyridine-α,β-dicarboxylic acid bis(propylenamide)-solid-phase material (**1.101**); carbonylated catechol-solid-phase material (**1.102**); catechol-solid-phase material (**1.103**); iminodiacetic acid-solid-phase material (**1.104**); phenylarsonic acid-solid-phase material (**1.105**); iminodimethylphosphonic acid-solid-phase material (**1.106**); serine-solid-phase material (**1.107**); 2,6-pyridinedicarboxaldehyde (**1.108**); 2,6-diacetylpyridine (**1.109**); 8-hydroxy-2-quinolinecarboxaldehyde (**1.110**); *N*,*N*,*N′*,*N′*,*N″*,*N″*-hexaoctylnitrilotriacetamide (**1.111**); phenanthroline diamide-solid-phase material (**1.112**); 1-(2-pyridylazo)-2-naphthol-solid-phase material (**1.113**); acetyl acetone-solid-phase material (**1.114**); *N*-methyl-*N*-phenyl-1,10-phenanthroline-2-carboxamide (**1.115**); *N*-octyl-*N*-tolyl-1,10-phenanthroline-2-carboxaide (**1.116**); 4-tert-octyl-4-((phenyl)diazenyl)phenol (**1.117**); 4-dodecyl-6-((4-(hexyloxy)phenyl)diazenyl) benzene-1,3-diol (**1.118**); glutamine-solid-phase material (**1.119**); diethylamine-substituted pentaerythritol-solid-phase material (**1.120**); benzotriazole (**1.121**); *N*-α-Fmoc-*N*-ε-boc-L-lysine-solid-phase material (**1.122**); aminocarbonylmethylglycine-solid-phase material (**1.123**); bis(3-methoxysalicylaldehyde)-*o*-phenylenedi-imine (**1.124**); *N*-(2-hydroxyethyl)salicylaldimine-solid-phase material (**1.125**); *N*,*N*′-bis(salicylidene)-1,3-ethylenediamine-solid-phase material (**1.126**); salicylamide-solid-phase material (**1.127**); 2-(2-nitrobenzylideneamino)guanidine (**1.128**); eriochrome black T (**1.129**); 1-2-(aminoethyl)-3-phenylurea-solid-phase material (**1.130**); 2,6-bis(5,6-dipropyl-1,2,4-

triazin-3-yl)pyridine (**1.131**); 2,(2,4-dihydroxyphenyl)-benzimidazole-solid-phase material (**1.132**); 3,4-hydroxypyridinone-solid-phase material (**1.133**); iminodiacetic acid-solid-phase material (Chelex 100) (**1.134**); *N*-2-hydroxyethyl ethylenediamine (**1.135**); benzoyl hydrazine-solid-phase material (**1.136**); amidoxime-solid-phase material (**1.137**); *N′*-[(2-hydroxy phenyl) methylene] benzohydrazide (**1.138**); *N*-[5-(trimethoxysilyl)-2-aza-1-oxopentyl]caprolactam-solid-phase material (**1.139**); dimethylamine-solid-phase material (**1.140**); 1-hydroxy-2-pyridinone-solid-phase material (**1.141**); and *N*-[(3-trimethoxysilyl)propyl]-ethylenediaminetriacetic acid-solid-phase material (**1.142**). Black circles in **1.85**, **1.86**, **1.88**–**1.92**, **1.94**–**1.98**, **1.101**–**1.105**, **1.112**–**1.114**, **1.119**, **1.120**, **1.122**, **1.123**, **1.125**–**1.127**, **1.130**, **1.132**–**1.137**, **1.139**, **1.141** and **1.142** represent the location of attachment to solid supports. 23

Figure 1.10: Separation factors reported for **1.85** as a function of atomic number where C_0 represents the starting concentration of rare-earth ions in solution: squares represent 1 mg/L, circles represent 2 mg/L, and triangles represent 5 mg/L. Adapted from Separation and Purification Technology, 231(115934), Artiushenko, O.; Ávila, E. P.; Nazarkovsky, M.; Zaitsev, V. Reusable hydroxamate immobilized silica adsorbent for dispersive solid phase extraction and separation of rare earth metal ions, Pages 1–10, Copyright (2019), with permission from Elsevier. 26

Figure 1.11: Uptake of Nd^{3+} as a function of time using **1.90** (circles) and **1.91** (squares). Adapted with permission of Royal Society of Chemistry from Adsorption performance of functionalized chitosan–silica hybrid materials toward rare earths, Roosen, J.; Spooren, J.; Binnemans, K. Volume 2(45), Copyright 2014; permission conveyed through Copyright Clearance Center, Inc. 27

Figure 1.12: Sulfur-donor ligands reported as part of solid-phase materials for enrichment of rare-earth elements since 2009: L-cysteine (**1.143**); 2-mercaptobenzimidole-solid-phase material (**1.144**); benzoyl thiourea-solid-phase material (**1.145**); and bis(2,4,4-trimethylpentyl)dithiophosphinic acid (Cyanex 301) (**1.146**). Black circles in **1.144** and **1.145** represent the location of attachment to solid supports. 29

Figure 1.13: Uptake of rare-earth ions La^{3+} (triangles), Nd^{3+} (squares), Gd^{3+} (circles), and Y^{3+} (upside-down triangles) as a function of pH using iron oxide nanoparticles functionalized with L-cysteine. Adapted from Journal of Environmental Chemical Engineering, 4(3), Ashour, R. M.; Abdel-Magied, A. F.; Abdel-khalek, A. A.; Helaly, O. S.; Ali, M. M. Preparation and characterization of magnetic iron oxide nanoparticles functionalized by L-cysteine: adsorption and desorption behavior for rare earth metal ions, Pages 3114–3121, Copyright (2016), with permission from Elsevier. 29

Figure 1.14: Alizarin Red S (**1.147**). 31

Figure 1.15: Visualization of the synthesis of a Eu^{3+}-imprinted polymer using vinyl pyridine and methacrylic acid as ligands, divinyl benzene as a polymerization agent, and 2,2′-azobisisobutyronitrile (AIBN) as an initiator. After Eu^{3+} is complexed with vinyl pyridine and methacrylic acid and polymerized with divinyl benzene, Eu^{3+} is removed using a leaching agent (**1.90**) resulting in the Eu^{3+}-imprinted polymer. Reprinted from Talanta, 106, Alizadeh, T.; Amjadi, S. Synthesis of Eu^{3+}-imprinted polymer and its application for indirect voltametric determination of europium, Pages 431–439, Copyright (2013), with permission from Elsevier. 32

Figure 2.1: Structure and design features of bis(ethylhexyl)amido DTPA. 40

Figure 2.2: ^{1}H-NMR Spectrum of Bis(ethylhexyl)amido DTPA. 42

Figure 2.3: ^{13}C-NMR Spectrum of Bis(ethylhexyl)amido DTPA. 43

Figure 2.4: SEM images of unmodified media. SEM images were taken using JEOL JSM 7600F (JEOL, USA), magnification of 35× and 100×. The voltage was 15 kV at low vacuum. Samples were sputter coated with gold, the current was 60 mA for 30 seconds then the images were acquired. 44

Figure 2.5: Inductively coupled plasma–mass spectrometry calibration of neodymium using ^{115}In as an internal standard. Nd^{III} curves are shown as an example of calibration curves, and all other metals showed similar accuracy. 47

Figure 2.6: Metal sorbed (mol sorbed/mol added) for bis(ethylhexyl)amido DTPA-associated media versus the equilibrium stability constants for DTPA.[20,282] The dotted line represents linear trendline with $R^2 = 0.91$. 50

Figure 2.7: (a) Sorption of trivalent rare-earth elements to the unmodified media. (b) Sorption of trivalent rare-earth elements to the ligand-associated media. The ligand-associated media shows preference for binding the mid to heavy rare-earth elements. Metal sorbed is C_b from **Equation 1**. The bars for each element on the primary (left) y-axis represent metal sorbed per metal added (mol/mol): black bars at pH 3.3 and grey bars at pH 0.9. The lines for each element on the secondary (right) y-axis represent metal sorbed per media added (mg/g): black line at pH 3.3 and grey line at pH 0.9. Error bars indicate the standard error of the mean of three independently prepared samples. 52

Figure 2.8: Nd^{III} sorption as a function of pH. Nd^{III} sorbed is C_b from Equation 1. Error bars indicate the standard error of the mean of three independently prepared samples. ...53

Figure 2.9: pH-cycling experiment with sorption and desorption of Nd^{III} from the organosilica-ligand system. Nd^{III} sorbed is C_b from Equation 1. Grey bars represent Nd^{III} bound between pH 1.5 and 1.6, and black bars represent Nd^{III} bound between pH 3.2 and 3.5. Error bars indicate the standard error of the mean of three independently prepared samples. 54

Figure 2.10: Comparison of acetate content in sorption experiments. Squares represent data from **Figure 2.8** where acetate (0.1 M) is present only in samples within pH range 3.6–5.6, and circles represent acetate (0.1 M) present in all solutions. 54

Figure 2.11: Metal sorption from fly ash leachate solutions at pH 3.0. Grey bars for each element represent percent metal extracted with unmodified media at pH 3.0, and black bars for each element represent metal extracted with the ligand-associated media. Error bars represent the standard error of the mean of three independently prepared samples. 56

Figure 2.12: Metal sorbed (mol sorbed/mol in leachate) for bis(ethylhexyl)amido DTPA-associated media versus the lanthanide equilibrium stability constants for DTPA.[20,282] The dotted line represents linear trendline with $R^2 = 0.94$. 57

Figure 3.1: Amphiphilic ligands described in this chapter. 61

Figure 3.2: ^{1}H-NMR Spectrum of **3.1**. 63

Figure 3.3: ^{13}C-NMR Spectrum of **3.1**. 64

Figure 3.4: ^{1}H-NMR Spectrum of **3.2**. 65

Figure 3.5: ^{13}C-NMR Spectrum of **3.2**. 66

Figure 3.6: Ligand-functionalized media loadings where the ligand on the media is represented by the number below each set of data on the x-axis. Error bars for **3.1** indicate the standard error of the mean of five independently prepared samples, and error bars for **3.2** indicate the standard error of the mean of seven independently prepared samples. 70

Figure 3.7: Washes of ligand-functionalized media. The ligand on the media is represented by the compound number below each set of data on the x-axis. Grey bars represent media washed in methanol; white bars represent media washed in pH 5.5 water; and black bars represent media washed in pH 0.9 water. Error bars indicate the standard error of the mean of three independently prepared samples for all data, except error bars for methanol wash for compound **3.1** represent the standard error of the mean of two independently prepared samples. A data point was removed by statistical analysis using a q test from the methanol wash for compound **3.1**. *Values measured for the pH 5.5 and pH 0.9 washes were below the limit of detection of LCMS (10 ppb). 71

Figure 4.1: (left) Eu^{II}-containing 222-cryptate **4.1** and (right) Eu^{II}-containing octaaza-cryptate **4.2**. 74

Figure 4.2: B3PW91/SDD optimized ground-state structures in SMD methanol: (top left) optimized structure of **4.1**; (top right) optimized structure of **4.2**; (bottom left) spin density (blue) mapped onto **4.1**; (bottom right) spin density (blue) mapped onto **4.2**. 80

Figure 4.3: UV–visible spectra from experiment and TD-DFT B3PW91/SDD calculations in SMD methanol. Experimental absorption (—) and emission (---) and calculated absorption (—) and emission (---) of **4.1** (top) and **4.2** (bottom). 81

Figure 4.4: Energy diagram depicting 4f–5d transitions and the respective natural-transition orbitals involved based on TD-DFT B3PW91/SDD calculations of ground-state-to-excited-state and excited-state-to-ground-state transitions for (left) **4.1** and (right) **4.2**. 82

Figure 4.5: Spectrum depicting 80 calculated transitions of the absorption of **4.1**. 82

Figure 4.6: Spectrum depicting 80 calculated transitions of the absorption of **4.2**. 83

Figure 4.7: Spectrum depicting the lowest nine calculated transitions of the emission of **4.2**. 83

Figure 4.8: Orbital energy diagram of the $5d_{z^2}$, $5d_{xy}$, and $4f_{z^3}$ orbitals for **4.1** (left) and **4.2** (right). The relatively large splitting energy in **4.2** is due to the presence of strong-field amine donors in the octaaza-cryptate compared to ethers in **4.1**. 84

CHAPTER 1

Coordination Chemistry of Solid–Liquid Adsorption of Rare-Earth Elements

1.1 Permissions and Description of Author Contributions

This chapter was adapted with permission from Hovey, J. L.; Dittrich, T. M.; Allen, M. J. *J. Rare Earths.* **2021**, https://doi.org/10.1016/j.jre.2022.05.012. Chapter 1 was written in collaboration with Dr. Timothy M. Dittrich and Dr. Matthew J. Allen. All authors contributed to the writing, editing, and formatting of the manuscript.

1.2 Introduction

The contents of this chapter pertain to the coordination chemistry of rare-earth elements using solid–liquid extraction, which are critical materials used in everyday technologies such as cell phones, laptop computers, hybrid and electric vehicles, wind turbines, and as catalysts in petroleum refining among other uses. Currently, the most widely used enrichment technique for rare-earth elements is a combination of fractional precipitation and liquid–liquid (or solvent) extraction which provides a reliable way to enrich rare-earth elements but takes many rounds to prepare pure rare-earth elements. Solid–liquid extraction involves the grafting of surface functional groups designed to bind rare-earth elements to a solid-phase material. Compared to liquid-liquid extraction, solid–liquid extraction features a single-phase media that facilitates the binding and elution to enrich rare-earth elements. This chapter explores the solid–liquid extraction of rare-earth elements using ligand-functionalized media with examples taken from reports published between 2009 and 2021.

In the era of constantly advancing technological efficiency, rare-earth elements are essential to new technologies because they exhibit a wide range of magnetic, electrochemical, and photochemical properties.[1–15] Rare-earth elements comprise the lanthanides plus scandium and yttrium, and their oxides are found mixed with each other in ore deposits such as monazite, bastnasite, xenotime, and ion-adsorption clays.[4,7,11,16] Due to the similar coordination chemistry and solubility of the elements, it is difficult to extract and purify them,[4,11,17,18] As the demand for

rare-earth elements increases, so does the need for new approaches to extract and recycle rare-earth elements from ores, magnets, batteries, optoelectronic devices, by-products of burning coal, and spent nuclear materials.

Despite the challenges associated with separations of rare-earth elements, the coordination chemistry of lanthanides is widely studied, and reported structural, kinetic, and thermodynamic properties inform extractions of the rare-earth elements from each other and from other elements.[7,19–21] In this thesis, *extraction* of rare-earth elements refers to the abstraction of rare-earth elements from solutions containing other chemical species; *separation* refers to the isolation of subgroups of rare-earth elements or individual rare-earth elements from other rare-earth elements; and *enrichment* refers to the increase in concentration of one or more of the rare-earth elements through extraction, separation, or both. Extraction, separation, and enrichment of rare-earth elements can be tuned by adjusting coordination chemistry,[22–24] Consequently, analysis of factors—including ligand denticity, pK_a, kinetic inertness, and thermodynamic stability—pertaining to the binding of ligands to rare-earth elements yields a general set of coordination-chemistry parameters to enable adjustment of rare-earth element extraction, separation, and enrichment processes.

A commonly used enrichment technique involves the coordination environment of rare-earth elements and is a combination of fractional precipitation and liquid–liquid (or solvent) extraction. Fractional precipitation of rare-earth elements refers to the addition of a chemical reagent to a solution of rare-earth ions to form insoluble complexes. Liquid–liquid extraction of rare-earth elements involves biphasic systems most often comprised of an organic layer doped with extractant (or ligand) designed to bind select metal ions from an acidic aqueous layer. These methods produce rare-earth oxides with purities >99.9% after more than 50 rounds of enrichment.[7] The methods are compatible with large-scale extractions, but they produce large amounts of organic waste.[25]

Another method of rare-earth element extraction that uses coordination chemistry is solid–liquid extraction. Solid–liquid extraction of rare-earth elements typically uses a solid-phase material made of two parts: a solid support that serves as an attachment surface and functionalized ligands that contain various functional groups for binding rare-earth elements. Surface-binding sites are either covalently or noncovalently incorporated into the solid-phase materials. Different solid-phase materials are used in solid–liquid extractions, including carbon- or silica-based matrices,[26–29] iron- or titanium-infused particles,[30–32] and biofilms consisting of bacteria or proteins,[33–36] and critical reviews of the solid supports and solid-phase materials used as matrices for rare-earth extraction can be found elsewhere.[37–40] Often if materials are functionalized with ligands, they can have synergistic properties, binding metal ions to both the solid support and the ligand. This chapter focuses on the coordination chemistry relevant to the use ligands on the solid-phase materials.

Ligand design for solid–liquid extraction and separation of rare-earth elements takes into account several considerations including metal charge density, donor-atom polarizability, ligand denticity, and binding-site pK_a (**Figure 1.1**). Rare-earth ions that have larger charge densities, such as the heavy rare earth elements relative to the light rare earth elements, tend to have increased electrostatic attraction with ligands. Because of the stronger metal–ligand interactions with rare-earth ions with larger charge densities, complexes of heavy rare-earth elements tend to be more inert than complexes of light rare-earth elements.[20]

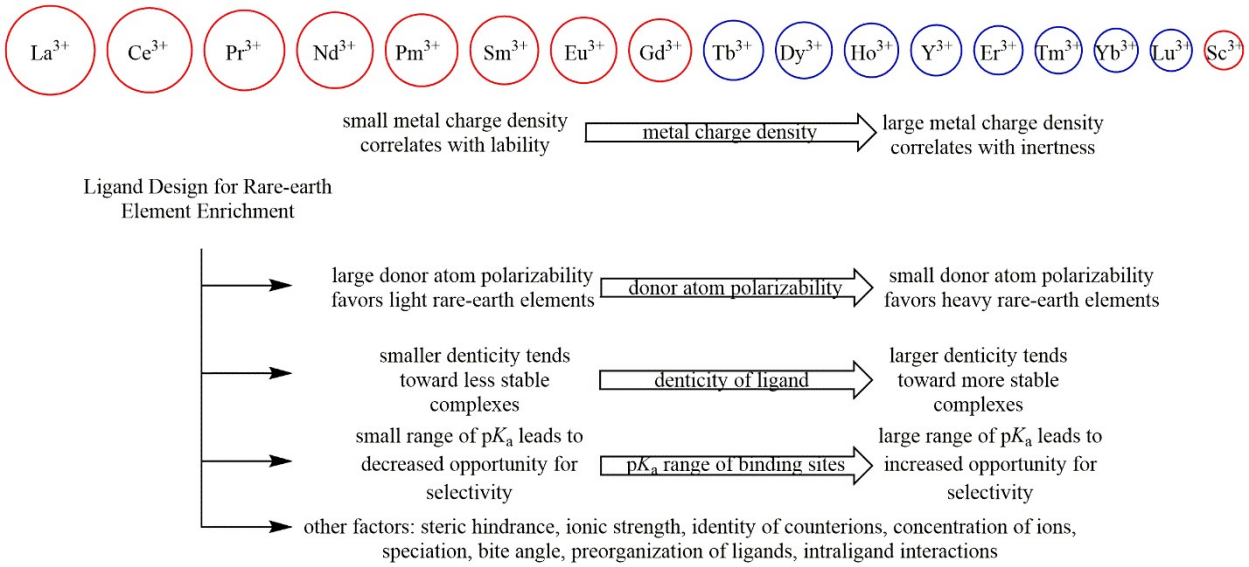

Figure 1.1. General design considerations of ligands for rare-earth element enrichment including metal charge density, donor atom polarizability, ligand denticity, and pK_a values of the ligand. Elements are listed in order of decreasing ionic radius of the +3 oxidation state. Blue circles represent heavy rare-earth elements and red circles represent light rare-earth elements. The size of the circles correlates to the trend of decreasing ionic radii across the series which also correlates to increasing charge density across the series.

Donor-atom polarizability is often described using hard–soft acid–base theory, where Lewis acids and bases are characterized on a continuum between hard and soft. Ions and atoms that are less polarizable, or less susceptible to distortion from an outside electronic field, are referred to as hard. More polarizable ions and atoms are referred to as soft. When analyzing trends in rare-earth element separations, the use of hard–soft acid–base theory enables qualitative comparison of donor-atom polarizability to rare-earth element selectivity, in which the light rare-earth ions are slightly more polarizable Lewis acids than the heavy rare earth ions and generally bind to more polarizable donor atoms (Lewis bases).[41]

Multidentate ligands generally have greater affinity for metal ions than monodentate ligands because of entropic considerations. Generally, larger denticities are associated with larger thermodynamic stabilities of the resulting rare-earth element complexes, up to the point of

saturation of the coordination sphere of the ions as a result of the chelate effect. In general, rare–earth ions in the +3 oxidation state tend to have coordination numbers of eight or nine.

Another important design feature of ligands for rare-earth element extractions is the range of pH in which the rare-earth ions will bind to ligands. In rare-earth element extractions, pH determines the speciation of metal ions and counterions in solution.[42] Other metal ions commonly found in recycled materials—such as Al^{3+}, Fe^{3+}, or Ni^{2+}—[29,43–45] can compete with the target metal ions and influence enrichment efficiencies. Because solution pH is related to the amount of protonation of the ligand, it is often beneficial to design ligands with a large range of pK_a values to increase selectivity. To illustrate this point, the three equilibria on the left of **Figure 1.2** represent the effect of pH on tridentate ligand speciation through deprotonation. As the pH increases, ligands are deprotonated, consistent with increasing pK_a values. The three equilibria on the right side of **Figure 1.2** represent the same ligand species in the same range of pH in the presence of a trivalent metal ion. As pH increases and the ligand is deprotonated, monodentate solvent molecules on the metal are displaced and the metal–ligand complex becomes increasingly stable, which is usually desirable to achieve increased enrichment of rare-earth elements.[7,29,46] Complex stability is defined by the conditional equilibrium complexation constant and is dependent on environmental variables such as ionic strength and pH.[20] In the example in **Figure 1.2**, lowering the pH results in a decrease of complex formation. Because competing cations such as Al^{3+}, Fe^{3+}, or Ni^{2+} are often present in much greater concentrations than the rare-earth ions, differences in the conditional equilibrium complexation constants create opportunities to selectively bind or elute rare-earth ions. Thus, the larger the range of pK_a values of a ligand, the more opportunity there is to selectivity elute rare-earth ions as a function of pH.

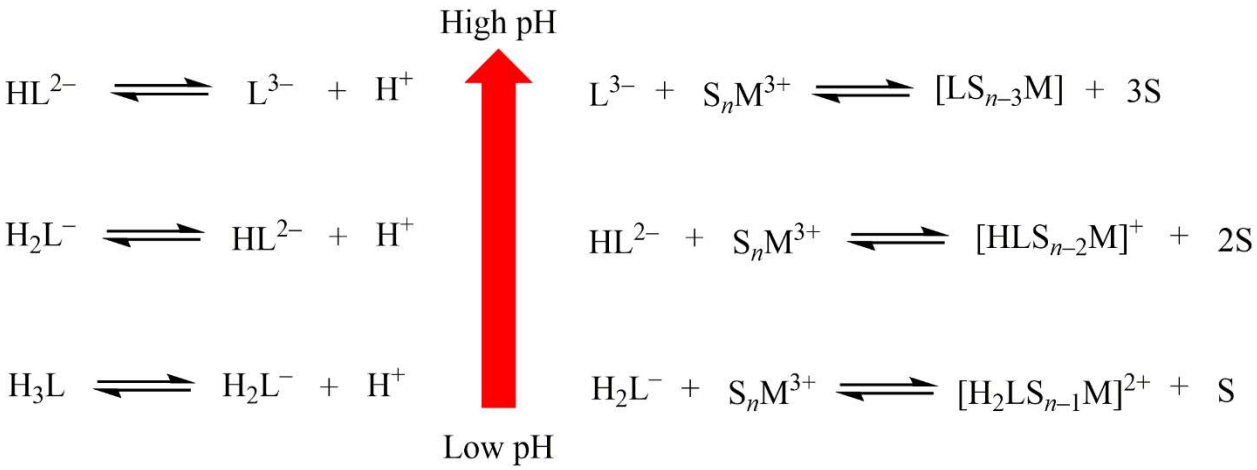

Figure 1.2. Relation between pK_a and complex formation. The left three equilibria represent the stepwise deprotonation of a multidentate triprotic ligand (H_3L) resulting from increasing the pH. The right three equilibria represent the complexation of each deprotonated species with a solvated trivalent metal ion (S_nM^{3+}), where *n* molecules of solvent are coordinated to the metal ion. This figure is an oversimplification for the purpose of illustration.

Despite the aforementioned trends, experimental variability causes anomalistic behavior, leading to unique enrichment behavior. Exceptions to trends arise from ligand features that include steric hindrance, saturated binding sites, variability in speciation caused by the identity of counterions and ionic strength, and size-exclusivity in ligands stemming from differences in bite angle, preorganization of the ligands, or intraligand interactions. These trends and exceptions are described in this chapter and offer insight into the impact that coordination chemistry has on the efficiency of the enrichment of rare-earth elements. This chapter analyzes the general design considerations for rare-earth element enrichment including metal charge density, donor-atom polarizability, ligand denticity, and binding-site pK_a for solid–liquid extraction organized by donor type with examples taken from reports published between 2009 and 2021. For a detailed review of rare-earth element extractions prior to 2009, readers are directed elsewhere.[47]

1.3 Solid-phase materials

Solid–liquid adsorptions of rare-earth ions use insoluble materials with affinity for rare-earth ions in an aqueous phase with no need for an organic phase during enrichment processes. There are several considerations to take into account when selecting or designing ligands for solid-phase materials, including donor-atom polarizability, denticity, and pK_a of the ligands as well as the kinetic inertness and thermodynamic stability of the resulting complexes. Other variables, such as steric bulk of the ligand and factors that influence speciation including choice of acid and ionic strength, play a role in selectivity. The ligands used in the solid-phase materials described in this section are divided into groups based on type of donor atoms. In each section, the ligands chosen for discussion are relevant to the design considerations discussed in **Figure 1.1** and provide insight into the relationship between coordination chemistry and rare-earth ion enrichment.

1.3.1 Carboxylic acids, alcohols, glycolic acids, glycolamic acids, and glycolamides

Ligands that contain carboxylic acids, alcohols, glycolic acids, glycolamic acids, and glycolamides in the solid–liquid separation of rare-earth elements described in this section are depicted in **Figure 1.3**.[43,46,48–78] The majority of studies reported for the solid–liquid enrichment of rare-earth ions using these systems report a preference for heavy rare-earth ions, likely based on the increased Lewis acidity of the heavy rare-earth elements compared to the light rare-earth elements.[46,55–65]

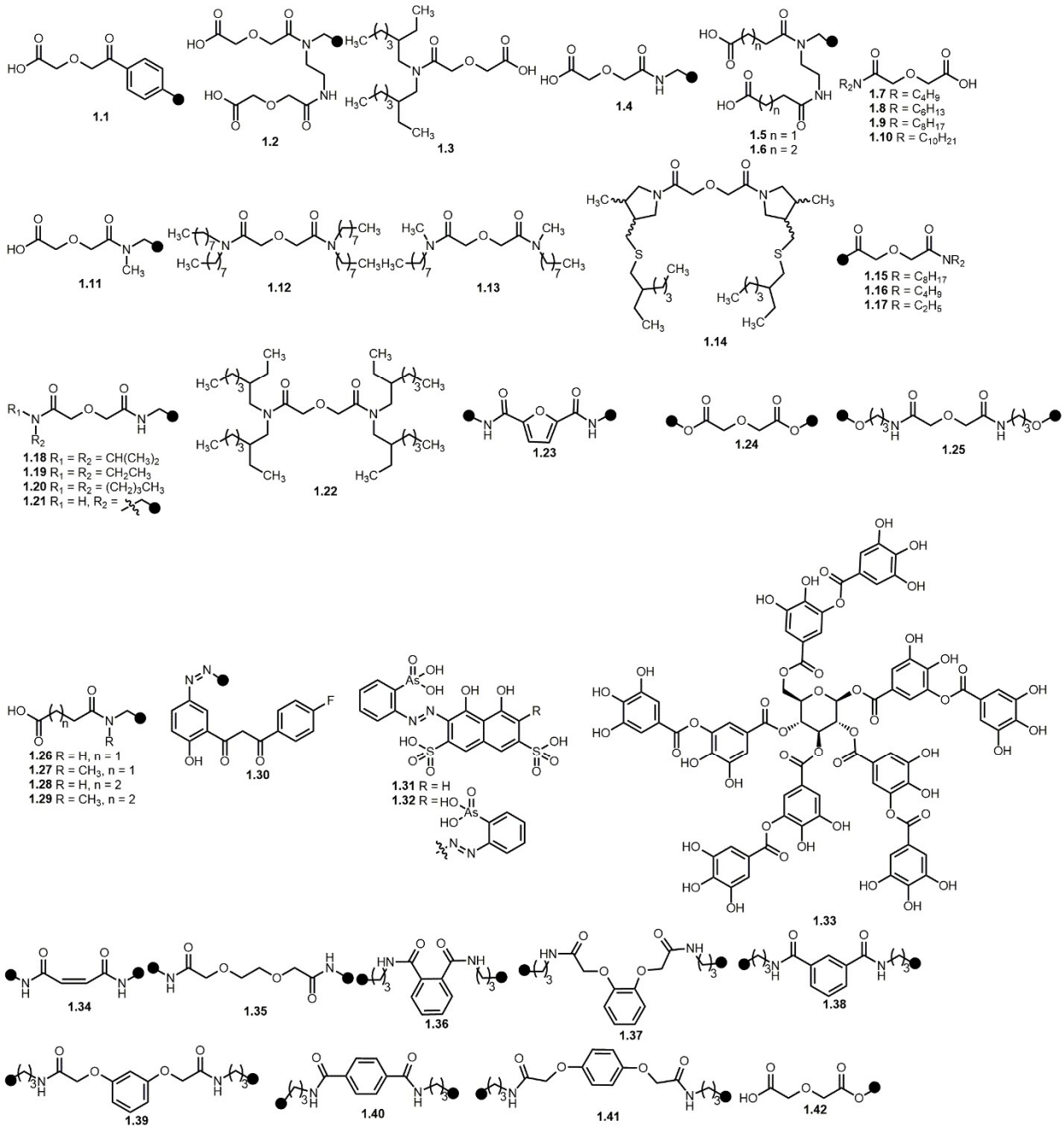

Figure 1.3. Oxygen-donor ligands reported as part of solid-phase materials for enrichment of rare-earth elements since 2009: diglycolic acid on polystyrene solid-phase material (**1.1**); di-substituted diglycolamic acid solid-phase material (**1.2**); *N,N*-di(2-ethylhexyl)-diglycolamide (DEHDGA) (**1.3**); diglycolamic acid solid-phase material (**1.4**); di-substituted succinamic acid solid-phase material (**1.5**); di-substituted glutaramic acid solid-phase material (**1.6**); bis-butyl

diglycolamic acid (**1.7**); bis-hexyl diglycolamic acid (**1.8**); bis-octyl diglycolamic acid (**1.9**); bis-decyl diglycolamic acid (**1.10**); mono-substituted *N*-methyl diglycolamic acid solid-phase material (**1.11**); *N,N,N′,N′*-tetraoctyldiglycolamide (TODGA) (**1.12**); *N,N′*-dimethyl-*N,N′*-dioctyldiglycolamide (DMDODGA) (**1.13**); 2,2'-oxybis(1-(3-(((2-ethylhexyl)thio)methyl)-4-methylpyrrolidin-1-yl)ethan-1-one) (DEHPDGA) (**1.14**); *N,N′*-dioctyl-diglycolic acid (DODGA) solid-phase material (**1.15**); *N*,*N*-dibutyl diglycolamic acid solid-phase material (**1.16**); and *N*,*N*-diethyl diglycolamic acid solid-phase material (**1.17**); *N,N*-diisopropyl *N′*-diglycolamide solid-phase material (**1.18**); *N,N*-diethyl *N′*-diglycolamide solid-phase material (**1.19**); *N,N*-dibutyl *N′*-diglycolamide solid-phase material (**1.20**); *N,N′*-diglycolamide solid-phase material (**1.21**); *N,N,N′,N′*-tetrakis-2-ethylhexyldiglycolamide (TEHDGA) (**1.22**); *N*,*N*-dioctylfuran-2,4-diamide (FDGA)-solid-phase material (**1.23**); diglycolylester (DGO) solid-phase material (**1.24**); and *N,N′*-bis-propyl diglycolamide (PDGA) solid-phase material (**1.25**); mono-substituted succinamic acid solid-phase material (**1.26**); mono-substituted *N*-methyl succinamic acid solid-phase material (**1.27**); mono-substituted glutaramic acid solid-phase material (**1.28**); mono-substituted *N*-methyl glutaramic acid solid-phase material (**1.29**); fluorinated β-diketone solid-phase material (**1.30**); Arsenazo I (**1.31**); Arsenazo III (**1.32**); tannic acid (**1.33**); maleamide-solid-phase material (**1.34**); 3,6-dioxaoctanedioic acid (DOODA)-solid-phase material (**1.35**); *N*,*N*-dioctyl-1,2-phthaloyl diamido-solid-phase material (**1.36**); *N*,*N*-dioctyl-1,2-phenylenedioxy diamido-solid-phase material (**1.37**); *N*,*N*-dioctyl-1,3-phthaloyl diamido-solid-phase material (**1.38**); *N*,*N*-dioctyl-1,3-phenylenedioxy diamido-solid-phase material (**1.39**); *N*,*N*-dioctyl-1,4-phthaloyl diamido-solid-phase material (**1.40**); *N*,*N*-dioctyl-1,4-phenylenedioxy diamido-solid-phase material (**1.41**); and diglycolic acid solid-phase material (**1.42**);. Black circles in **1.1**, **1.2**, **1.4**–**1.6, 1.11**, **1.15**–**1.21**, **1.23**–**1.30**, and **1.34**–**1.42** represent the location of attachment to solid supports.

Diglycolic acids, diglycolamic acids, and diglycolamides (**Figure 1.3**, **1.1**–**1.25**, and **1.42**) generally coordinate to rare-earth ions in a tridentate fashion through an ether oxygen and two carbonyl or carboxylate oxygens. One such diglycolic-acid-modified polystyrene nanofiber solid-phase material (**1.1**) was reported through the synthetic modification of electrospun fiber supports using diglycolic acid (15% w/w).[66] The sorption of Ce^{3+} and Nd^{3+} from solution (100 ppm, HNO_3, pH 6) by the modified nanofiber media showed comparable adsorption capacities of 152.5 and 146.2 mg/g, respectively. Investigations into the selectivity of **1.1** revealed that the material is still selective for Ce^{3+} when in competition with Co^{2+}, Ni^{2+}, and Sr^{2+} (100 ppm each, HNO_3, pH 6) binding 100.3 mg/g Ce^{3+}, 2.01 mg/g Co^{2+}, 4.99 mg/g Ni^{2+}, and 3.30 mg/g Sr^{2+}.[66] The main reason for the preferential binding of rare-earth elements was determined to be a combination of size-specific binding in the solid-phase material leading to a chelate effect and larger charge density in the rare-earth ions compared to d-block ions. Because diglycolic acid binds 3:1 with the rare-earth elements and 2:1 with the smaller d-block ions, the relatively large rare-earth element (ionic radius of Ce^{3+} **=** 1.02 Å) was generally entropically preferred over Ni^{2+} (0.69 Å), Co^{2+} (0.65–0.745 Å), and Sr^{2+} (1.18 Å).[19] Even though Sr^{2+} is larger than Ce^{3+}, it is probable that there was relatively low competition between the ions because of the larger charge density of Ce^{3+} compared to Sr^{2+}.

Increases in denticity also influence the enrichment of rare-earth ions. Silica solid-phase supports electrostatically modified with chromophores Arsenazo I (**1.31**) and Arsenazo III (**1.32**) were reported resulting in quantitative adsorption of rare-earth elements from a solution of La^{3+}, Nd^{3+}, Sm^{3+}, Gd^{3+}, Ho^{3+}, and Er^{3+} (0.1 ppm each, HNO_3 at pH 5.5–7 for **31** and pH 2–6 for **32**).[67] Although both chromophores bind rare-earth elements to form 1:1 complexes, the major difference in the coordination chemistry is the presence of one arsenic acid in **1.31** versus two arsenic acid groups in **1.32**, leading to more thermodynamically stable complexes of rare-earth elements with **1.32** compared to **1.31**. The difference in size is also significant between the two ligands: because **1.32** is larger than **1.31**, the surface of the silica has the capacity to fit only 42% of the larger ligand **1.32** (~0.0075 mmol/g) compared to the smaller ligand **31** (~0.018 mmol/g).[67]

In this noncovalently bound solid-phase material, the difference in size and denticity of the two ligands resulted in a media prepared with **1.32** that was more selective for the rare-earth elements relative to the media prepared with **1.31**.

The nature of the matrix in which metal ions are introduced to the solid-phase materials is also important because it impacts the chemical species that are introduced for adsorption.[68–70] One such example is *N,N*-di(2-ethylhexyl)-diglycolamide (DEHDGA) functionalized Amberlite IRA-910 resin (**1.3**).[68] Solid-phase material **1.3** exhibits preference for the heavy rare-earth elements over light rare-earth elements and selectivity for the trivalent rare-earth ions over other trivalent ions, specifically Fe^{3+} and Al^{3+} (HCl, pH 1.5). The preference for rare-earth ions over Fe^{3+} is likely due to the anionic speciation of Fe^{3+} in high concentrations of HCl and provides an opportunity for preconcentration of the heavy rare-earth elements from a solution of competing trivalent metal ions.

A diglycolamic acid modified solid-phase material (**1.4**) was used at low pH (HCl, pH 1) to enrich Sc^{3+} from a solution of Sc^{3+}, La^{3+}, Ce^{3+}, and Al^{3+} (20, 300, 750, and 2,000 ppm, respectively).[70] This finding is a result of the differences in size of Sc^{3+}, La^{3+}, and Ce^{3+} (0.745, 1.032, and 1.02 Å, respectively).[19] Because the main species at pH 1 is Sc^{3+} (**Figure 1.4**), the ionic radius of Sc^{3+} was complimentary to the pore size of their solid-phase material (0.89 Å), whereas La^{3+} and Ce^{3+} were not complimentary sizes. These studies underline the idea that the ionic radius plays a critical role in variability between adsorption studies using solid-phase materials for rare-earth element adsorption.

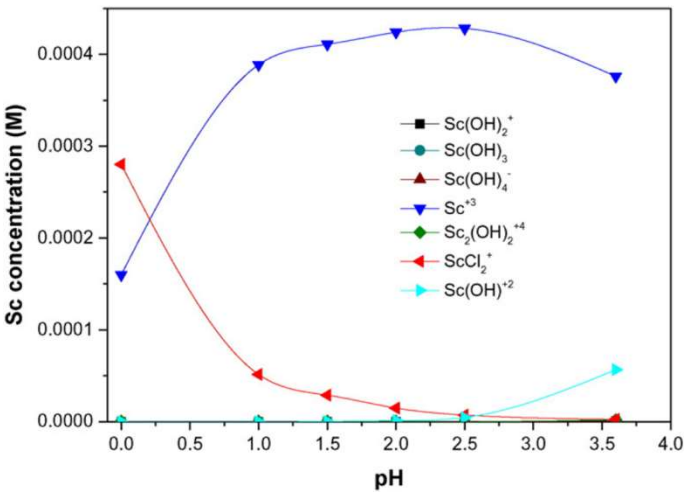

Figure 1.4. Speciation of Sc^{3+} in chloride medium as a function of pH. Reprinted from Hydrometallurgy, 165 (Part 1), Van Nguyen, N.; Iizuka, A.; Shibata, E.; Nakamura, T. Study on adsorption behavior of a new synthesized resin containing glycol amic acid group for separation of scandium from aqueous solutions, Pages 51–56, Copyright (2015), with permission from Elsevier.

Although one of the most notable trends among the solid-phase materials described in this section is the selectivity for heavy rare-earth elements, there are some instances where the mid-lanthanide ions are preferred.[43,71–74] The preference for mid-lanthanide ions usually stems from adjusting the ligand in the solid-phase material: designing a preorganized solid-phase material typically leads to unique rare-earth ion selectivity (**Figure 1.3**, **1.21**, **1.23**–**1.25**, **1.34**–**1.41**). For example, a solid-phase material featuring maleamide, **1.34**, that links a maleamide group to mesoporous silica nanoparticles using two amide linkages (**Figure 1.5a**) were used to enrich rare-earth elements from a solution of Sm^{3+}, Eu^{3+}, Gd^{3+}, Tb^{3+}, Dy^{3+}, Ho^{3+}, and Er^{3+} (20 ppm each, HNO_3, pH 4) and exhibited the following selectivity: $Gd^{3+} > Tb^{3+} > Eu^{3+} > Sm^{3+} > Er^{3+} \approx Dy^{3+} > Ho^{3+}$ (**Figure 1.5b**).[71] The preorganized ligand assembly likely created a size-specific environment, leading to the preference for ions with ionic radii between 0.94 and 0.90 Å.[19]

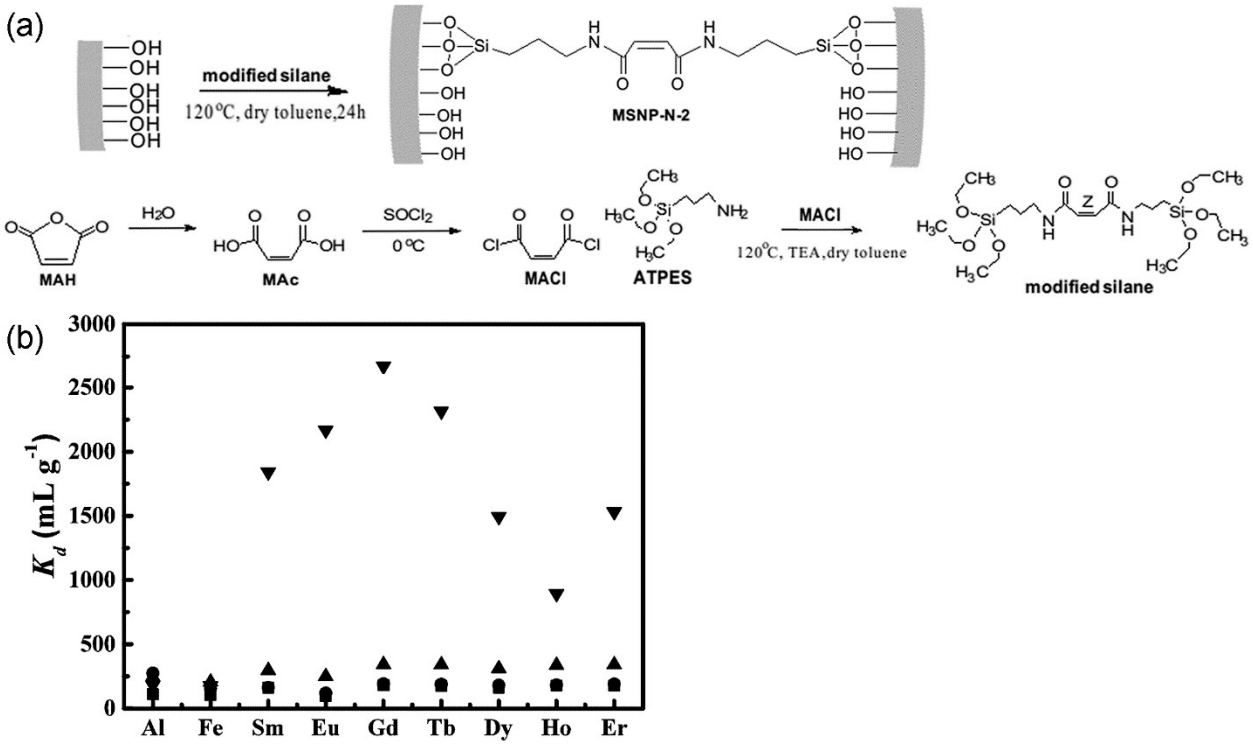

Figure 1.5. (a) Preparation of preorganized maleamide-solid-phase material for the enrichment of mid-lanthanide ions where the grey rectangles represent the solid support, MAH is maleic anhydride, MAc is maleic acid, and MACl is maleic acid chloride, and APTES is 3-aminopropyltriethoxysilane; (b) distribution constants of metal ions using **1.34** where MSNP-OH (squares) is the pre-ATPES mesoporous silica nanoparticle, MSNP-N (circles) is post-ATPES treated mesoporous silica nanoparticle, MSNP-N-1 (triangles) is monosubstituted mesoporous silica nanoparticle, and MSNP-N-2 (upside-down triangles) is disubstituted mesoporous silica nanoparticle. Adapted with permission of Royal Society of Chemistry from Design of mesoporous silica hybrid materials as sorbents for the selective recovery of rare earth metals, Zheng, X.; Wang, C.; Dai, J.; Shi, W.; Yan, Y. Volume 3, Copyright 2015; permission conveyed through Copyright Clearance Center, Inc.

Larivière, Kleitz and coworkers provided examples of diglycolamide solid-phase material that exhibits selectivity for the mid-lanthanide ions.[73] A macroporous silica support covalently functionalized with diglycolamide ligands through both of the amide moieties was reported,

creating a rigidly linked disubstituted ligand (**1.21**). A synthetic solution of all trivalent rare-earth ions except Pm^{3+} (2 ppb each, HNO_3, pH 4) was introduced to the media, and Eu^{3+} and Gd^{3+} were preferentially adsorbed to the solid-phase material up to ~3 times more than other rare-earth ions when in competition with the other rare-earth ions and competing cations such as Al^{3+}, and Fe^{3+}. The selectivity for mid-lanthanide ions was attributed to the relatively rigid structure of the synthetically modified solid-phase material providing fixed spacing for binding of the mid-sized ions[73]

By adjusting the angle at which the coordinating atoms of a ligand bind to a metal ion, known as bite angle, selectivity for rare-earth ions is adjusted (**Figure 1.3** compounds **1.21**, **1.23**, **1.35–1.41**).[75–78] Two classes of ligands were covalently attached to KIT-6 mesoporous silica: phenylenedioxy diamides and phthaloyl diamides (**Figure 1.6**). The separation of all of the rare-earth elements except Pm^{3+} (30 ppb each, HNO_3, pH 4) was analyzed using three bidentate phthaloyl diamides *N*,*N*-dioctyl-1,2-phthaloyl diamido-solid-phase material (**1.36**), *N*,*N*-dioctyl-1,3-phthaloyl diamido-solid-phase material (**1.38**), *N*,*N*-dioctyl-1,4-phthaloyl diamido-solid-phase material (**1.40**) with different bite angles (**1.40** > **1.38** > **1.36**, **Figure 1.6**).[75] The extraction and separation of rare-earth elements (30 ppb HNO_3, pH 4) was analyzed from bauxite leachate using tetradentate phenylenedioxy diamide ligands *N*,*N*-dioctyl-1,2-phenylenedioxy diamido-solid-phase material (**1.37**), *N*,*N*-dioctyl-1,3-phenylenedioxy diamido-solid-phase material (**1.39**), *N*,*N*-dioctyl-1,4-phenylenedioxy diamido-solid-phase material (**1.41**) with bite angles **1.41** > **1.39** > **1.37.**[76] In general, ligands with smaller bite angles showed preference for the heavy rare-earth elements, and ligands with larger bite angles showed preference for the light rare-earth elements.[75–78] Another comparison between the phthaloyl diamides and phenylenedioxy diamides from these two reports is the impact of the chelate effect on rare-earth ion enrichment. Bidentate **1.36** and tetradentate **1.37** had distribution coefficients (or the amount of metal ion bound to the solid-phase material) of 53,500 and ~80,000 mL/g Lu^{3+} (30 ppb, HNO_3, pH 4),[75,76] respectively, demonstrating that the chelate effect is important to rare-earth binding.

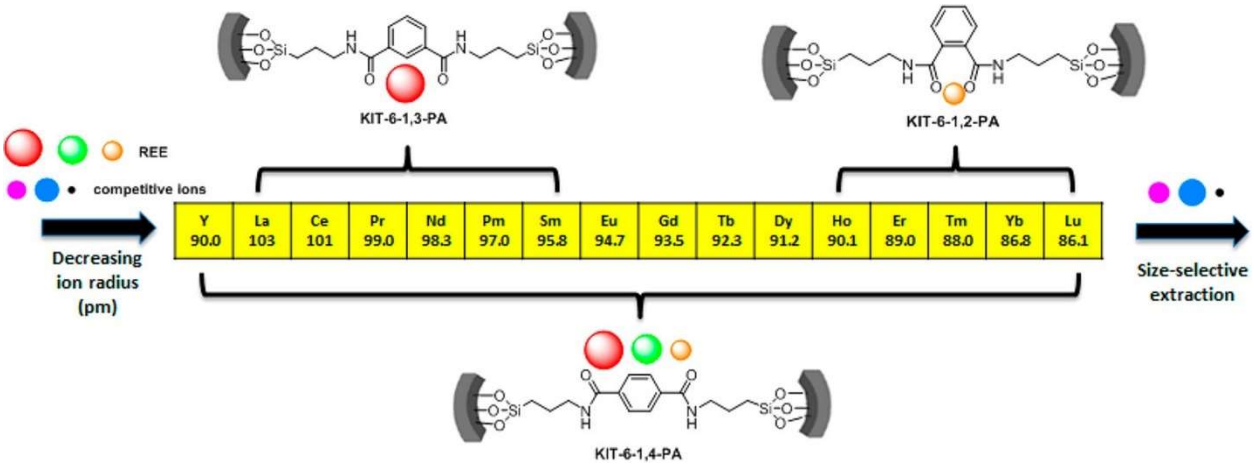

Figure 1.6. Solid-phase media reported in rare-earth element binding studies with ligands featuring varying bite angles: (a) KIT-6-1,2-PA (**1.36**) top right, KIT-6-1,3-PA (**1.38**) top left, KIT-6-1,3-PA (**1.40**) bottom. Media generally display a direct relationship between bite angle and preference for ions based on radius. Reprinted with permission from Hu, Y.; Drouin, E.; Larivière, D.; Kleitz, F.; Fontaine, F-G. Highly efficient and selective recovery of rare earth elements using mesoporous silica functionalized by preorganized chelating ligands. *ACS Appl. Mater. Interfaces.* **2017**, *9*, 38584. Copyright 2017 American Chemical Society.

In addition to general considerations for coordination chemistry, this section has outlined the general trend for selectivity for heavy rare-earth ions by carboxylic acid, alcohol, glycolic acid, glycolamic acid, or glycolamide solid-phase materials, the role denticity plays in ligand design, the effect of pH on rare-earth ion binding, the importance of sample matrix on the uptake of rare-earth ions by solid-phase materials, and the effect of preorganization and bite angle adjustment on ligand design for mid-lanthanide ion selectivity. It is also important to consider the main speciation of target ions in the sample environment to give efficient enrichment: for example, if the species will be anionic or cationic, the sizes of the species, and electrostatic interactions with solid-phase material. In addition, there are some examples of the preorganization of ligands resulting in selectivity for mid-lanthanide ions. Taking into consideration that heavy rare-earth elements are the most commonly enriched group of rare-earth elements by solid-phase materials

featuring carboxylic acids, alcohols, glycolic acids, glycolamic acids, or glycolamides, and the preorganized ligands shift the preference to the mid rare-earth elements, it is possible to use coordination chemistry to separate the rare-earth ions into three main categories: light, medium, and heavy.

1.3.2 Phosphoric acids, phosphate esters, phosphazenes, and phosphoryl-containing ligands

Phosphoric acids, phosphate esters, phosphazenes, and phosphoryl-containing solid-phase materials tend to have softer oxygen donors than carboxylic acids, alcohols, glycolic acids, glycolamic acids, or diglycolamides because the phosphorous atom is softer than oxygen.[41] Although many phosphorus-containing ligands were designed to bind softer actinide ions from solutions containing mixtures of lanthanides and actinides from spent nuclear fuel, the slight gradient shift in polarizability of phosphorus-containing ligands used in solid-phase materials for rare-earth element adsorption results in mixed selectivity among the rare-earth ions.[79–133] Phosphorus-containing solid-phase materials reported since 2009 include phosphoric acids, phosphonic acids, phosphate esters, phosphine oxides, and other phosphorus-containing ligands (**Figure 1.7**, compounds **1.43–1.84**).

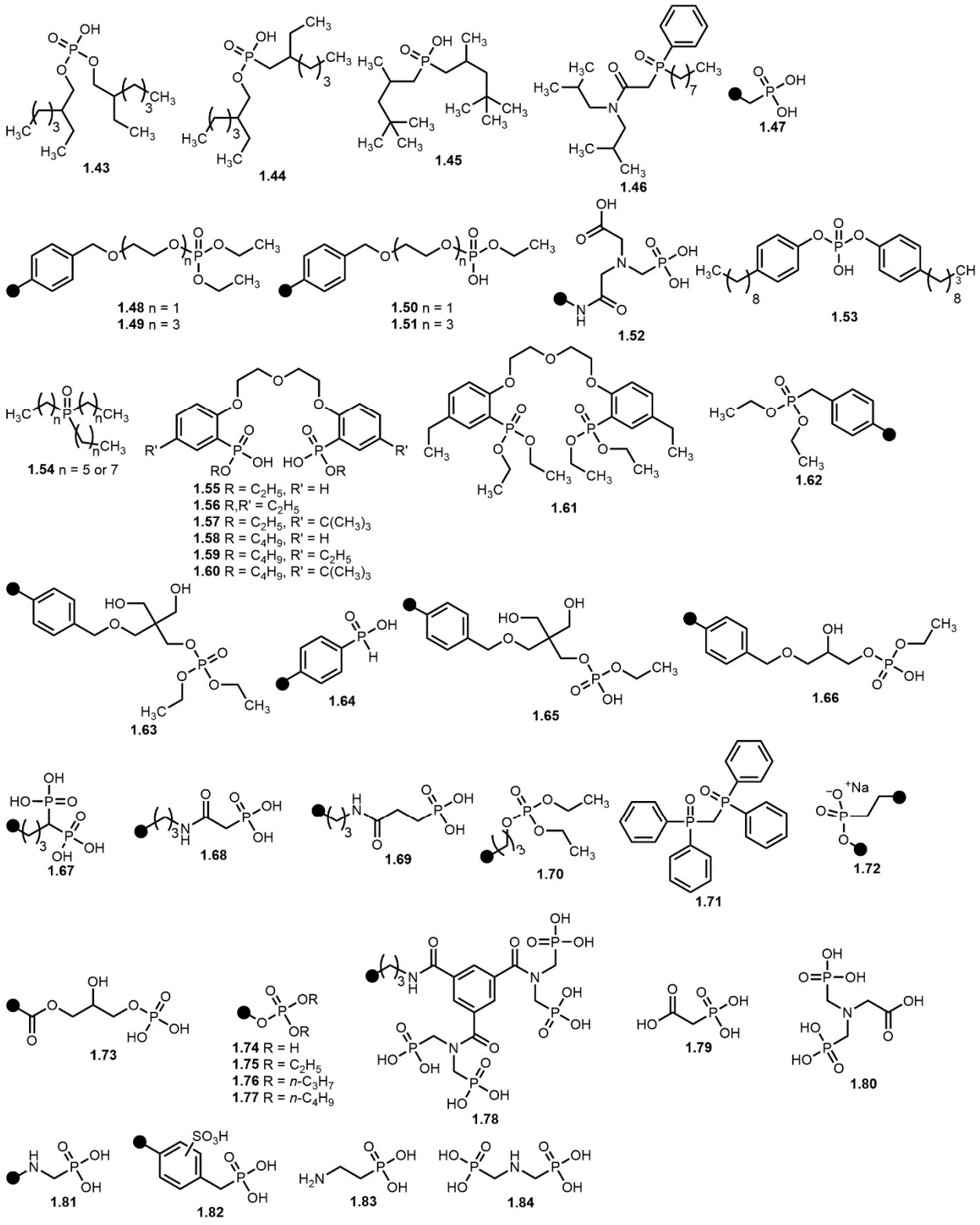

Figure 1.7. Phosphorous-containing ligands reported as part of solid-phase materials for enrichment of rare-earth elements since 2009: bis(2-ethylhexyl)phosphoric acid (HDEHP,

D2EHPA, TOPS 99, or P204) (**1.43**); 2-ethylhexylphosphonic acid mono-2-ethylhexyl ester (HEHEHP, D2EHPA, PC88A, or P507) (**1.44**); di-(2,4,4-trimethylpentyl) phosphinic acid (HTMPeP, Cyanex 272) (**1.45**); octyl(phenyl)-*N*,*N*-diisobutylcarbamoylmethylphosphine oxide (CMPO) (**1.46**); diprotic phosphonic acid (DPA)-solid-phase material (**1.47**); ethylene glycol phosphate diethyl ester (pEG1)-polyvinylbenzyl material (**1.48**); triethylene glycol phosphate diethyl ester (pEG3)-polyvinylbenzyl material (**1.49**); ethylene glycol monoprotic phosphate ethyl ester (pEG1M)-polyvinylbenzyl material (**1.50**); and triethylene glycol monoprotic phosphate ethyl ester (pEG3M)-polyvinylbenzyl material (**1.51**); *N*-(phosphonomethyl)iminodiacetic acid (PMIDA)-solid-phase material (**1.52**); dinonyl phenyl phosphoric acid (**1.53**); Cyanex 923 (**1.54**); 1,5-bis[2-(oxyethoxyphosphoryl)phenoxy]-3-oxapentane (**1.55**); 1,5-bis[2-(oxyethoxyphosphoryl-4-ethyl)phenoxy]-3-oxapentane (**1.56**); 1,5-bis[2-(oxyethoxyphosphoryl-4-tert-butyl)phenoxy]-3-oxapentane (**1.57**); 1,5-bis[2-(oxybutoxyphosphoryl)phenoxy]-3-oxapentane (**1.58**); 1,5-bis[2-(oxybutoxyphosphoryl-4-ethyl)phenoxy]-3-oxapentane (**1.59**); 1,5-bis[2-(butoxyoxyphosphoryl-4-tert-butyl)phenoxy]-3-oxapentane (**1.60**); 1,5-bis[2-(diethoxyphosphoryl-4-ethyl)phenoxy]-3-oxapentane (**1.61**); phosphonate diester-polyvinylbenzyl material (**1.62**); phosphorylated pentaerythritol-polyvinylbenzyl material (**1.63**); phosphinic acid-polyvinylbenzyl material (**1.64**); monoprotic phosphorylated pentaerythritol-polyvinylbenzyl material (**1.65**); monoprotic phosphorylated glycerol-polyvinylbenzyl material (**1.66**); diphosphonic acid-solid-phase material (**1.67**); acetamide phosphonic acid-solid-phase material (**1.68**); propionamide phosphonic acid-solid-phase material (**1.69**); (trimethoxysilyl)propyl diethylphosphonate-solid-phase material (**1.70**); tetraphenylmethylenediphosphine oxide (**1.71**); sodium-treated phosphonate-solid-phase material (**1.72**); phosphoric acid-solid-phase material (T-PAR solid support) (**1.73**); phosphonate-solid-phase material (**1.74**); *n*-ethyl phosphonate-solid-phase material (**1.75**); *n*-propyl phosphonate-solid-phase material (**1.76**); *n*-butyl phosphonate-solid-phase material (**1.77**); benzene triamido-tetraphosphonic acid-solid-phase material (**1.78**); phosphonoacetic acid (**1.79**); *N*,*N*-bisphosphono(methyl)glycine (**1.80**); aminophosphonic acid-solid-phase material (**1.81**);

sulfonic acid/phosphonic acid-solid-phase material (**1.82**); aminoethylphosphonic acid (**1.83**); and imino-bis-methylphosphonic acid (**1.84**). Black circles in **1.47**–**1.52**, **1.62**–**1.70**, **1.72**–**1.78**, **1.81**, and **1.82** represent the location of attachment to solid supports.

Stemming from a large body of research of the separation of lanthanides from actinides in spent nuclear fuel using liquid–liquid extraction,[134] there is significant insight into the use of bis(2-ethylhexyl)phosphoric acid (HDEHP) **1.43** and 2-ethylhexylphosphonic acid mono-2-ethylhexyl ester (HEHEHP) **1.44** for the adsorption of rare-earth elements from solutions of competing ions depending on separation conditions.[79,83,87,88,91,92,96–99,103] The majority of solid–liquid adsorption studies involving **1.43** report a preference for heavy rare-earth elements with some reports of preference for light rare-earth elements.[79,83–103] Similarly for ligand **1.44**, rare-earth ion selectivity is dependent on separation conditions.[105–108] To elaborate on the differences in binding between **1.43** and **1.44**, a comparative publication analyzed bidentate ligands **1.43**, **1.44**, and di-(2,4,4-trimethylpentyl) phosphinic acid (HTMPeP) **1.45** anchored onto reverse-phase C18 silica for their ability to separate lanthanide ions (10 ppm each, 2 M HNO_3).[79] As the number of P–O bonds decreases (**1.43** > **1.44** > **1.45**), the pK_a of the acidic proton increases (2.04, 2.75, and 3.62 for **1.43**, **1.44**, and **1.45**, respectively). All three solid-phase materials demonstrate a preference for heavy rare-earth ions, and the trend in binding capacity decreases for the solid-phase materials using ligands **1.43** > **1.44** > **1.45** (**Figure 1.8**).[79] The difference in binding suggests that the change in pK_a among the three ligands impacted the equilibrium complexation constants.

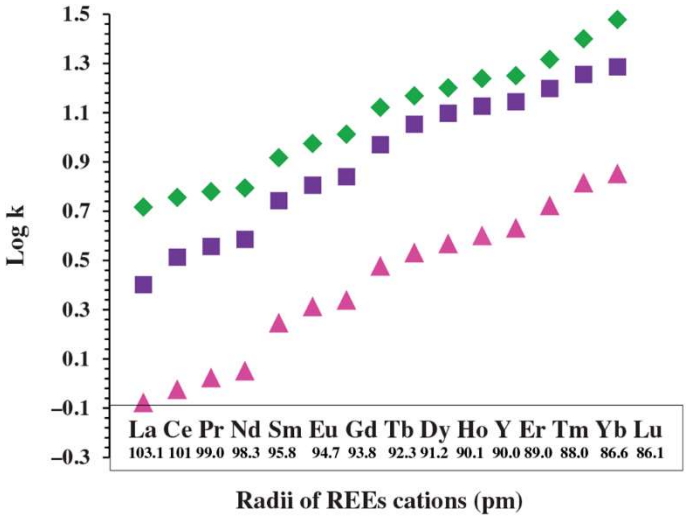

Figure 1.8. Affinity of rare-earth elements by solid-phase material using ligands **1.43** (diamonds), **1.44** (squares), and **1.45** (triangles) described by retention factors (log k) as a function of ionic radii. Adapted with permission from Ramzan, M.; Kifle, D.; Wibetoe, G. Comparitive study of stationary phases impregnated with acidic organophosphorous extractants for HPLC separation of rare earth elements. *Sep. Sci. Technol.* **2016**, *51*, 494. Copyright © 2016 Taylor & Francis Group.

An example of a solid-phase material that was selective for light rare-earth elements used the ligand octyl(phenyl)-*N*,*N*-diisobutylcarbamoylmethylphosphine oxide **1.46** adsorbed onto silica to bind Nd^{3+}, Gd^{3+}, Sr^{2+}, Zr^{4+}, Mo^{6+}, Ru^{3+}, Pd^{2+}, Cs^{+}, and trace amounts of Am^{3+} (5 mM in 3 M HNO_3).[80] The results show a breakthrough curve from a column experiment (flow rate: 1 cm^3/min; 25 °C) where the order of elution is Cs^{+}, Sr^{2+}, Ru^{3+}, Pd^{2+}, Gd^{3+}, Nd^{3+}, Am^{3+}, Zr^{4+}, then Mo^{6+}. Although it is unclear why this selectivity of ions is present, ligand **1.46** might be a good starting point for selective extraction of light rare-earth elements.

To compare the effects of changing a phosphonic acid functionality to a phosphate ester or phosphate diester, one study compared five ligands on polyvinylbenzyl chloride for the adsorption of Lu^{3+} and La^{3+} (0.1 mM in 0.1 M H_3PO_4).[81] The five ligands were diprotic phosphonic acid **1.47**, ethylene glycol phosphate diethyl ester **1.48**, triethylene glycol phosphate diethyl ester **1.49**, ethylene glycol monoprotic phosphate ethyl ester **1.50**, and triethylene glycol monoprotic

phosphate ethyl ester **1.51**. The results indicate a general preference for Lu^{3+} over La^{3+} up to three-fold and rare-earth ion binding following the order: **1.51** > **1.50** > **1.47** > **1.49** > **1.48**. Comparison of binding among the solid-phase materials led to the conclusion that the phosphate ester media sorbed rare-earth ions better than the phosphonic acid media because the phosphonic acid media binding was hindered by hydrogen-bond interactions between the hydroxyl groups. Rare-earth element affinity was found to be enhanced by the ion exchange of the monoprotic solid-phase material more than the phosphate diester media containing no exchangeable acidic protons.[81] The ligands with three ethylene glycol groups coordinated rare-earth ions better than the ligands with one ethylene glycol group because the oxygens in ethylene glycol coordinated to the rare-earth ions, enhancing the chelate effect. This example highlights the impact of designing a ligand that binds to rare-earth ions through ion exchange or through neutral donor coordination and the direct correlation between denticity and rare-earth ion complex affinity.

Phosphorus-containing ligands provide insight from the history of actinide enrichment, and there is a large amount of research for the separation of actinide ions from rare-earth ions.[80,115,135,136] Similar to **Section 1.2.1**, design considerations to keep in mind for the coordination chemistry of phosphorus-containing ligands include the pK_a of the acidic protons on the ligand, the speciation resulting from the acidic matrix of the system, and the denticity of the ligand. The pK_a of the acidic protons on the phosphate group is influenced by the amount of electron withdrawing groups on the ligand that affects the enrichment of rare-earth ions. It is also important to note that mixed selectivity of rare-earth ions can be caused by differences in speciation that result in unique selectivity of rare-earth ions. In addition, ligands with larger denticities tend to have higher affinities for rare-earth ions than those with smaller denticities.

1.3.3 Hydroxamates, polyamido acetic acids, Schiff bases, pyridine derivatives, phenanthroline, benzotriazoles, aza-crown ethers, amides, and imines

There is a large body of research surrounding the use of nitrogen-based ligands, specifically hydroxamates, polyamido acetic acids, Schiff bases, pyridine derivatives, phenanthroline, benzotriazoles, aza-crown ethers, amides, and imines in solid-phase materials for the enrichment of rare-earth elements (**Figure 1.9** compounds **1.85**–**1.142**).[29,44,45,116,121,137–200] These ligands feature a mixture of nitrogen and oxygen donor atoms that tend to be softer donors than carboxylic acids, alcohols, glycolic acids, or diglycolamides.[41] The majority of studies in this group of donor atoms report selectivity for the heavy rare-earth elements, but there is some mixed selectivity throughout.

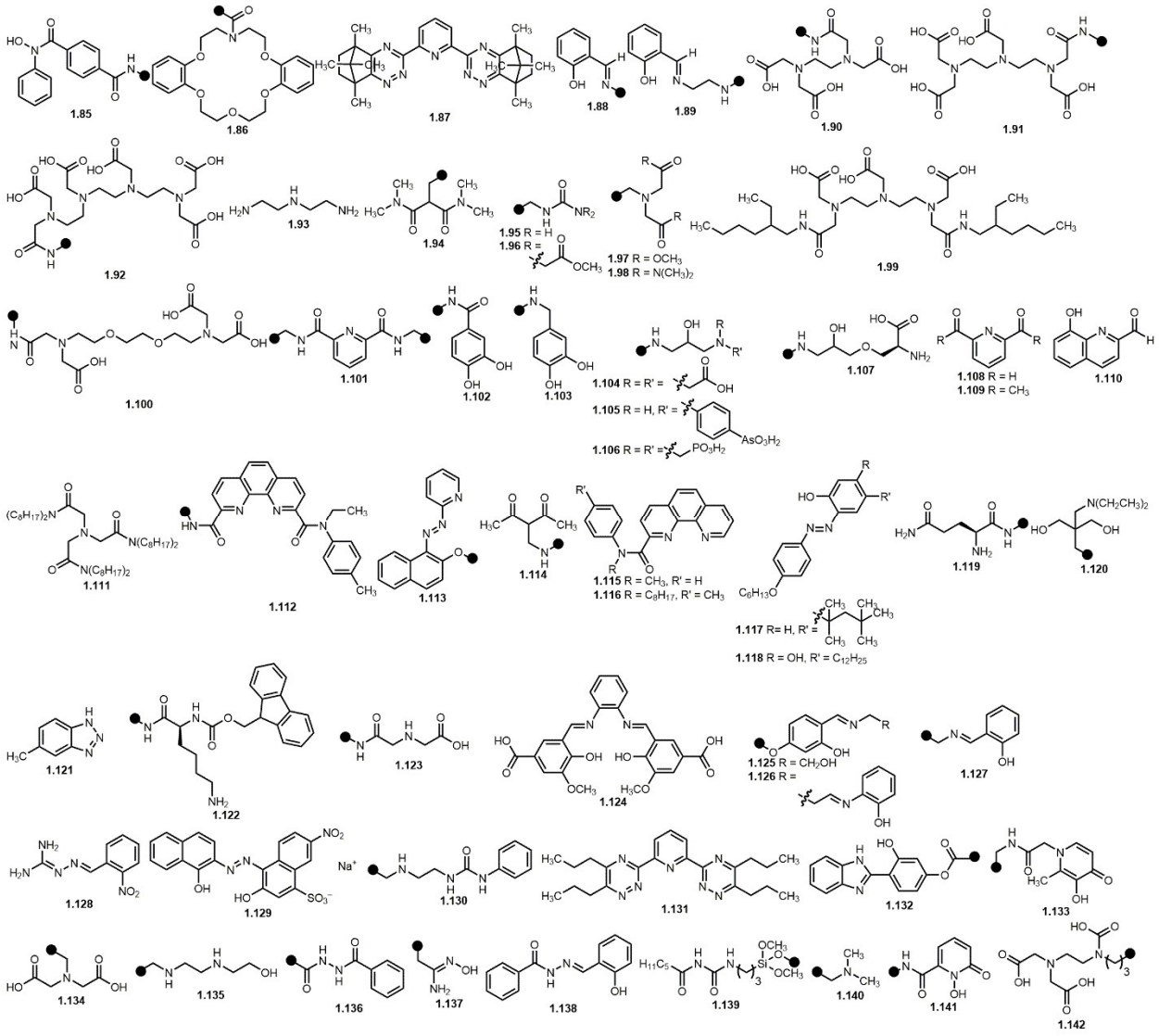

Figure 1.9. Nitrogen-containing ligands reported as part of the solid-phase materials for enrichment of rare-earth elements since 2009: *N*-benzoyl-*N*-phenylhydroxylamine-solid-phase material (**1.85**); monoaza dibenzo 18-crown-6 ether-solid-phase material (**1.86**); 2,6-bis(5,6,7,8-tetrahydro-5,8,9,9-tetramethyl-5,8-methano-1,2,4-benzotriazin-3-yl)pyridine (**1.87**); *N*-propyl salicylaldimine-solid-phase material (**1.88**); ethylenediaminepropyl salicylaldimine-solid-phase material (**1.89**); ethylenediaminetetraacetic acid-solid-phase material (**1.90**); diethylenetriaminepentaacetic acid-solid-phase material (**1.91**); triethylenetetraminehexaacetic acid-solid-phase material (**1.92**); diethylenetriamine (**1.93**); tetramethylmalonamide-solid-phase material (**1.94**); urea-solid-phase material (**1.95**); *N*-aminopropylen-amidoiminodiacetic acid-

solid-phase material (**1.96**); dimethoxy iminodiacetate-solid-phase material (**1.97**); iminodiacetamide-type solid-phase material (**1.98**); *N*,*N*′-bis(ethylhexylamido) diethylenetriaminetriacetic acid (**1.99**); ethyleneglycol tetraacetic acid (**1.100**); pyridine-α,β-dicarboxylic acid bis(propylenamide)-solid-phase material (**1.101**); carbonylated catechol-solid-phase material (**1.102**); catechol-solid-phase material (**1.103**); iminodiacetic acid-solid-phase material (**1.104**); phenylarsonic acid-solid-phase material (**1.105**); iminodimethylphosphonic acid-solid-phase material (**1.106**); serine-solid-phase material (**1.107**); 2,6-pyridinedicarboxaldehyde (**1.108**); 2,6-diacetylpyridine (**1.109**); 8-hydroxy-2-quinolinecarboxaldehyde (**1.110**); *N*,*N*,*N*′,*N*′,*N*″,*N*″-hexaoctylnitrilotriacetamide (**1.111**); phenanthroline diamide-solid-phase material (**1.112**); 1-(2-pyridylazo)-2-naphthol-solid-phase material (**1.113**); acetyl acetone-solid-phase material (**1.114**); *N*-methyl-*N*-phenyl-1,10-phenanthroline-2-carboxamide (**1.115**); *N*-octyl-*N*-tolyl-1,10-phenanthroline-2-carboxaide (**1.116**); 4-tert-octyl-4-((phenyl)diazenyl)phenol (**1.117**); 4-dodecyl-6-((4-(hexyloxy)phenyl)diazenyl) benzene-1,3-diol (**1.118**); glutamine-solid-phase material (**1.119**); diethylamine-substituted pentaerythritol-solid-phase material (**1.120**); benzotriazole (**1.121**); *N*-α-Fmoc-*N*-ε-boc- L-lysine-solid-phase material (**1.122**); aminocarbonylmethylglycine-solid-phase material (**1.123**); bis(3-methoxysalicylaldehyde)-*o*-phenylenedi-imine (**1.124**); *N*-(2-hydroxyethyl)salicylaldimine-solid-phase material (**1.125**); *N*,*N*′-bis(salicylidene)-1,3-ethylenediamine-solid-phase material (**1.126**); salicylamide-solid-phase material (**1.127**); 2-(2-nitrobenzylideneamino)guanidine (**1.128**); eriochrome black T (**1.129**); 1-2-(aminoethyl)-3-phenylurea-solid-phase material (**1.130**); 2,6-bis(5,6-dipropyl-1,2,4-triazin-3-yl)pyridine (**1.131**); 2,(2,4-dihydroxyphenyl)-benzimidazole-solid-phase material (**1.132**); 3,4-hydroxypyridinone-solid-phase material (**1.133**); iminodiacetic acid-solid-phase material (Chelex 100) (**1.134**); *N*-2-hydroxyethyl ethylenediamine (**1.135**); benzoyl hydrazine-solid-phase material (**1.136**); amidoxime-solid-phase material (**1.137**); *N*′-[(2-hydroxy phenyl) methylene] benzohydrazide (**1.138**); *N*-[5-(trimethoxysilyl)-2-aza-1-oxopentyl]caprolactam-solid-phase material (**1.139**); dimethylamine-solid-phase material (**1.140**); 1-hydroxy-2-pyridinone-solid-

phase material (**1.141**); and *N*-[(3-trimethoxysilyl)propyl]-ethylenediaminetriacetic acid-solid-phase material (**1.142**). Black circles in **1.85**, **1.86**, **1.88**–**1.92**, **1.94**–**1.98**, **1.101**–**1.105**, **1.112**–**1.114**, **1.119**, **1.120**, **1.122**, **1.123**, **1.125**–**1.127**, **1.130**, **1.132**–**1.137**, **1.139**, **1.141** and **1.142** represent the location of attachment to solid supports.

Selectivity for the heavy rare-earth elements was observed in a study using *N*,*N*′-bis(ethylhexylamido)diethylenetriaminetriacetic acid-type ligand (**1.99**) noncovalently associated with an organically modified silica gel as the solid-phase material.[29] The solid-phase material was used to extract all of the rare-earth ions except Pm^{3+} (5ppm each, HNO_3, pH 3.3) resulting in a 3.5-fold preference for the heavy rare-earth elements compared to the light rare-earth elements. Because unsubstituted DTPA has a wide range of pK_a values, 2.00–10.48.[20] the enrichment of rare-earth ions using ligand **1.99**-solid-phase material featured pH-dependent binding: at pH 3.3, the solid-phase material extracted 21 mg/g rare-earth ions and at pH 0.9, the solid-phase material bound 1.6 mg/g rare-earth ions. The pH-dependent nature of the system is an important tool not only for reusability of the solid-phase material, but also could be used to increase the enrichment of rare-earth ions where differences in selectivity are observed at different pH as illustrated in **Figure 1.2**.

Another example of a solid-phase material with selectivity for heavy rare-earth elements includes *N*-benzoyl-*N*-phenylhydroxylamine functionalized to silica gel (**1.85**).[137] All of the lanthanides excluding Pm^{3+} and Sm^{3+} (1 ppm, HNO_3, pH 5) were introduced to **1.85** resulting in a separation factor (the ratio of uptake of two metal ions) of ~80 for Lu^{3+}/La^{3+}, compared to a separation factor of ~20 for Gd^{3+}/La^{3+}.[137] The separation factors were determined to be dependent on the amount of ligand bound to the solid-phase material (**Figure 1.10**) indicating that the solid-phase material becomes saturated with metal ions at a certain threshold (around 5 ppm starting concentration of rare-earth ions). As a general design consideration for ligands to increase the selectivity for rare-earth ions, it is important to keep in mind the impact of ligand loading on the solid support because it relates to target ion selectivity.

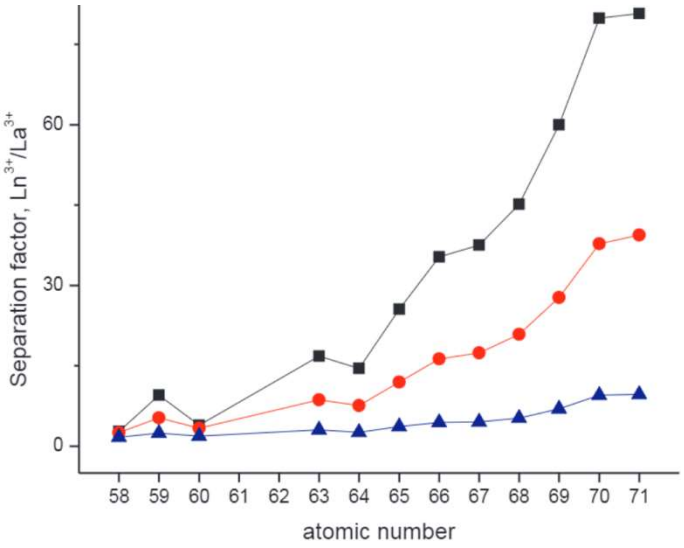

Figure 1.10. Separation factors reported for **1.85** as a function of atomic number where C_0 represents the starting concentration of rare-earth ions in solution: squares represent 1 mg/L, circles represent 2 mg/L, and triangles represent 5 mg/L. Adapted from Separation and Purification Technology, 231(115934), Artiushenko, O.; Ávila, E. P.; Nazarkovsky, M.; Zaitsev, V. Reusable hydroxamate immobilized silica adsorbent for dispersive solid phase extraction and separation of rare earth metal ions, Pages 1–10, Copyright (2019), with permission from Elsevier.

Although the majority of studies in this section report selectivity for heavy rare-earth elements, there are also reports of mixed selectivity among the hydroxamates, polyamido acetic acids, Schiff bases, pyridine derivatives, phenanthroline, benzotriazoles, aza-crown ethers, amides, and imines in solid-phase materials. For example, monoaza dibenzo 18-crown-6 ether was attached to styrene divinylbenzene to form solid-phase material **1.86** and enrich La^{3+}, Nd^{3+}, and Sm^{3+} (1.5 mM, HCl, pH 4.5).[138] Solid-phase material **1.86** retained La^{3+} over Nd^{3+} and Sm^{3+}, likely because of the cavity size of **1.86** creating a size-preference for the largest ion, La^{3+}.

Towards the goal of achieving increased separation among the rare-earth ions, a silica/polymer composite solid support was functionalized with 2,6-bis(5,6,7,8-tetrahydro-5,8,9,9-tetramethyl-5,8-methano-1,2,4-benzotriazin-3-yl)pyridine, **1.87**, for the extraction of Y^{3+}, La^{3+}, Ce^{3+}, Pr^{3+}, Nd^{3+}, Sm^{3+}, Eu^{3+}, Gd^{3+}, Dy^{3+}, Er^{3+}, Yb^{3+}, and Lu^{3+} (1 mM, HNO_3).[139] Distribution

coefficients of the mid-lanthanide ions Dy^{3+} and Er^{3+} were an order of magnitude greater than heavy rare-earth ion Lu^{3+} and four orders of magnitude greater than light rare-earth ion La^{3+}. The authors suggest that the selectivity towards mid rare-earth ions could be caused by the cavity size of the solid-phase material having a complimentary size to the mid rare-earth ions.[139]

An example of the chelate effect in solid-phase materials is in the functionalization of a chitosan-silica solid support with ethylenediaminetetracetic acid (**1.90**) and diethylenetriaminepentaacetic acid (**1.91**) for the enrichment of Nd^{3+} (0.51 mM, HNO_3).[141] The results indicate that the solid support functionalized with **1.91** had ~25% higher adsorption of Nd^{3+} at pH 2.5 than the solid support functionalized with **1.90** (**Figure 1.11**), which can be explained by the additional carboxylic acid and amine donors in **1.91** compared with **1.90**. This observation demonstrates how modifying the denticity of ligands is a useful way to adjust enrichment among target metal ions.

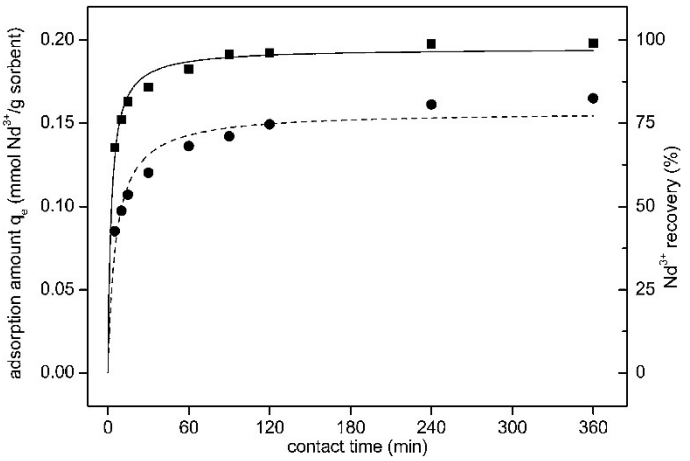

Figure 1.11. Uptake of Nd^{3+} as a function of time using **1.90** (circles) and **1.91** (squares). Adapted with permission of Royal Society of Chemistry from Adsorption performance of functionalized chitosan–silica hybrid materials toward rare earths, Roosen, J.; Spooren, J.; Binnemans, K. Volume 2(45), Copyright 2014; permission conveyed through Copyright Clearance Center, Inc.

Mixed oxygen and nitrogen donor ligands provide insight into the adjustment of ligand basicity for rare-earth ion enrichment. Although most of the solid-phase materials with

hydroxamates, polyamido acetic acids, Schiff bases, pyridine derivatives, phenanthroline, benzotriazoles, aza-crown ethers, amides, or imines exhibit selectivity for the heavy rare-earth ions, there are some reports of mixed selectivity of rare-earth ions. Compared to **Section 1.2.1**, the ligands in this section are reported to have less predictable selectivity among the rare-earth elements, which is likely caused by the presence of softer nitrogen donors compared to oxygen donors. When designing enrichment experiments, important variables that impact both rare-earth element uptake and selectivity include the range of pK_a values of the ligand, the number of available metal binding sites on the solid-phase solid support, variability in cavity size enabling selectivity of mid rare-earth elements, and ligand denticity varying the selectivity of rare-earth ions. In the examples shown, pH-dependent binding was observed with a ligand featuring a wide range of pK_a values, rare-earth ion uptake is directly proportional to the amount of ion binding sites on the solid-phase solid support, and selectivity can be altered by adjusting the rigidity of the ligand through macrocyclic ligand design or through differences in cavity size. In addition to these considerations, an increase in ligand denticity provides a means to adjust rare-earth ion selectivity through a decrease in entropy.

1.3.4 Thiazols, thiols, sulfides, and sulfoxides

Because sulfur-based ligands have the largest donor atom polarizability of the ligands discussed in this chapter, there are few reports of their use for the enrichment of rare-earth elements.[101,102,201–204] Because of their “softer” nature, thiazols, thiols, and sulfoxides have mixed selectivity in rare-earth element enrichment, but can be useful in the separation of rare-earth elements, such as the mid-lanthanide ions that are otherwise comparatively difficult to separate. Thiazols, thiols, sulfides, and sulfoxides reported in solid-phase materials for the enrichment of rare-earth elements since 2009 are reported in **Figure 1.12**, **1.143**–**1.146**.

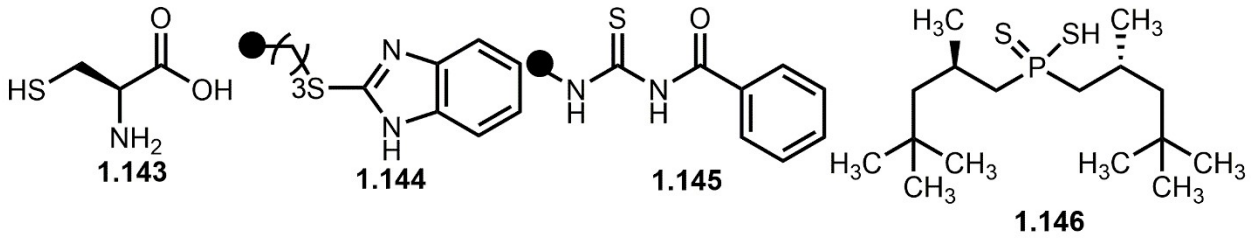

Figure 1.12. Sulfur-donor ligands reported as part of solid-phase materials for enrichment of rare-earth elements since 2009: L-cysteine (**1.143**); 2-mercaptobenzimidole-solid-phase material (**1.144**); benzoyl thiourea-solid-phase material (**1.145**); and bis(2,4,4-trimethylpentyl)dithiophosphinic acid (Cyanex 301) (**1.146**). Black circles in **1.144** and **1.145** represent the location of attachment to solid supports.

An example of a sulfur-containing ligand for rare-earth ion enrichment is the functionalization of iron oxide nanoparticles with L-cysteine (**1.143**) for the separation of La^{3+}, Nd^{3+}, Gd^{3+}, and Y^{3+} (200 ppm, HNO_3).[201] The results indicate uptake of the rare-earth ions in the order Nd^{3+} > La^{3+} > Gd^{3+} > Y^{3+} (**Figure 1.13**).[201] The solid-phase material exhibited mixed selectivity, but this method might be a reasonable pathway to separate Y^{3+} from mixed solutions of rare-earth ions.

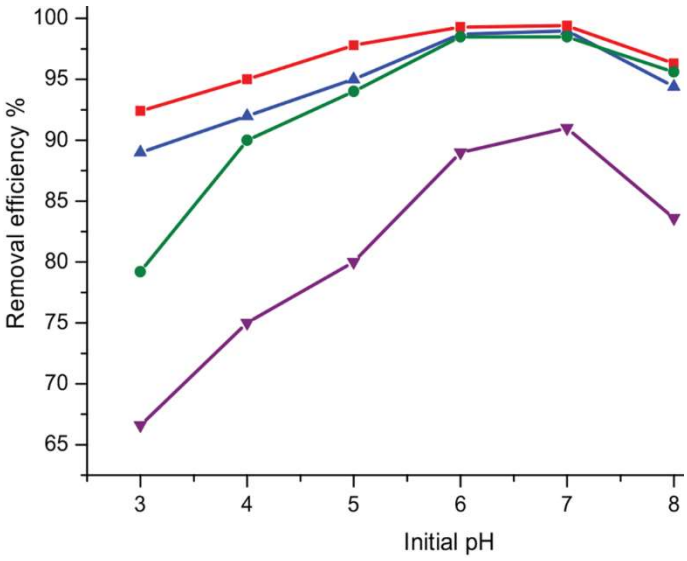

Figure 1.13. Uptake of rare-earth ions La^{3+} (triangles), Nd^{3+} (squares), Gd^{3+} (circles), and Y^{3+} (upside-down triangles) as a function of pH using iron oxide nanoparticles functionalized with L-

cysteine. Adapted from Journal of Environmental Chemical Engineering, 4(3), Ashour, R. M.; Abdel-Magied, A. F.; Abdel-khalek, A. A.; Helaly, O. S.; Ali, M. M. Preparation and characterization of magnetic iron oxide nanoparticles functionalized by L-cysteine: adsorption and desorption behavior for rare earth metal ions, Pages 3114–3121, Copyright (2016), with permission from Elsevier.

Sulfur-based ligands such as thiazols, thiols, sulfides, and sulfoxides feature donor atoms with large donor atom polarizability, which should display selectivity for lighter rare-earth ions, but there is mixed selectivity among this group of ligands. Despite sulfur-based ligands being less predictable for rare-earth ion enrichment than ligands with less polarizable donor atoms, the mixed selectivity provides an opportunity to separate ions among the rare-earths that are typically difficult to separate such as the mid-lanthanide ions or light-rare-earth ions.

1.4 Ion-imprinted polymers

In addition to solid-phase materials for solid–liquid rare-earth element adsorption, another method of rare-earth element enrichment uses crosslinked polymers imprinted with the target metal ion, where the imprinted metal ion is removed after synthesis to create the finished media with exposed ligand designed for ion-specific binding. Ion-imprinted media are used for many different ions,[205–207] including rare-earth ions[208–226] and the polymer is designed to create a binding site to match the size and coordination sphere of the target ion. Ion-imprinted polymers are designed to address ligand features for rare-earth ion enrichment including donor atom polarizability, ligand denticity, pK_a range of binding sites, steric hindrance, bite angle, and preorganization of ligands.

Towards the size-selective extraction of rare-earth ions, an ion-imprinted polymer was formed from a polymerization of ethylene glycol dimethacrylate, methacrylic acid, and a photoactive ligand Alizarin Red S (**1.147**) (**Figure 1.14**).[208] After the polymer was formed in the presence of Gd^{3+}, the ion was removed using HCl (0.1 M), leaving Gd^{3+}-sized binding sites open for rare-earth element separation. Separations were performed using a group of rare-earth

elements La^{3+}, Ce^{3+}, Eu^{3+}, Gd^{3+}, Lu^{3+} (3 ppm each, HCl, pH 6) and a separate extraction of Gd^{3+} (3 ppm, HCl, pH 6) against a series of competing ions including Al^{3+}, Fe^{3+}, Cu^{2+}, Zn^{2+}, and Sr^{2+} (10 ppm each, HCl, pH 6). The system was not selective for Gd^{3+} in the presence of other rare-earth ions but showed preference for the heavier rare-earth elements and other trivalent metal ions in the competition experiments. The lack of selectivity for Gd^{3+} can be attributed to the nature of the ligand that tends to form stable complexes with metal ions of larger charge density.[208]

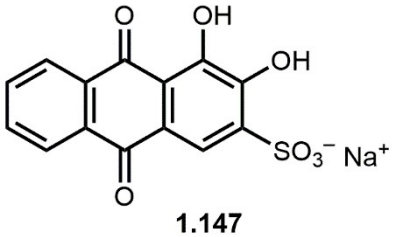

1.147

Figure 1.14. Alizarin Red S (**1.147**).

Eu^{3+}-imprinted polymer nanoparticles were synthesized using vinyl pyridine and methacrylic acid as ligands that were polymerized using divinyl benzene and 2,2′-azobisisobutyronitrile as an initiator (**Figure 1.15**).[209] The Eu^{3+} was leached from the polymer using **1.90** and a carbon paste electrode was functionalized with the prepared polymer. The prepared polymer-functionalized electrode was introduced to individual solutions of rare-earth ions (La^{3+}, Ce^{3+}, Sm^{3+}, Eu^{3+}, Gd^{3+}, or Dy^{3+}, 1×10^{-6} M, HCl, pH 7) containing Cu^{2+} (5×10^{-6} M, HCl, pH 7). To measure rare-earth ion selectivity to the system, oxidative stripping differential pulse voltammetry was used to detect the amount of Cu^{2+} displaced from the electrode. When a target ion outcompetes Cu^{2+}, the measured current for the Cu^{2+} peak decreases, and the results indicate that the peak decreased by ~20% when in competition with Eu^{3+} and did not decrease in the presence of any of the other tested rare-earth ions, indicating that the Eu^{3+}-imprinted polymer is selective for Eu^{3+}.[209] Among other preorganized ligands reported for rare-earth ion enrichment,

ion-imprinted polymers provide another tool to extract mid-lanthanide ions through preorganization of ligands.

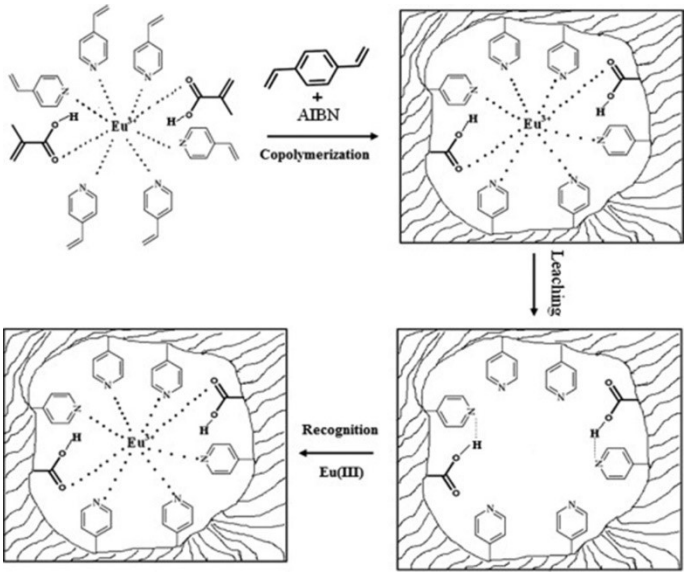

Figure 1.15. Visualization of the synthesis of a Eu^{3+}-imprinted polymer using vinyl pyridine and methacrylic acid as ligands, divinyl benzene as a polymerization agent, and 2,2′-azobisisobutyronitrile (AIBN) as an initiator. After Eu^{3+} is complexed with vinyl pyridine and methacrylic acid and polymerized with divinyl benzene, Eu^{3+} is removed using a leaching agent (**1.90**) resulting in the Eu^{3+}-imprinted polymer. Reprinted from Talanta, 106, Alizadeh, T.; Amjadi, S. Synthesis of Eu^{3+}-imprinted polymer and its application for indirect voltametric determination of europium, Pages 431–439, Copyright (2013), with permission from Elsevier.

Although ion-imprinted polymers address ligand features for rare-earth ion enrichment including donor atom polarizability, ligand denticity, pK_a range of binding sites, steric hindrance, bite angle, and preorganization of ligands, it is important to keep in mind other variable factors including matrix speciation and intraligand interactions when designing templated extraction solid-phase materials. The two examples of ion-imprinted polymers in this section for the enrichment of rare-earth ions give some insight into the much larger body of research using templated extraction solid-phase materials to enrich target ions. Readers are encouraged to consult other reviews for more information regarding ion-imprinted polymers.[227–230]

1.5 Polymers, solid supports, and hydrogels

Systems with well-defined coordination environments have been discussed with solid-phase materials exhibiting variable surface ligand distribution. There are many examples of rare-earth ion enrichment using polymers, solid supports, or hydrogels with variable surface ligand distribution and ill-defined coordination environments.[26–28,30–32,231–255] It is important to analyze how these solid supports impact solid–liquid extraction for the enrichment of rare-earth ions because commercially available solid supports provide a streamlined and relatively cost-effective approach compared to the solid-phase materials described in **Sections 1.2** and **1.3** of this chapter.

A study analyzed an amine–epoxy monolith polymerized from tetraethylenepentamine with an epoxide such as diepoxide, triepoxide, or tetraepoxide for their uptake of lanthanides (La^{3+}, Nd^{3+}, Eu^{3+}, Dy^{3+}, and Yb^{3+} ~0.14 mM each, HCl).[231] The monoliths feature amine (and possibly hydroxyl) binding sites and the monolith formed from triepoxide and tetraethylenepentamine precursors had selectivity for the heavy rare-earth ions, binding roughly double the amount of Yb^{3+} ions compared to La^{3+} at pH 2.5 and >90% uptake of all rare-earth ions at pH 6.4.[231] In this example, the full range of binding sites is not known, but the system is effective in the removal of rare-earth ions. Knowledge of the surface binding sites enables gauging of the general selection of ions based on donor atom polarizability and pK_a range of binding sites, but the full coordination sphere is often not elucidated to enable detailed insight into design analysis.

Even though polymers, solid supports, and hydrogels have variable coordination environments, they provide effective enrichment of rare-earth elements as seen in the provided example. A controllable ligand design feature in this case is the identity of the donor atoms on the precursor molecules that guide the general selectivity of the polymeric species for rare-earth ions, and subsequently, adjust the pK_a range of the donor atoms on the surface binding sites. Polymers, solid supports, and hydrogels impact the field of rare-earth element enrichment by extracting rare-earth ions from mixtures of other ions to streamline the process of rare-earth ion separation.

1.6 Conclusions and Future Outlook

The use of solid–liquid adsorption for the enrichment of rare-earth ions enables for adjustments in selectivity through the use of coordination chemistry in the design of ligands for solid-phase materials. Several actions may be taken towards the general goal of decreasing the number of steps needed to obtain pure rare-earth oxides including using a rare-earth-ion-specific polymer, solid support, or hydrogel as a preliminary step to extract rare-earth ions from other competing ions in solution, improving the selectivity of ligands used in solid-phase materials, and increasing the amount of surface-bound ligand for the extraction of rare-earth elements. General design considerations for improving rare-earth ion separation include adjusting ligand donor atom polarizability, ligand denticity, and the pK_a range of the binding sites on the ligand. Currently, the rare-earth ions can be readily separated into three main groups using solid–liquid adsorption methodologies: heavy, mid, and light rare-earth elements. To separate the heavy rare-earth elements, a ligand with a smaller donor atom polarizability such as oxygen can be used. From the two resulting fractions (heavy- and light- rare-earth ions) a preorganized ligand with binding cavity complimentary to the ionic radii of the mid-lanthanide ions can be used to create heavy, mid, and light rare-earth element fractions. From the three fractions of rare-earth ions, the future of solid–liquid adsorption would benefit from creating a single column or set of columns with solid-phase materials designed to fully separate the individual rare-earth ions, providing an organic solvent-free method to efficiently remove rare-earth ions from aqueous solutions.

1.7 Thesis Overview

Because of the demand for rare-earth elements from the rapidly improving efficiency of today's technology, there is a need for an efficient, reusable, and reliable method to enrich rare-earth elements from spent materials. Although liquid–liquid extraction provides and efficient and reliable method to enrich rare-earth elements, solid–liquid extraction provides an opportunity for reuse of materials, which increases the efficiency of enrichment and extraction. To compliment the methods discussed in **Chapter 1** for the solid–liquid extraction of rare-earth elements,

Chapter 2 describes the development of a pH-dependent solid-phase media for use in extraction of rare-earth elements from waste materials such as leachate from fly ash, and **Chapter 3** discusses further modifications to the ligand on the solid-phase media. **Chapter 4** delves into the use of one of the rare-earth elements, europium, in a computational study analyzing the luminescent effects of coordination chemistry of divalent europium.

In **Chapter 2**, a solid-phase media is described that binds and elutes rare-earth elements for extraction and enrichment. The synthesis and methodology for a solid-phase media that exhibits pH-dependent binding of aqueous rare-earth elements is found in **Chapter 2**. The media shows pH-dependent binding of Nd^{III} and retains efficiency over at least six cycles of binding and elution. Mixed solutions of rare-earth elements demonstrated a preference for mid and heavy rare-earth elements based on thermodynamic binding preferences of the ligand, and selectivity for rare-earth elements over iron and aluminum were observed with coal fly ash leachate. This method is expect this new recovery method to be a significant step towards aqueous-based extraction and enrichment of critically important rare-earth elements.

Chapter 3 describes my contributions towards the adjustment of the hydrophobic moieties in amphiphilic ligand used in **Chapter 2** to analyze the properties of grafting ligands to organically modified silica for the enrichment of rare-earth ions. The derivatives of diethylenetriamine pentaacetic acid (DTPA) feature oxygen and nitrogen donors to bind the rare-earth elements and hydrophobic moieties designed to bind to the solid support. By controlling the length of the hydrophobic moieties in the DTPA derivatives—butyl or hexyl moieties—greater noncovalent interactions were expected to occur with ligands featuring longer chains with the solid support. We found that the ligand featuring butyl moieties adsorbed less than the ligand featuring hexyl moieties. The ligand with butyl hydrophobic binding groups also showed increased wash-off at pH 5.5 compared to the ligand with hexyl hydrophobic binding groups, likely due to the differences in solubility between the two ligands in aqueous environments. The results presented in this chapter lend to the rational design of noncovalently bound solid-phase media.

In **Chapter 4**, the properties of the rare-earth element europium was explored through a computational study of the photophysical properties of two divalent europium cryptates. The calculations provided an explanation for the bright yellow luminescence of the Eu^{II}-containing octaaza-cryptate compared to the less intense blue luminescence of the structurally similar Eu^{II}-containing 2.2.2-cryptate. Calculations using time-dependent density functional theory with the B3PW91 functional, the Stuttgardt–Dresden relativistic core potential basis for europium, and SMD implicit solvation were used to compute the excitation and emission spectra of both complexes. Emission was also calculated with state-specific solvation. The results were compared with experimental luminescence data acquired in methanol. Natural-transition orbitals revealed similar spin-allowed transitions between the 4f and 5d orbitals on the europium ion in both complexes. For the 2.2.2-cryptate, the emissive state was hidden underneath the broad ultraviolet absorption; therefore, the state was not experimentally differentiated in the spectra, despite being present in the calculated spectra. For the octaaza-cryptate, the emissive state was observed as a separate band, shifted to lower energy than the broad ultraviolet absorption. Using ligand-field arguments, sharp differences in luminescence and the bathochromic shift of the emissive state were attributed to a greater splitting of the 5d orbitals of the octaaza-cryptate relative to the 2.2.2-cryptate.

Chapter 5 provides a summary of the contributions from **Chapters 2–4**, and the potential future directions of the research are discussed.

CHAPTER 2

Sorption of Rare-Earth Elements onto a Ligand-Associated Media for pH-Dependent Extraction and Recovery of Critical Materials

2.1 Permissions and Description of Author Contributions

This chapter was adapted with permission from Hovey, J. L.; Dardona, M.; Allen, M. J.; Dittrich, T. M. *Sep. Purif. Technol.* **2021**, *258*, 118061–118068. The studies described in this chapter were performed in collaboration with Mohammed Dardona, Dr. Timothy M. Dittrich, and Dr. Matthew J. Allen. In addition to writing and editing the manuscript, my contributions to the research included the synthesis and characterization of the bis(ethylhexyl)amido DTPA ligand, preparation of the solid-phase materials, pH versus loading experiments, and cycling pH experiments. Within Chapter 2, “we” and “our” refers to the authors of the manuscript Hovey, J. L.; Dardona, M.; Allen, M. J.; and Dittrich, T. M.

2.2 Introduction

In this chapter, the extraction of rare-earth elements from solutions of different pH values and from competing metal ions in leachate solutions for reuse using solid-phase materials is discussed. The studies done in this chapter aim to identify the selectivity of the solid-phase material and the pH-dependent binding of the system in aqueous solutions of metal ions. The ingenuity of the system is found in the pH-dependent nature of the ligand leading to control over the binding and elution of rare-earth ions, desirable for reuse of the system to create an organic solvent-free method of extracting rare-earth elements from spent materials.

The unique optical, magnetic, and catalytic properties of rare-earth elements make these elements critical to many industrial processes and technologies including cell phones, laptops, and electric vehicles.[1–13,17] Production of such technologies can be problematic and costly because of difficulties in separation and purification of the required rare-earth elements.[7,11,12,17] Global production of these elements relies on ores such as monazite,[4,7,11,256] bastnasite, [4,7,11,256] xenotime, [4,7,11] and ion-adsorption clays. [4,7,11,16,256]In 2018, China was responsible for >70% of the

world mine production of rare-earth elements.[257] Recent geopolitical issues have increased interest in recovering these elements from non-traditional sources such as electronic waste[4–7] and fly ash, waste produced from burning coal for electricity generation.[134,258–260] An economical procedure to extract rare-earth elements from such abundant by-products is highly desirable. The most common technique for separating rare-earth elements from the valueless gangue metals in an aqueous solution on a commercial scale is liquid–liquid (or solvent) extraction.[11,12,261–264] While solvent extraction has many advantages including efficiency and relatively small space requirements, there are large quantities of organic solvent waste that require additional costs and have potential environmental implications. Recent advances have been made towards using room-temperature molten salts known as ionic liquids,[8,265–268] for rare-earth element separations; however, these remain expensive and will require further developments to reduce organic waste streams.

In contrast to liquid–liquid extractions, solid–liquid separations remove the need for organic solvent in the separation process and have the potential to increase the efficiency and selectivity of extractions.[61,68,75,77,91,111,113,142,146,147,149,152,155,156,269–272] Many ligands have been used with solid–liquid extractions, but most efforts have focused on high capacity and selectivity at the expense of recovery, limiting the reusability of these materials.[147,152,270–272] One particularly interesting ligand used to overcome this limitation in solid–liquid extractions is diethylenetriaminepentaacetic acid (DTPA) covalently linked to solid supports.[142,146,149,156] These systems demonstrate pH-responsive binding to rare-earth elements. Moderately acidic solutions (pH ~0.5) are used to elute the rare-earth elements into concentrated solutions for further processing. The binding of DTPA covalently linked to solid supports has been shown to be influenced by the presence of surface functional groups remaining from the inability to perfectly functionalize solid supports or by instability of the support to pH ranges needed to elute bound rare-earth elements. [142,146,149,156] A study done by Karamalidis and coworkers analyzed grafting different lanthanide-chelating ligands onto resin beads using two equlibrium adsorption isotherms:

the Langmuir model to analyze monomolecular adsorption and the Freundlich model for multilayer adsorption.[149] They found that the Langmuir model best represented the binding sites with strong affinity for rare-earth elements at the ligand binding site, and the Freundlich model best described the weak interactions between the aminated resin and the rare-earth elements.[149] Although a multisite modeling approach was necessary to calculate the total rare-earth element uptake on their aminated resin, they determined that the Langmuir model could be used as an indicator for binding strength for DTPA and rare-earth elements because the binding of DTPA is much stronger than the resin to rare-earth elements.[149] The complexation thermodynamics of DTPA with rare-earth elements also were studied by Grimes and Nash who reported generally larger complexation constants of unmodified DTPA with the heavier rare-earth elements suggesting that DTPA-associated media would also show similar binding preference for the heavy rare-earth elements.[20] To overcome the limitations associated with covalent attachment of DTPA to solid supports, we hypothesized that modification of DTPA with hydrophobic groups would enable noncovalent interaction with a hydrophobic support to enable isolation of rare-earth elements. Here, we present hydrophobicly modified pH-dependent ligands on solid support for use in extractions of rare-earth elements.

To design a ligand-associated media for enrichment of rare-earth elements, the main ligand selection criteria were (1) the presence of hydrophobic moieties to attach the ligand to a hydrophobic solid support, (2) the presence of pH-sensitive moieties to control sorption of aqueous metal species, and (3) selectivity for the more valuable mid and heavy rare-earth elements over competing metals with lower value such as lanthanum, cerium, iron, and aluminum. In addition to the wide use of DTPA in lanthanide separations chemistry, we were also inspired by the rich history of Gd^{III}DTPA as a contrast agent for magnetic resonance imaging because it dissociates rapidly upon lowering pH.[273–275] Notably, DTPA has acid dissociation constants (pK_a 2.00–10.48)[20] that suggest effective dissociation of rare-earth elements is possible if binding occurs at a higher pH than elution. Because the rare earths can precipitate above ~pH 5.5, we

expected a functional pH range to be below pH 5. To interact with both solid support and metals, bis(ethyhexyl)amido DTPA, a pH-sensitive multidentate chelator (**Figure 2.1**), was selected because of its ability to bind rare-earth elements effectively and also to release them in a reasonable pH range (pH 1–5).

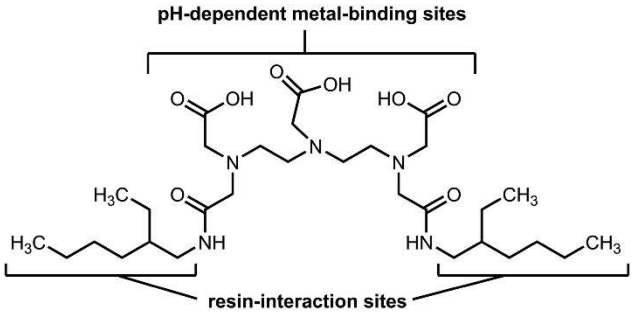

Figure 2.1. Structure and design features of bis(ethylhexyl)amido DTPA.

For solid–liquid extraction, the choice of solid support is critically important. Swellable organically modified silica was chosen as the solid support because it has a high surface area, a high capacity for organics, and features hydrophobic ethylbenzyl silane groups that are ideal for interaction with aliphatic regions of adsorbed ligands.[276–278] DTPA was synthetically modified to include two hydrophobic ethylhexyl groups needed to anchor the ligand to the media through hydrophobic interactions,[279,280] leaving three carboxylic groups to drive pH-responsive metal binding. A 20% (wt/wt) media was synthesized by adding a methanolic solution of ligand to the organosilica, removing solvent using a centrifuge vacuum system, rinsing with purified water, and drying the resulting media under reduced pressure. Aqueous metal ion sorption was tested in batch experiments. Once metals bind to the ligand-associated media, they can be eluted by lowering the pH to result in an enriched solution of rare-earth elements while the ligands remain attached to the surface. To the best of our knowledge, this is the first reported use of a hydrophobic attachment mechanism to make a DTPA-associated media. These results are also the first report of synthesizing bis(ethylhexyl)amido DTPA (modified DTPA) for sorption applications.

2.3 Materials and Methods

2.3.1 Ligand Synthesis

Bis(ethylhexyl)amido diethylenetriaminepentaacetic acid was prepared following a published procedure.[281] Commercially available chemicals were of reagent-grade purity or better and were used without further purification unless otherwise noted. Ethylhexylamine and diethylenetriaminepentaacetic acid bis-anhydride were purchased from TCI Chemicals and used as purchased. Water was purified using a water purification system (ELGA PURELAB Ultra Mk2 high purity water, 18.2 MΩ•cm resistivity). A solution of ethylhexylamine (4.39 g, 0.0340 mol) in anhydrous dimethylformamide (50 mL) under an atmosphere of argon was heated to 70 °C. Diethylenetriaminepentaacetic acid bis-anhydride (6.02 g, 0.0168 mol) was added to the solution while stirring. The reaction was stirred for 4 h at 70 °C. Solvent was removed, and the resulting light-yellow oil was solidified by adding acetone (30 mL). The solid was recrystallized from boiling ethanol to yield 6.58 g (79%) of the desired product as a white microcrystalline solid.

2.3.2 Ligand Characterization Methods

To characterize the purity of products, ^{1}H-NMR and ^{13}C-NMR spectra were acquired (Agilent MR-400, 399.78 MHz for ^{1}H and 100.53 MHz for ^{13}C). Chemical shifts are reported relative to residual solvent signals (CD_3OD: ^{1}H δ 4.95, ^{13}C δ 49.15). NMR data are assumed to be first order, and the multiplicity is reported as “s” = singlet, “t” = triplet, and “m” = multiplet. Italicized elements are those that are responsible for the shifts. Correlation spectroscopy (COSY), distortionless enhancement by polarization transfer (DEPT), and heteronuclear multiple quantum coherence (HMQC) spectra were used to assign spectral peaks.

To characterize the identity of products, high-resolution mass spectrometry (HRMS, Waters LCT Premier Xe time-of-flight high-resolution mass spectrometer) was used in the Lumigen Instrument Center in the Department of Chemistry at Wayne State University. pH values were determined using a benchtop pH meter (Accumet AE150, FisherScientific). NMR and MS data for bis(ethylhexyl)amido DTPA are in agreement with reported values (**Figures 2.2** and

2.3).[281] ^{1}H NMR (400 MHz, CD_3OD): δ = 3.83 (s, 2H; CH_2CO_2), 3.50 (s, 4H; CH_2CO), 3.46 (s, 4H; CH_2CO), 3.40 (t, J = 6 Hz, 4H; NCH_2CH_2), 3.20–3.12 (m, 8H; NCH_2CH_2 and NCH_2CH), 1.56–1.46 (m, 2H; C*H*), 1.42–1.23 (m, 16H; CH_2), 0.98–0.86 (m, 12H; CH_3); ^{13}C NMR (100.53 MHz, CD_3OD): δ = 174.9, 173.0, 170.5, 58.9 (*C*H_2CO), 56.9 (*C*H_2CO), 56.4 (*C*H_2CO_2), 54.6 (N*C*H_2CH_2), 51.6 (*C*H_2), 43.6 (*C*H_2), 40.7 (*C*H), 32.2 (*C*H_2), 30.1 (*C*H_2), 25.3 (*C*H_2), 24.3 (*C*H_2), 14.6 (*C*H_3), 11.3 (*C*H_3). HRMS (*m/z*): $[M + Na]^+$ calcd. for $C_{30}H_{57}N_5O_8$, 638.4099; found, 638.4096.

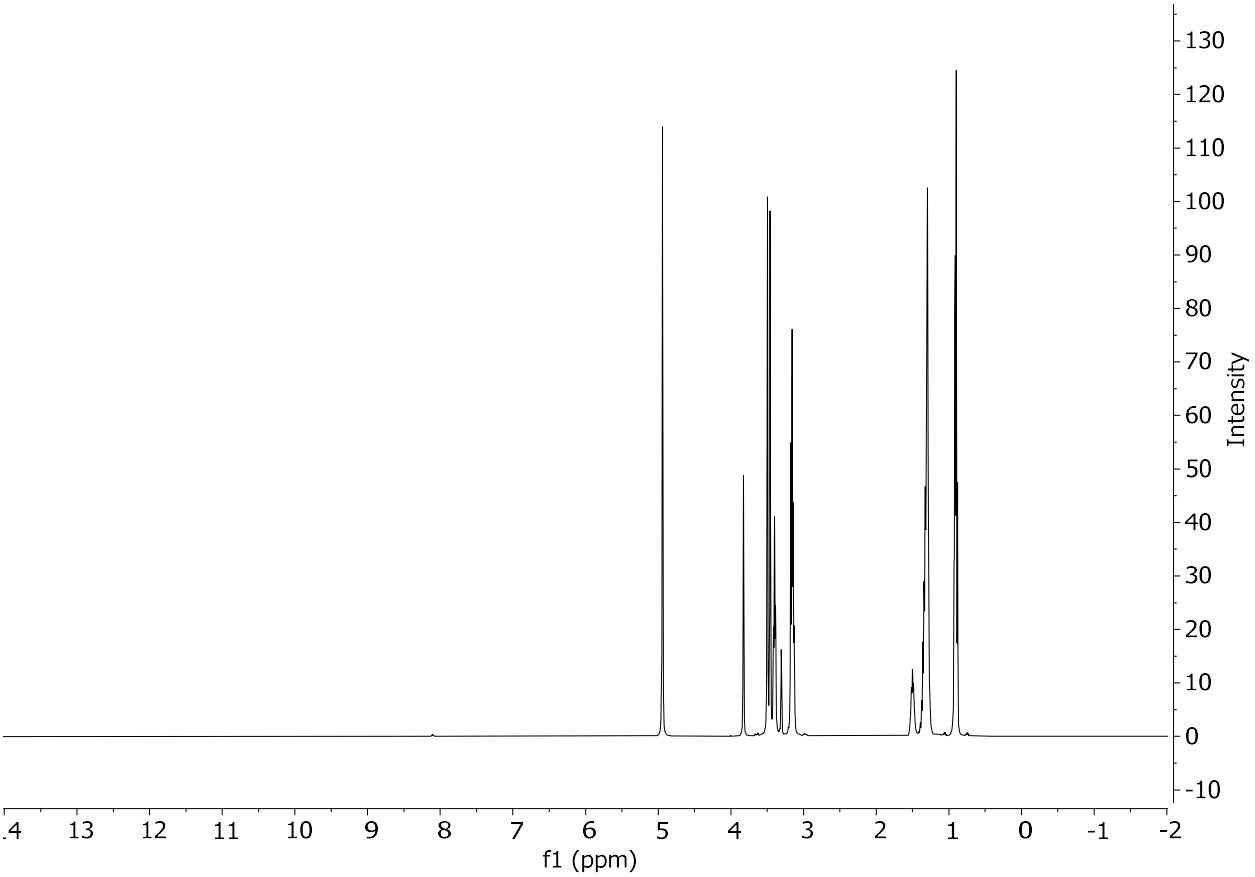

Figure 2.2. ^{1}H-NMR Spectrum of Bis(ethylhexyl)amido DTPA.

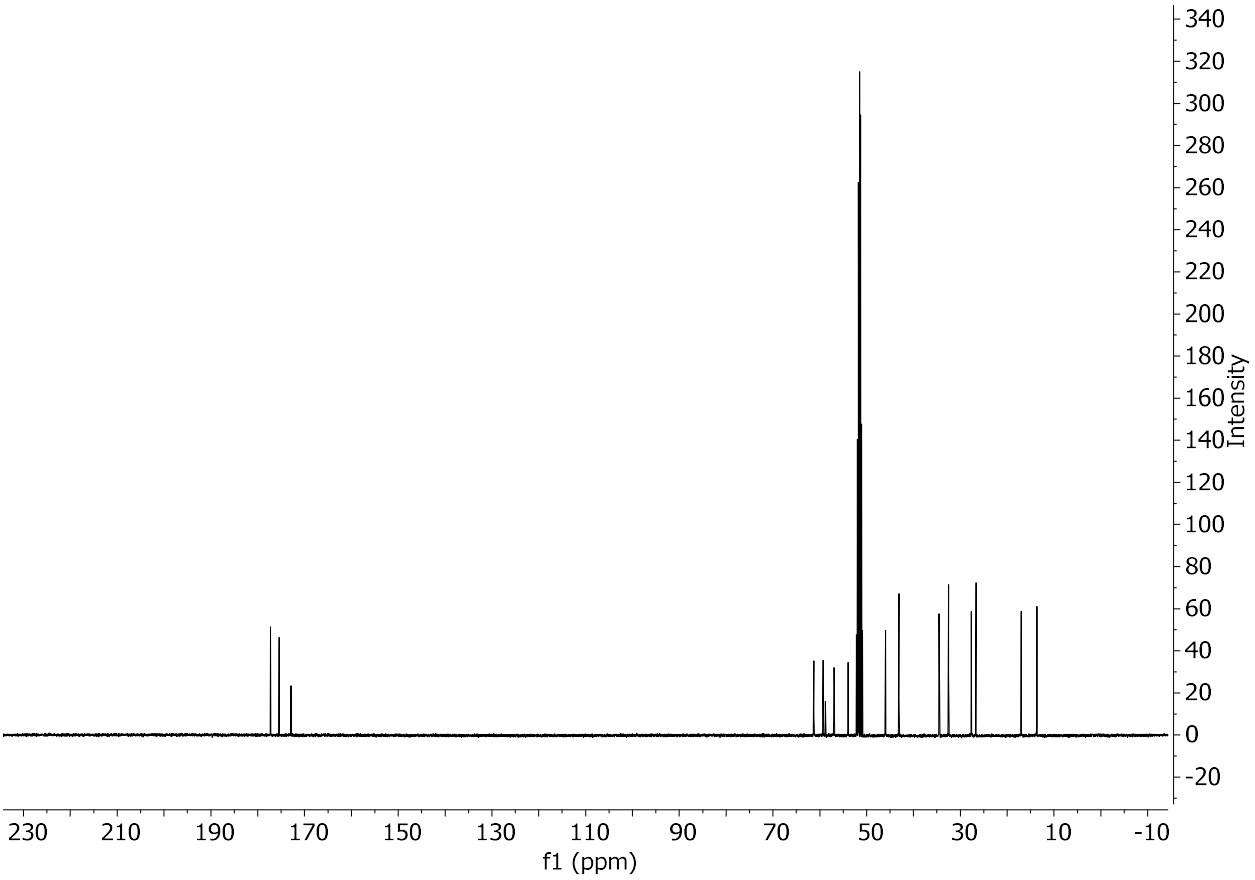

Figure 2.3. ^{13}C-NMR Spectrum of Bis(ethylhexyl)amido DTPA.

2.3.3 Sorbent Media Synthesis

The sorbent was synthesized by attaching the hydrophobic ethylhexyl chains of the ligand to the hydrophobic organosilica, leaving three carboxyl groups to interact with aqueous cations (**Figure 2.1**). A swellable organically modified silica, or organosilica, was purchased as the hydrophobic solid support (Osorb®, ABS Materials, Wooster, OH, lot #0035). Before modification, the organosilica had a reported surface area of >600 m^2/g (BET N_2 method), a pore volume of 0.65 mL/g, and an average pore size <6 nm.[277] SEM images were taken of the osorb material (**Figure 2.4**). Batches of organosilica media (4.03 ± 0.01 g) were loaded with bis(ethylhexyl)amido DTPA by adding solutions of bis(ethylhexyl)amido DTPA (50 mL, 32.6 ± 0.1 mM) in methanol to the organosilica in 50 mL screw-top polypropylene centrifuge tubes. The suspensions were rotated at 19 revolutions per minute for 1 h at ambient temperature. Methanol was removed

(Vacufuge Concentrator 5301) at 45 °C for approximately 3 h to visible dryness. Portions of purified water (3 × 40 mL) were used to rinse the media. The ligand-associated media was filtered using a Buchner funnel, filter paper (Qualitative 90 mm, Whatman), and water-aspiration vacuum filtration. The media was returned to the vial and residual solvent was removed under reduced pressure.

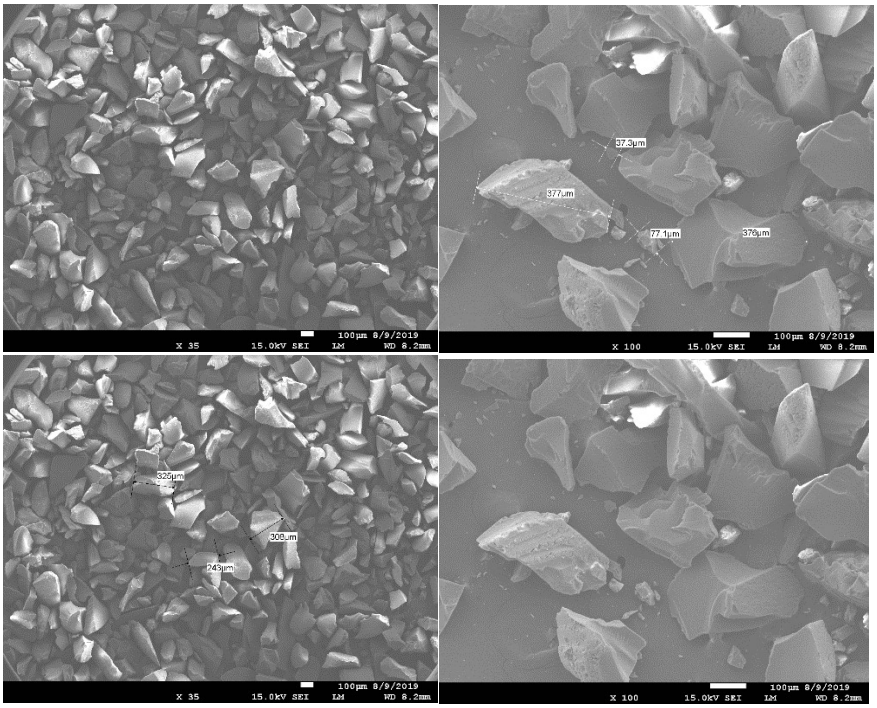

Figure 2.4. SEM images of unmodified media. SEM images were taken using JEOL JSM 7600F (JEOL, USA), magnification of 35× and 100×. The voltage was 15 kV at low vacuum. Samples were sputter coated with gold, the current was 60 mA for 30 seconds then the images were acquired.

We made ~25 g of ligand-associated media by attaching bis(ethylhexyl)amido DTPA (5 g dissolved in methanol) to organosilica (20 g) in batches of 5–7 grams [for example, bis(ethylhexyl)amido DTPA (1 g) + organosilica (4 g)]. This procedure resulted in 20% (wt/wt) loading of bis(ethylhexyl)amido DTPA on the organosilica media that was used in all of the sorption experiments presented here. The media was a darker yellow than the unmodified

organosilica. The dried media also had good handling properties for transferring between vials and did not clump or have static issues.

2.3.4 16-Element Competition Studies

Solutions of all 16 naturally occurring rare-earth elements (Sc, Y, and the lanthanides minus Pm) were prepared by diluting a standard solution [250 mL, ICP–MS-B in nitric acid (2%, aqueous), each of the 16 rare-earth elements (10 ppm), High Purity Standards] into a 500 mL volumetric flask and diluting to the mark with purified water resulting in 80 ppm total concentration of rare-earth elements. The 16-element competition experiments were conducted with 80 ppm total rare-earth element concentration (5 ppm × 16 elements) to interpret competition between individual elements in a lower concentration range than the proof-of-concept experiments. The pH of the resulting solution was 0.9 and was used as the low pH point for the experiment. The pH of a separate sample of rare-earth element solution (80 ppm) was adjusted to pH 3.3 using NaOH (5 M, VWR). For each sample, prepared rare-earth element solutions (40 mL) were pipetted into preweighed ligand-associated media (104 ± 2 mg) in 50 mL screw-cap polypropylene centrifuge vials. Control samples used unmodified organosilica (104.6 ± 0.5 mg) as purchased. The sample vessels were capped and rotated at 5 revolutions per minute for 24 h. Dilutions for ICP–MS were prepared by filtering aliquots (500 µL) from the sample vessels into disposable glass test tubes using 1 mL polypropylene syringes and 0.2 µm nylon hydrophilic filters (Basix, 8mm, Fisher). Samples were filtered, diluted, and analyzed by ICP–MS as described above. All rare-earth element standards (12 points between 0.005 and 200 ppb) were prepared by diluting commercially available standard (170 ppm total rare-earth elements) with a solution of OmniTrace acid (2% nitric).

2.3.5 pH versus Loading experiments

Solutions of Nd^{III} (50 mL, 300 ppm) were prepared by pipetting 1.5 mL of Nd^{III} in aqueous nitric acid (4%, 10,000 ppm, High Purity Standards) into 50 mL screw-cap polypropylene centrifuge vials and diluting with purified water or 0.1 M acetate buffer (48.5 mL). A 300 ppm Nd^{III}

concentration was selected for initial proof-of-concept experiments to represent the anticipated upper range of total rare-earth element concentrations possible in acidic coal fly ash leachate. pH was adjusted using NaOH (0.5 M, Honeywell) or nitric acid (2% OmniTrace). Each reaction was begun by pipetting a prepared solution of Nd^{III} (40 mL) into preweighed ligand-associated media (253 ± 3 mg) in 50 mL screw-cap polypropylene centrifuge vials. The reaction vessels were rotated at 19 revolutions per minute for 1 h (Tube Revolver/Rotator, ThermoScientific). Serial dilutions for ICP–MS were prepared by filtering aliquots (500 µL) from the reaction vessel into disposable glass test tubes using plastic 1 mL syringes and 0.2 µm hydrophilic filters (4 mm, PFTE, Millex-LG). Filtered solutions (200 µL) were diluted with purified water (19.8 mL). From the diluted solutions, 500 µL was further diluted with a solution of OmniTrace acid (9.5 mL 2% nitric, 0.5% hydrochloric). All Nd^{III} standards (5 points between 5 and 200 ppb) were prepared by diluting commercially available standard (10,000 ppm Nd^{III}) with a solution of OmniTrace acid (2% nitric, 0.5% hydrochloric). ICP–MS measurements were performed in triplicate with independently prepared solutions, and the values are reported as the mean ± standard error of the mean of the independent measurements. Calibration curves can be seen in **Figure 2.5**.

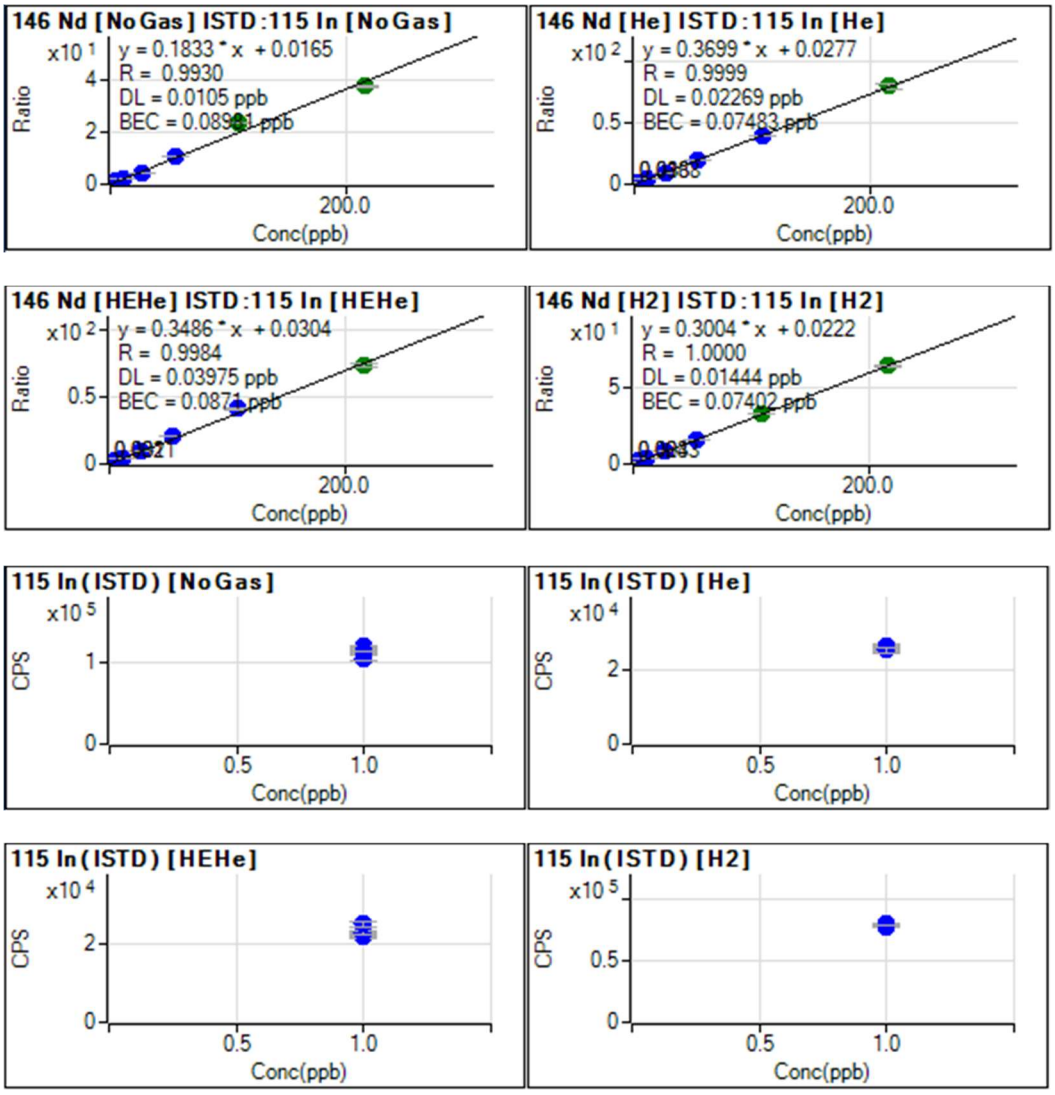

Figure 2.5. Inductively coupled plasma–mass spectrometry calibration of neodymium using ^{115}In as an internal standard. Nd^{III} curves are shown as an example of calibration curves, and all other metals showed similar accuracy.

2.3.6 Cycling pH experiments

Samples were prepared by mixing ligand-associated media (253 ± 2 mg) with Nd^{III} in 0.1 M acetate buffer (40 mL, 300 ppm) and adjusting the pH (3.3 ± 0.2) using concentrated nitric acid. Controls containing no media were prepared by adding the Nd^{III} solution (300 ppm, 40 mL) to a clean 50 mL polypropylene centrifuge tube. Tubes were rotated for 1 h, and the pH was measured and recorded. Aliquots (100 µL) were removed from each sample and filtered into disposable

glass test tubes using hydrophilic filters (0.2 µm, 4 mm PFTE, Millex-LG). Filtered aliquots (50 µL of each filtered sample) were diluted to 5 mL using purified water, and the solutions were further diluted (500 µL to 10 mL) using a solution of OmniTrace acid (9.5 mL 2% nitric, 0.5% hydrochloric). Concentrations of Nd^{III} were determined using ICP–MS. The pH of the samples was adjusted (1.5 ± 0.1) using concentrated HNO_3 (adding the same volume of nitric acid to the controls as to the samples), and samples were equilibrated for 20 min by rotating at 19 revolutions per minute. The pH was measured, and a sample was collected (100 µL), filtered, and diluted (1:200). The same process as described above for the first loading and strip cycle was repeated five additional times.

2.3.7 Rare-Earth Element Recovery from Fly Ash Leachate

Fly ash was sampled from a local coal-fired power plant, and acid digested by adding fly ash (5.0 ± 0.1 g) to HCl (aqueous, 20 mL, 4 M, OmniTrace) in a 50 mL polypropylene centrifuge tube and rotating for 22 h. The solution was centrifuged (30 min, 3500 rpm, IEC International Centrifuge, HT) and filtered (Quantitative Grade 41, Whatman), and the pH was raised to 3.0 by adding NaOH (aqueous, 8 M, Fisher). The resulting solution was centrifuged (30 min, 3500 rpm, IEC International Centrifuge, HT) and filtered a second time (Quantitative Grade 41, Whatman), and the resulting leachate was used in sorption experiments.

For each sample, prepared leachate solutions (10 mL) were added to preweighed ligand-associated media (51.5 ± 0.4 mg) in 50 mL screw-cap polypropylene centrifuge vials. Control samples used organosilica (51.6 ± 0.5 mg) as purchased. The sample vessels were capped and rotated at 5 revolutions per minute for 24 h. Dilutions for ICP–MS analysis were prepared by filtering aliquots (500 µL) from the sample vessels into disposable glass test tubes using 3 mL polypropylene syringes and 0.2 µm nylon hydrophilic filters (Basix, 13 mm, Fisher). The nickel and rare-earth element solutions were diluted from the filtered aliquots (10 µL) with OmniTrace acid (9.99 mL, 2% nitric). Aluminum and iron samples were further diluted: 1 mL was diluted with a solution of OmniTrace acid (9 mL, 2% nitric) and the diluted solutions (1 mL) were diluted with a solution of OmniTrace acid (9 mL, 2% nitric). The calibration curve (11 points between 0.005

and 200 ppb) was prepared by diluting several standards to a single standard in OmniTrace acid (1000 ppb, 10 mL, 2% nitric): multielement standard containing Al, As, Ba, Be, Cd, Ca, Ce, Cr, Co, Cu, Dy, Er, Eu, Gd, Ga, Ho, Fe, La, Pb, Lu, Mg, Mn, Nd, Ni, P, K, Pr, Rb, Sm, Se, Ag, Na, Sr, S, Tl, Th, Tm, U, V, Yb, Zn, Cs, B [IV-ICP–MS-71A in nitric acid (3%), each of the 43 elements listed (10 ppm each), High-Purity Standards], Sc (10,000 ppm, hydrochloric acid, 10%, High-Purity Standards), Tb in aqueous nitric acid solution (100 ± 0.6 ppm, nitric acid, 2%, High-Purity Standards), and Y (9.99 ± 0.06 ppm, nitric acid, 2%, High-Purity Standards).

2.4 Results and Discussion

2.4.1 16-Element Competitive Sorption Experiments

The complexation constants for DTPA are well established, but to the best of our knowledge, there has been no report of complexation constants with all of the rare-earth elements and the bis(ethylhexyl)amido DTPA analog. However, we garnered knowledge about our system from reports of the binding of DTPA with rare-earth elements.[20,149] A 16-element sorption competition experiment was designed as a screening test to determine whether or not bisethylhexylamido DTPA has the same complexation constants as aqueous DTPA. By comparing the rare-earth element uptake of our ligand-associated media to the 16 REE complexation constants reported for aqueous DTPA,[20] we can test if (1) the addition of two ethylhexyl chains to DTPA, and (2) the attachment of the chains to organosilica, do not change the sorption order and sorption magnitude of the 16 rare earth elements being studied.

Batch sorption experiments were conducted using solutions with 16 rare-earth elements at pH 3.3 with bis(ethylhexyl)amido DTPA-associated organosilica (**Figure 2.6**). Enough metal must be present to ensure that there was excess remaining in solution at equilibrium. We chose to use 10,000 ppm ICP–MS standard for our stock solution and sacrifice a small amount of error (<1%) introduced by the molarity variance between elements. There is a strong linear correlation (R^2 = 0.91) between the normalized amount of metal sorbed (mol sorbed/mol added) for

bis(ethylhexyl)amido DTPA-associated media and the reported equilibrium complexation constants for dissolved DTPA for a solution at pH 3.3.

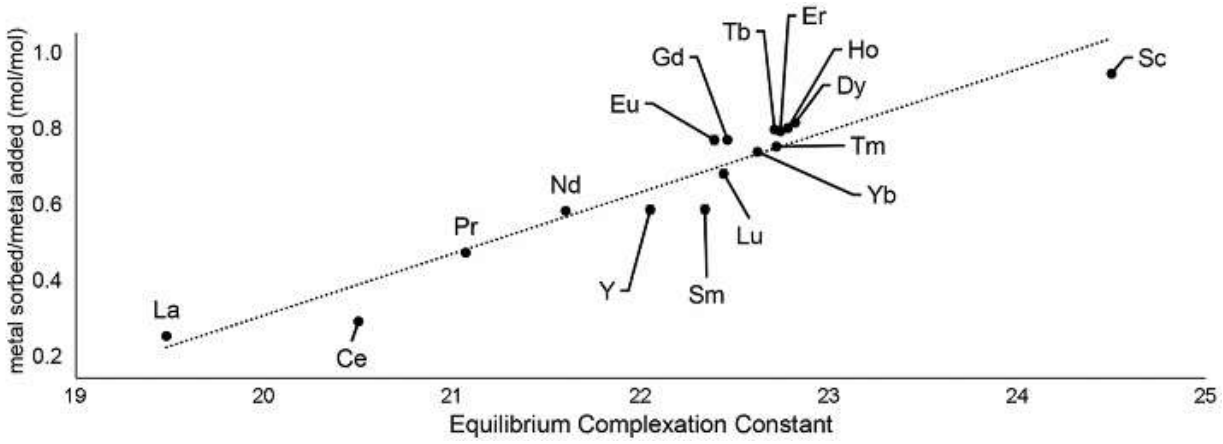

Figure 2.6. Metal sorbed (mol sorbed/mol added) for bis(ethylhexyl)amido DTPA-associated media versus the equilibrium stability constants for DTPA.[20,282] The dotted line represents linear trendline with $R^2 = 0.91$.

Because the bis(ethylhexyl)amido DTPA has three remaining carboxylic acid functional groups of the five present on DTPA (two carboxyl groups are sacrificed to attach the two hydrophobic chains), this correlation suggests the remaining three carboxyl groups are responsible for the complexation constants of DTPA. Although this method can only indirectly verify if a set of known complexation constants for a ligand are still mostly valid for the modified molecule (DTPA and bisethylhexylamido DTPA, in this case), this method can be a useful screening method for efficient decision making in custom media design. This proof-of-concept experiment aided in the thermodynamic characterization of our ligand-associated media, showing that the addition of two ethylhexyl chains to DTPA and the hydrophobic interaction with the organosilica does not change the sorption order of the 16 rare-earth elements being studied.

Batch sorption experiments were conducted using solutions with 16 rare-earth elements at pH 0.9 and 3.3 with both unmodified organosilica and bis(ethylhexyl)amido DTPA-associated organosilica (**Figure 2.7**). These pH values were selected to bracket the anticipated working

range of the ligand–rare-earth element system. The amount of metal sorbed was calculated using **Equation 1**,

$$C_b = \left(\frac{(C_i - C_u)V}{1{,}000(m)}\right) \quad \textbf{(1)}$$

where C_b is the amount of metal sorbed to the media (mol), C_i is the initial metal concentration in solution (ppm), C_u is the unbound metal in solution after sorption (ppm), m is the molar mass of the metal (g/mol), and V is the volume of metal solution (L). Control experiments with only metal and no media present were conducted for each experiment to monitor for precipitation and were used to determine C_i. The metal sorbed, C_b, was divided by the amount of ligand associated with the media. **Figure 2.7a** shows control experiments of unmodified media at both pH 0.9 and pH 3.3 and **Figure 2.7b** shows ligand-associated media binding rare-earth elements at both pH 0.9 and pH 3.3. The unmodified media shows little to no sorption of rare-earth elements at both high and low pH (**Figure 2.7a**). Ligand-associated media binds 6 and 130 times more rare-earth elements than unmodified media at pH 0.9 and 3.3, respectively, at these concentrations.

At pH 0.9, the sorption of all rare-earth elements excluding scandium is insignificant (**Figure 2.7b**). Metal sorption increases significantly at pH 3.3, where a total of 0.69 mol of rare-earth elements are extracted per mol of added metal (21 mg rare-earth elements per g of media). At pH 0.9, only 0.13 mol rare-earth elements per mol of added metal are extracted (1.6 mg metal per g media), with scandium accounting for 76% of the total bound metal at the lower pH. The solution at pH 3.3 shows notable selectivity of binding heavy over light rare-earth elements with lanthanum and cerium exhibiting the lowest sorption overall. Because only Sc binds to the ligand-associated media at pH 0.9, the selectivity for Sc presents an opportunity to remove Sc at a low pH with ligand-associated media prior to exposing solutions to ligand-associated media at higher pH.

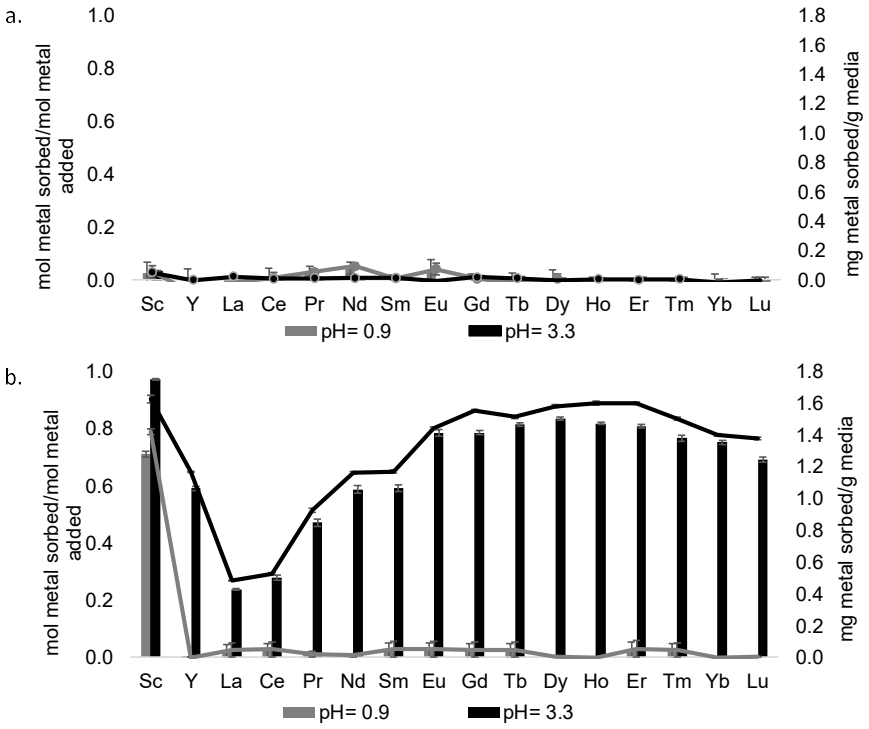

Figure 2.7. (a) Sorption of trivalent rare-earth elements to the unmodified media. (b) Sorption of trivalent rare-earth elements to the ligand-associated media. The ligand-associated media shows preference for binding the mid to heavy rare-earth elements. Metal sorbed is C_b from **Equation 1**. The bars for each element on the primary (left) y-axis represent metal sorbed per metal added (mol/mol): black bars at pH 3.3 and grey bars at pH 0.9. The lines for each element on the secondary (right) y-axis represent metal sorbed per media added (mg/g): black line at pH 3.3 and grey line at pH 0.9. Error bars indicate the standard error of the mean of three independently prepared samples.

2.4.2 pH-dependent Sorption and Cycling of Nd^{III}

Due to the critical nature of neodymium in many technologies,[283] we focused our cycling studies on Nd^{III}. The effective pH range of Nd^{III} sorption to the ligand-associated media was determined by measuring metal binding as a function of pH (**Figure 2.8**). Six solutions of Nd^{III} (300 ppm) in dilute nitric acid (<0.2% v/v) were prepared within a range of pH (0.8–5.4). The amount of metal sorbed after 1 h was calculated using Equation 1. The metal sorbed, C_b, was

divided by the amount of ligand associated with the ligand-associated media to yield the data in **Figure 2.8**.

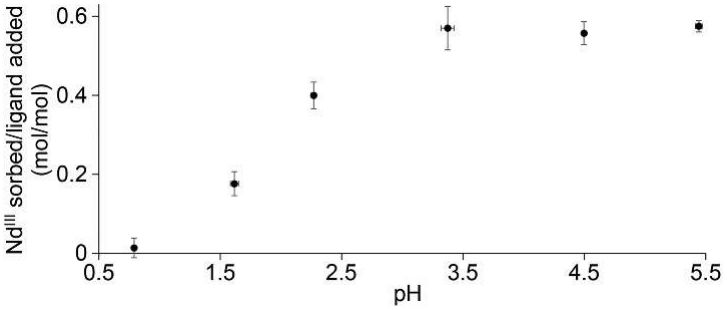

Figure 2.8. Nd^{III} sorption as a function of pH. Nd^{III} sorbed is C_b from Equation 1. Error bars indicate the standard error of the mean of three independently prepared samples.

We observed an insignificant amount of metal binding at pH 0.8 (<0.01 ± 0.03 mol Nd^{III} sorbed per mol of added ligand). As the pH increases, the ligand-associated media sorbed more metal per mole of added ligand, reaching a plateau at pH 3.4 ± 0.1 with 0.57 ± 0.06 mol Nd^{III} sorbed per mol of added ligand. This observation is consistent with the pH-dependence of DTPA complexation where the metal binding sites (carboxylic acids and amines) are largely protonated below pH 2. DTPA has a pK_{a_3} of 4.3;[20] therefore, the plateau in binding above pH 3.6 is reasonable. A plausible reason for the value of less than 1:1 metal/added ligand in **Figure 2.8** is the presence of inaccessible binding sites that are blocked by the solid support, as is often the case in solid-phase chemistry.[156]

A cycling experiment was performed to study the regeneration of our ligand-associated media. Nd^{III} solutions (300 ppm) were mixed with ligand-associated media in 0.1 M acetate buffer (pH 3.3) and cycled between pH 3.3 and 1.5 (**Figure 2.9**). To confirm that acetate does not impact Nd^{III} binding, experiments using acetate buffer versus no acetate buffer can be seen in **Figure 2.10**. As was observed in our pH-dependent metal binding experiments, more Nd^{III} binds at the higher pH than at the lower pH for each cycle. The overall mean binding at pH 3.3 is 0.51 ± 0.02 mol Nd^{III} per mol added ligand. The overall mean binding at pH 1.5 is 0.19 ± 0.01 mol Nd^{III} per mol added ligand. From this cycling experiment, a clear trend of binding Nd^{III} at a mildly acidic pH

and eluting Nd^{III} at lower pH is apparent. Furthermore, we did not observe a significant decrease in the binding efficiency between the first and sixth cycles, suggesting that the ligand-associated media has the potential for many rounds of reuse.

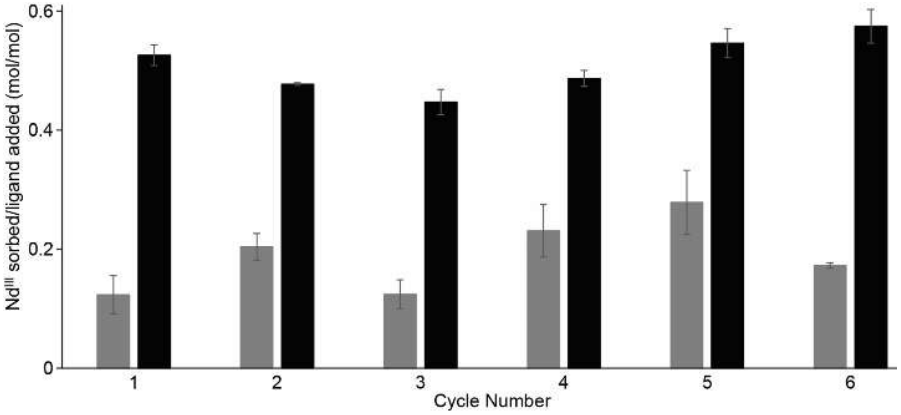

Figure 2.9. pH-cycling experiment with sorption and desorption of Nd^{III} from the organosilica-ligand system. Nd^{III} sorbed is C_b from Equation 1. Grey bars represent Nd^{III} bound between pH 1.5 and 1.6, and black bars represent Nd^{III} bound between pH 3.2 and 3.5. Error bars indicate the standard error of the mean of three independently prepared samples.

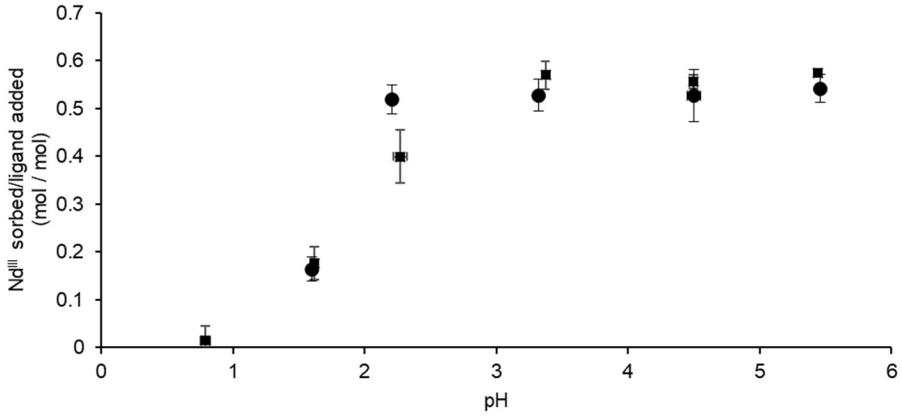

Figure 2.10: Comparison of acetate content in sorption experiments. Squares represent data from **Figure 2.8** where acetate (0.1 M) is present only in samples within pH range 3.6–5.6, and circles represent acetate (0.1 M) present in all solutions.

2.4.3 Proof-of-concept: Rare-earth element recovery from coal fly ash leachate

To evaluate the potential of using the DTPA-associated media for rare-earth element extraction from a more complex solution, we tested the ligand-associated media sorption performance with a coal fly ash digestion leachate in a nitric acid system raised to pH 3 for sorption experiments. In addition to coal fly ash being an abundant waste product with significant amounts of rare-earth elements,[133,257–260] fly ash leachates contain large concentrations of competing trivalent ions such as aluminum and iron. The concentrations of rare-earth elements and Al, Fe, and Ni in the fly ash leachate used in this study are shown in **Table 2.1**. The rare-earth elements and Ni were measured at concentrations between 0.06 and 4.2 ppm with much higher concentrations of Al (5,500 ppm), and Fe (1,800 ppm). Although not a main consideration for this paper, Ni is included as a point of comparison of the trivalent rare-earth elements with divalent metals.

Table 2.1: Metal concentrations of fly ash leachate measured by ICP–MS. Reported values are the mean concentration of three replicates.*

Element	Leachate Concentration (ppm)
Al	5500
Sc	0.82
Fe	1800
Ni	4.2
Y	4.2
La	4.1
Ce	8.2
Pr	1.0
Nd	3.7
Sm	0.78
Eu	0.19
Gd	0.82
Tb	0.13
Dy	0.76
Ho	0.15
Er	0.43
Tm	0.06
Yb	0.37
Lu	0.06

* The standard error of the mean was <5% for all measurements

Sorption experiments were performed to test the ability of both unmodified organosilica and DTPA-associated organosilica to sorb rare-earth elements (**Figure 2.11**) in the presence of iron and aluminum at several orders or magnitude higher than the rare-earth elements (~700- to 90,000-fold excess) (**Table 2.1**). At these concentrations, the unmodified organosilica only sorbed Al, Fe, and Sc, while all other rare-earth elements and nickel did not significantly sorb. These experiments demonstrate that sorption of rare-earth elements to ligand-associated media occurs as a result of the modification with hydrophobic bis(ethylhexyl)amido DTPA. Interestingly, these data also suggest that the unmodified organosilica could be used as a means to pretreat samples to remove iron or aluminum or to select for scandium among the other rare-earth elements at these concentrations.

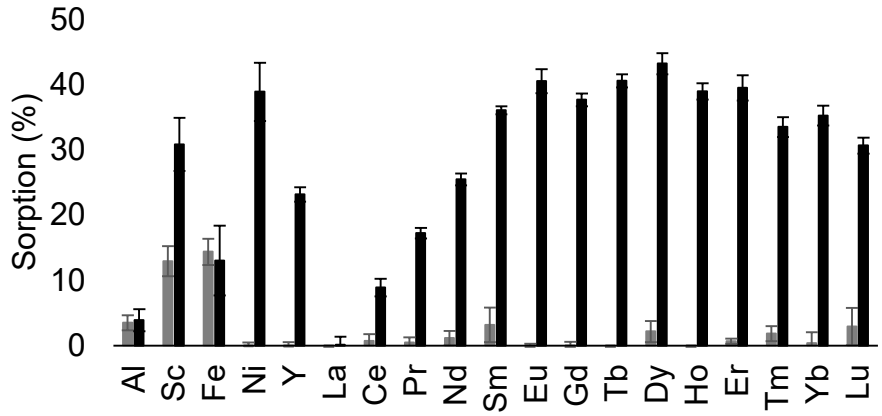

Figure 2.11. Metal sorption from fly ash leachate solutions at pH 3.0. Grey bars for each element represent percent metal extracted with unmodified media at pH 3.0, and black bars for each element represent metal extracted with the ligand-associated media. Error bars represent the standard error of the mean of three independently prepared samples.

Fly ash leachate was treated with our ligand-associated media using the same procedure as the 16-element experiments described above. The ligand-associated media showed a sorption preference toward mid and heavy rare-earth elements (**Figure 2.12**), even in the presence of large concentrations of Al and Fe. There is a strong linear correlation (R^2 = 0.94) between the normalized amount of metal sorbed (mol sorbed/mol added) for bisethylhexylamido DTPA-

associated media and the reported equilibrium complexation constants for dissolved DTPA for a pH 3.3 solution.[20,282]

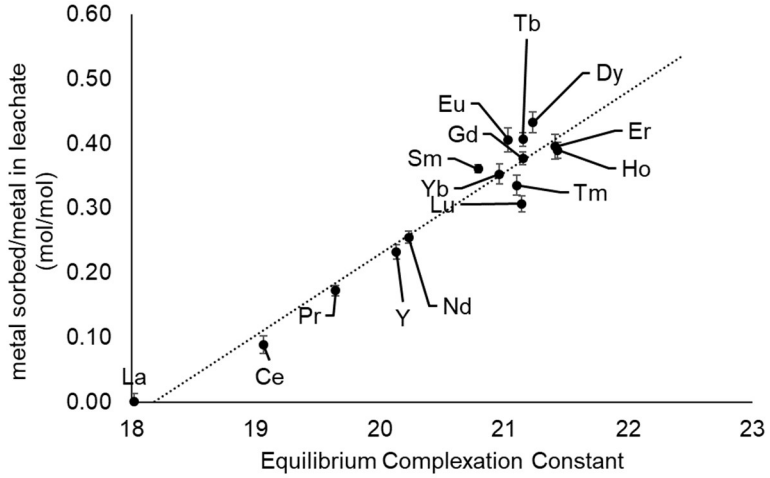

Figure 2.12. Metal sorbed (mol sorbed/mol in leachate) for bis(ethylhexyl)amido DTPA-associated media versus the lanthanide equilibrium stability constants for DTPA.[20,282] The dotted line represents linear trendline with $R^2 = 0.94$.

Notably, even though iron and aluminum were present at concentrations several orders of magnitude higher than the rare-earth elements in the leachate (**Table 2.1**), iron and aluminum competed poorly with the rare-earth elements. We attribute this unique selectivity to the speciation at low pH.[284] Nickel sorbed at a similar level to the mid and heavy rare-earth elements. These experiments demonstrate that the observed selectivity of rare-earth element binding is not altered when in competition with iron and aluminum; however, nickel competes with rare-earth elements for binding. These results indicate that a resin of this type would be more useful for coal fly ash leachate compared to recycled batteries that would contain larger amounts of nickel.

2.5 Conclusions

We have synthesized a new pH-dependent media by noncovalently adding hydrophobic moieties to DTPA and attaching them to organosilica. The ligand-associated media sorption capacity increases as a function of pH in the pH range 1–5, which is well-suited for metal recovery from acid leach solutions. We have also demonstrated that the ligand-associated media can be

reused for at least six cycles, binds rare-earth elements with selectivity for the heavier elements over cerium and lanthanum, and can extract rare-earth elements when in competition with other metals found in fly ash. The selectivity for heavy rare-earth elements over cerium and lanthanum is a key finding because of the critical importance of the elements. The technology described here is an inroad to organic solvent-free methods of recovering essential elements from a variety of sources.

CHAPTER 3

Adjusting Chain Length of Amphiphilic Ligands for the Preparation of Solid-Phase Media Designed to Enrich Rare-Earth Elements

3.1 Description of Author Contributions

The studies in this chapter were carried out in collaboration with Nicholas Peraino and Matthew J. Allen. My contributions to the studies described in this chapter include the synthesis and characterization of the bis(butyl)amido DTPA ligand and the bis(hexyl)amido DTPA ligand, preparation of the solid-phase materials, washes of the solid-phase materials, and preparation of calibration curves and samples for quantitative chromatography. Within Chapter 3, Nicholas Peraino carried out quantitative chromatography measurements.

3.2 Introduction

In this chapter, the hydrophobic interactions between ligands and hydrophobic organosilica were probed by adjusting the length of the hydrophobic chains on the ligands. The studies in this chapter aimed to characterize the interactions involved in the design of solid-phase media with noncovalently bound ligands. By characterizing both the initial adsorption of ligands and the adsorption of the ligands after washing the solid-phase media in different solvents, the aim of the studies described in this chapter was to establish ligand properties that provide efficient and reusable solid-phase media designed for the enrichment of rare-earth elements.

Rare-earth elements are crucial to the development of everyday technologies including displays, batteries, permanent magnets, catalysts in petroleum refineries, and other applications.[1–13,17] The rare-earth elements are among the most critically scarce elements with calculated consumption of rare-earth elements in the United States outweighing the calculated supply from mining and reused materials.[7] The paucity of local primary sources of rare-earth elements has shifted the focus from mining rare-earth elements to the enrichment of rare-earth elements in secondary sources such as recycled electronic waste,[4–7] coal fly ash,[133,258–260] or

spent nuclear fuel.[80,135,136] Some common methods used to enrich rare-earth elements include liquid–liquid extraction combined with fractional precipitation or solid–liquid extraction. Liquid–liquid extraction involves a biphasic system where the extractant, or ligand, is added to the organic phase and used to extract the rare-earth ions from the aqueous phase. Combined with fractional precipitation, where counterions are used to precipitate rare-earth ions from solution, liquid–liquid extraction produces purities of rare-earth oxides >99.9% after more than 50 rounds of separations.[7] Although liquid–liquid extraction is widely used commercially to provide rare-earth oxides, there is a significant amount of organic waste produced from many rounds of separations.[25] An organic-solvent-free method of rare-earth element enrichment is solid–liquid extraction, where solid-phase materials are comprised of solid supports with ligands that are either covalently or noncovalently associated with the solid support. A benefit of using solid–liquid extraction is the solid-phase material is designed to bind rare-earth ions from a single aqueous phase. In addition to omitting the use of organic solvent during extractions, the solid–liquid extraction method provides the opportunity to increase selectivity and efficiency of rare-earth element enrichment by modifying both the ligand and solid support. By adjusting the interactions between ligands and solid supports, ligands can be synthetically modified to enhance enrichment of rare-earth ions.

The strategy described in this chapter for rare-earth-element enrichment involves grafting ligands to organically modified silica for the enrichment of rare-earth ions in a pH-dependent fashion, and the specific study central to this chapter analyzes the effects of adjusting the interactions between ligands and solid support on the amount of metal adsorbed to the solid-phase media. Amphiphilic ligands (**3.1** and **3.2**) were selected for study because they are derivatives of diethylenetriamine pentaacetic acid (DTPA) were chosen with metal-binding moieties featuring oxygen and nitrogen donors and hydrophobic moieties to facilitate noncovalent interactions with hydrophobic solid supports (**Fig. 3.1**). Because DTPA is widely used for binding rare-earth elements, the thermodynamics and kinetics of binding are well-studied and aid in the

application for rare-earth element extraction.[20,282,142,146,149,156] One of the main reasons behind the choice of ligand was to enable binding of rare-earth ions in a pH-dependent fashion. DTPA features pK_a values that range from 2.00 to 10.5,[20] resulting in a trend where the rare-earth ions bind at a higher pH (pH = 3.3) and elute at a lower pH (pH = 1).[29] In the interest of reusability of the solid-phase media, it is important to choose a solid support and ligand that are stable at the pH values at which the metals are extracted and eluted. To address the impact of adjusting the ligand used in rare-earth-element enrichment, DTPA was synthetically modified with different hydrophobic moieties selected to study noncovalent interactions with hydrophobic organically modified silica.

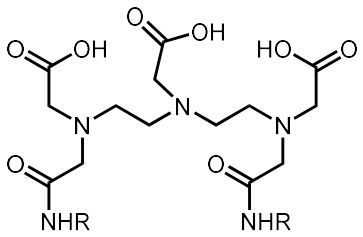

3.1: R = C_4H_9
3.2: R = C_6H_{13}

Figure 3.1. Amphiphilic ligands described in this chapter.

The focus of the study described in this chapter is to analyze the effects of adjusting the length of the hydrophobic moieties on ligand loading and wash off. Ligands **3.1** and **3.2** feature butyl and hexyl hydrophobic functional groups. The bis(ethylhexylamido) DTPA ligand is discussed in **Chapter 2** for rare-earth ion enrichment and the selection criteria for ligands **3.1** and **3.2** included synthetic feasibility and solubility.[29] Because the ligands were expected to interact with solid supports through hydrophobic interactions, the central hypothesis of this chapter is that ligands featuring longer chains will exhibit stronger noncovalent interactions to the solid support. Consequently, stronger ligand-resin interactions would be expected to shift equilibrium toward ligand-bound solid-phase material and result in more ligand bound to the solid support. Experimentally, this hypothesis was tested by measuring the amount of ligand on the solid-phase

media. Further, the material that has the most ligand interactions would also feature the most stable ligand-solid support interactions leading to the least amount of ligand washed off through reuse of the solid-phase material. Wash off was measured by exposing solid-phase media to different environments relevant to rare-earth element enrichment such as methanol, pH 5.5 water representative of a binding pH, and pH 0.9 water representative of an elution environment.

3.3 Materials and Methods

3.3.1. Ligand Synthesis

Ligands **3.1** and **3.2** were prepared by using procedures similar to those reported elsewhwere.[285,286] Commercially available chemicals were of reagent-grade purity or better and were used without further purification unless otherwise noted. NMR characterization was performed using ^{1}H- and ^{13}C-NMR spectroscopy (Agilent MR-400, 399.78 MHz for ^{1}H and 100.53 MHz for ^{13}C). Chemical shifts are reported relative to residual solvent signals (CD_3OD: ^{1}H δ 3.31, ^{13}C δ 49.15). NMR data are assumed to be first order, and the multiplicity is reported as “s” = singlet, “t” = triplet, and “m” = multiplet. Italicized elements are those that are responsible for the shifts. Correlation spectroscopy (COSY), distortionless enhancement by polarization transfer (DEPT), and heteronuclear multiple quantum coherence (HMQC) spectra were used to assign spectral peaks. The identity of products was characterized by high-resolution mass spectrometry (HRMS, Thermo Scientific LTQ Orbitrap XL high-resolution mass spectrometer). Water was purified using a water purification system (ELGA PURELAB Ultra Mk2 high purity water, 18.2 MΩ•cm resistivity). A swellable organically modified silica, or organosilica, was purchased as the hydrophobic solid support (Osorb®, ABS Materials, Wooster, OH, lot #0035). Samples were rotated using a Tube Revolver/Rotator, ThermoScientific. Quantitative chromatography was accomplished with a Waters Acquity UPLC.

General ligand synthesis procedure:

To a stirring solution of amine (butylamine: 4.12 g, 0.0563 mol, or hexylamine: 5.72 g, 0.0565 mol) in anhydrous dimethylformamide (100 mL) under an atmosphere of Ar at 70 °C was

added diethylenetriaminepentaacetic acid bis-anhydride (10.0 g, 0.0280 mol). The resulting reaction mixture was stirred for 4 h at 70 °C. Solvent was removed under reduced pressure, and the resulting solid was crystallized from boiling ethanol to yield **3.1**: 6.00 g (43%) or **3.2**: 12.1 g (77%) as a white microcrystalline solid.

N,*N*′-Bis(butylamido)diethylenetriaminetriacetic acid (**3.1**):

^{1}H NMR (399.78 MHz, CD_3OD) (**Figure 3.2**): δ = 3.82 (s, 2H; C*H*$_2$CO$_2$), 3.57–3.35 (m, 12H; C*H*$_2$CO, NC*H*$_2$CH$_2$), 3.28–3.19 (m, 4H, C*H*$_2$), 3.19–3.08 (m, 4H; NC*H*$_2$CH$_2$), 1.60–1.44 (m, 4H; C*H*$_2$), 1.44–1.26 (m, 4H; C*H*$_2$), 1.02–0.84 (m, 6H; C*H*$_3$); ^{13}C NMR (100.53 MHz, CD_3OD) (**Figure 3.3**): δ = 175.0, 173.0, 170.5, 58.9(*C*H$_2$CO), 56.7 (*C*H$_2$CO), 56.4 (*C*H$_2$CO$_2$), 54.8 (N*C*H$_2$*C*H$_2$), 51.6 (N*C*H$_2$*C*H$_2$), 40.3 (*C*H$_2$), 32.7 (*C*H$_2$), 21.3 (*C*H$_2$), 14.3 (*C*H$_3$). HRMS (*m*/*z*): [M + Na]$^{+}$ calcd. for $C_{22}H_{41}N_5O_8Na$, 526.2847; found, 526.2841.

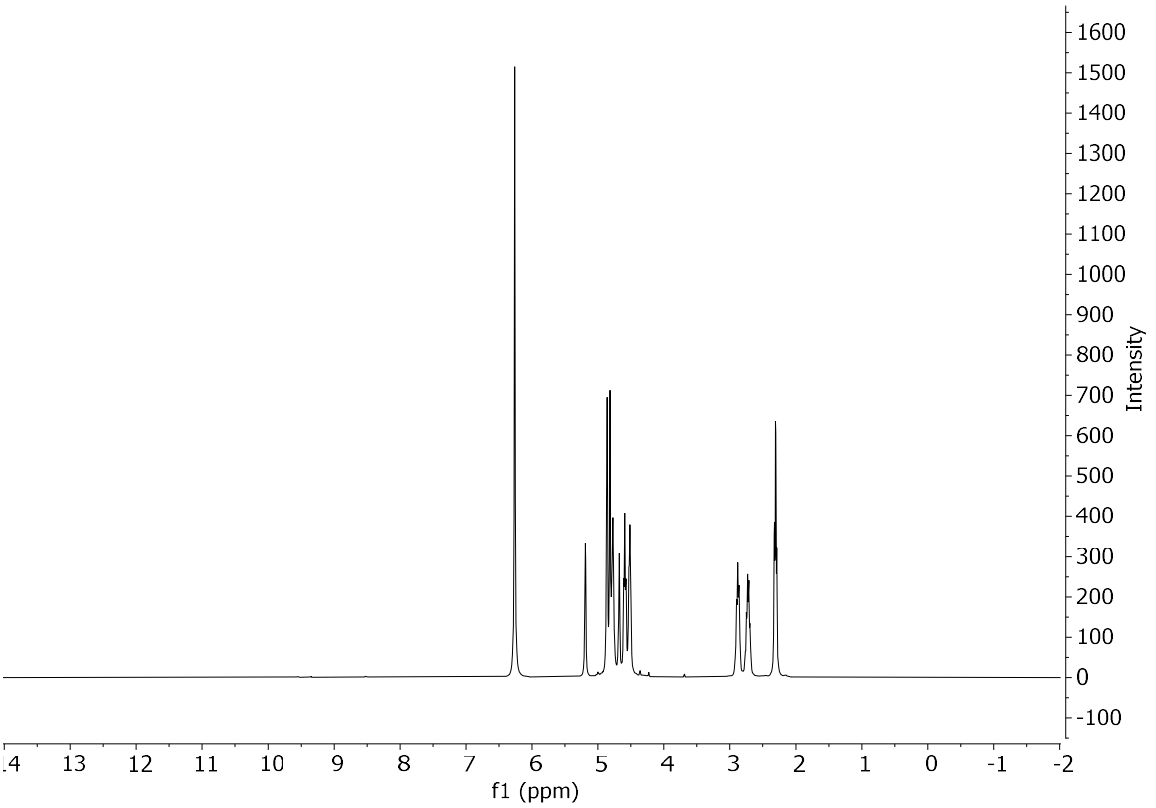

Figure 3.2. ^{1}H-NMR Spectrum of **3.1**.

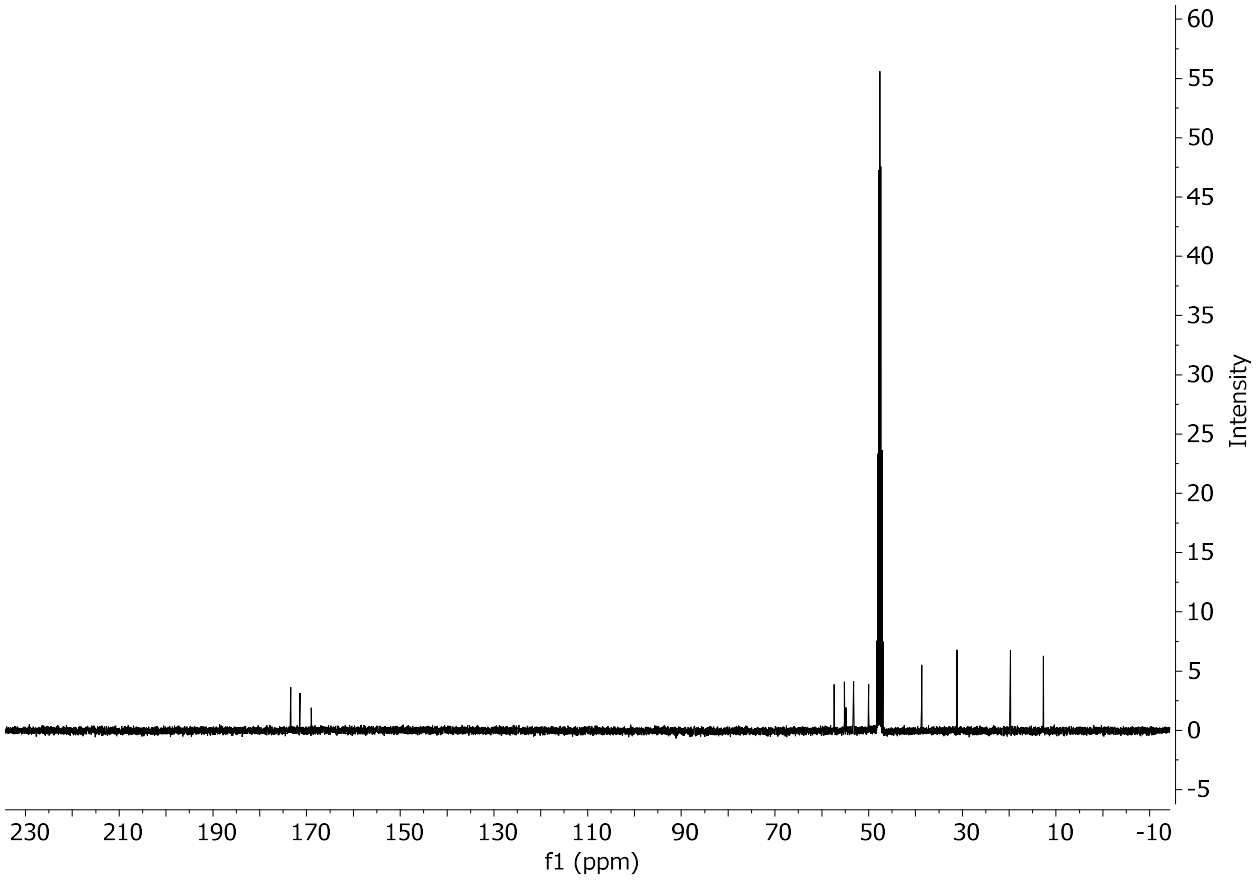

Figure 3.3. ^{13}C-NMR Spectrum of **3.1**.

N,*N*′-Bis(hexylamido)diethylenetriaminetriacetic acid (**3.2**):

^{1}H NMR (399.78 MHz, CD_3OD) (**Figure 3.4**): δ = 3.78 (s, 2H; CH_2CO_2), 3.45 (s, 4H; CH_2CO), 3.40 (s, 4H; CH_2CO), 3.36 (t, 4H, J = 6 Hz; NCH_2CH_2), 3.16 (t, 4H, *J* = 6 Hz; CH_2), 3.10 (t, 4H, *J* = 6 Hz; NCH_2CH_2), 1.53–1.42 (m, 4H; CH_2), 1.35–1.21 (m, 12H; CH_2), 0.90–0.81 (m, 6H; CH_3); ^{13}C NMR (100.53 MHz, CD_3OD) (**Figure 3.5**): δ = 174.9, 173.0, 170.5, 58.9 (*C*H_2CO), 56.7 (*C*H_2CO), 56.4 (*C*H_2CO_2), 54.8 (NCH_2*C*H_2), 51.5 (NCH_2*C*H_2), 40.6 (*C*H_2), 32.9 (*C*H_2), 30.6 (*C*H_2), 28.0 (*C*H_2), 23.8 (*C*H_2), 14.6 (*C*H_3). HRMS (*m*/*z*): $[M + Na]^+$ calcd. for $C_{26}H_{49}N_5O_8Na$, 582.3473; found, 582.3476.

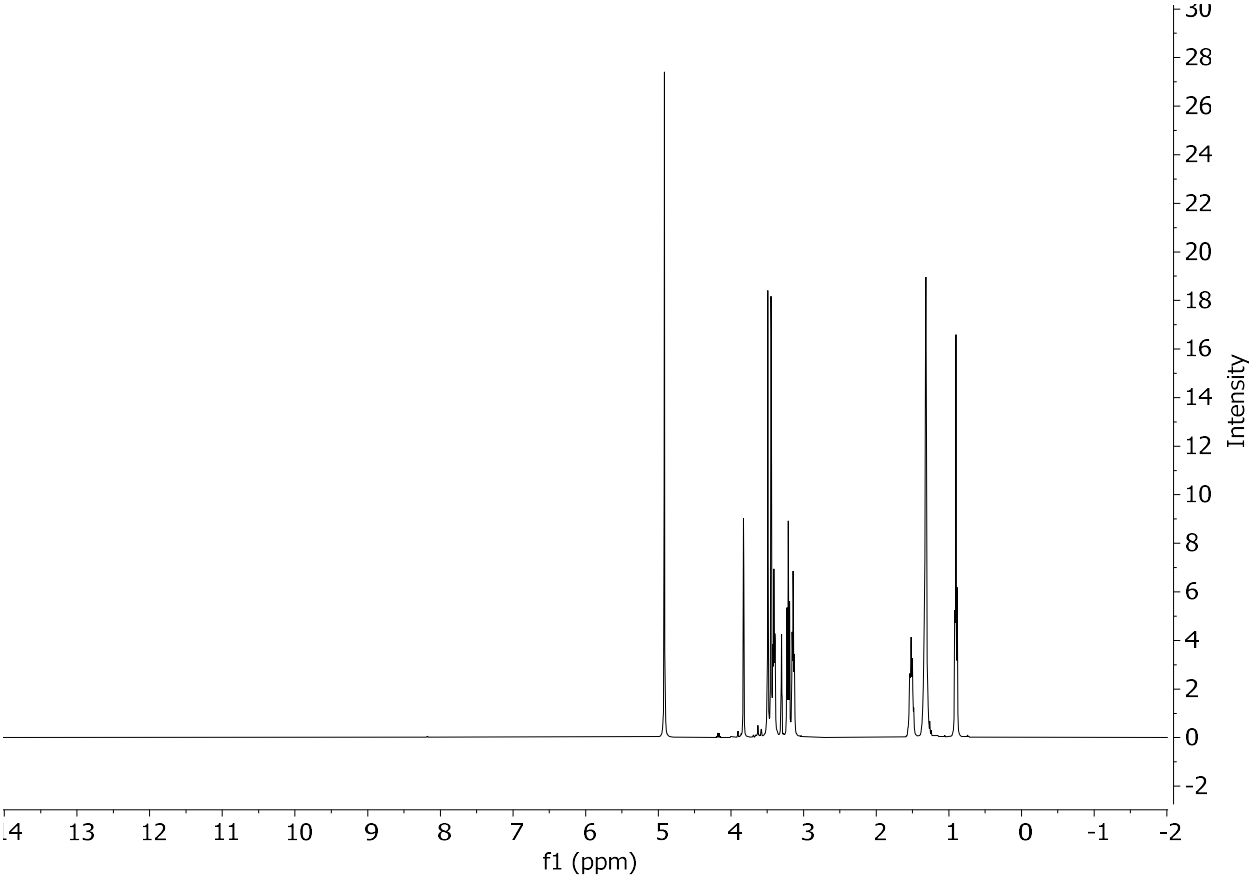

Figure 3.4. ^{1}H-NMR Spectrum of **3.2**.

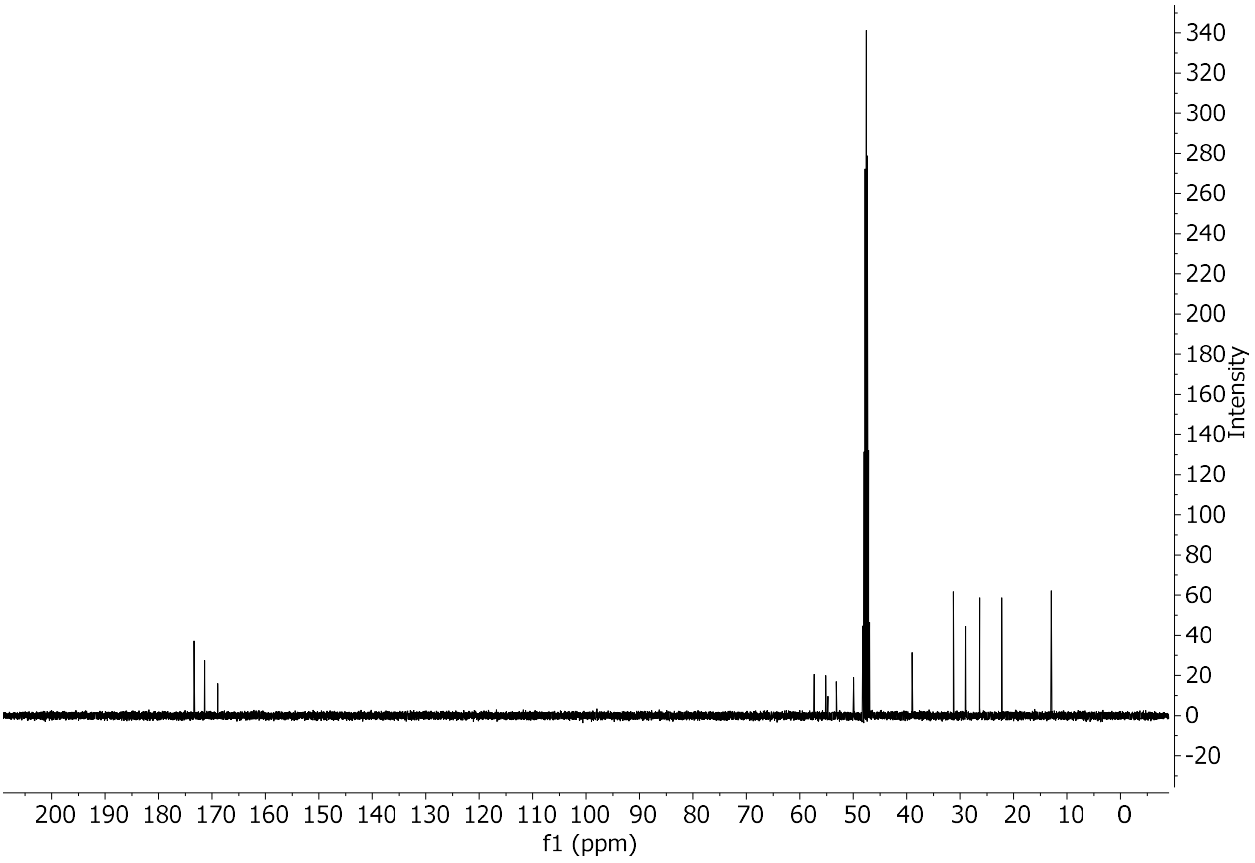

Figure 3.5. ^{13}C-NMR Spectrum of **3.2**.

3.3.2 Preparation of Ligand-Functionalized Media

All ligand-functionalized media were prepared at a concentration below which aggregation was expected based on reported critical micelle concentration of the hexadecyl bisamide derivative of DTPA.[287] Samples of organosilica media were loaded with ligand by adding a solution of **3.1** (500 mL, 0.516 ± 0.004 mM) or **3.2** (500 mL, 0.515 ± 0.003 mM) in methanol to preweighed organosilica (741 ± 1 mg) in a 1 L round bottom flask. The suspensions were rotated at 30 revolutions per minute for 1 h at ambient temperature. The samples of ligand-functionalized media were filtered using water-aspiration vacuum filtration with a Buchner funnel and filter paper (Qualitative 90 mm, Whatman) and filtrates were collected in 500 mL plastic screw-cap polypropylene containers. The media was returned to the vial and residual solvent was removed under reduced pressure. Dilutions for liquid-chromatography–mass spectrometry (LCMS)

analysis were prepared by diluting the collected water filtrates to 500 mL using a 500 mL volumetric flask with methanol. Aliquots (1 mL) were removed from each sample and filtered into disposable glass test tubes using hydrophilic filters (0.2 µm, 4 mm PFTE, Millex-LG). Filtered aliquots (50 µL of each filtered sample via glass syringe) were added to a 22 mL glass vial and diluted to 10 mL using a water/methanol solution (80/20 v/v, 9.95 mL). Each sample (80 µL) was further diluted using a water/methanol solution (80/20 v/v, 1.92 mL). The samples were filtered into 2 mL screw cap glass LCMS vials and sealed with a septum cap using hydrophilic filters (0.2 µm, 4 mm PFTE, Millex-LG). The calibration curve for **3.1** was prepared starting with a working solution of **3.1** (25 mL, 1000 ppm). The working solution (3 mL) was filtered into a disposable glass test tube using hydrophilic filters (0.2 µm, 4 mm PFTE, Millex-LG) and diluted (25 µL to 25 mL) using a 25 mL volumetric flask using water/methanol (80/20 v/v). The solution was further diluted using a 10 mL volumetric flask (1 mL to 10 mL) using water/methanol (80/20 v/v) and the resulting 100 ppb solution was used to prepare the calibration curve for **3.1** (5 points between 5 and 100 ppb) using water/methanol (80/20 v/v). The calibration curve for **3.2** was prepared starting with a working solution of **3.2** (250 mL, 100 ppm). The working solution (1 mL) was filtered into a disposable glass test tube using hydrophilic filters (0.2 µm, 4 mm PFTE, Millex-LG) and diluted using a 10 mL volumetric flask (1 mL to 10 mL vial pipet) using water/methanol (80/20 v/v). The resulting 100 ppb solution was used to prepare the calibration curve for **3.1** (5 points between 5 and 100 ppb) using water/methanol (80/20 v/v). Chromatography was performed with 10 µL injection of sample dissolved in water/methanol (80/20 v/v); elution with A: water containing formic acid (0.1%); B: acetonitrile containing formic acid (0.1%); a Phenomenex Aeris widepore C4 200 3.6 µm x 50 mm x 2.1 mm column; and a Thermo LTQ-XL operating in CID MS/MS mode with an isolation width of 1.5 Da scanning for **3.1** (504.3 @20CID to 215.13, 316.26 @ 4.13 min) and **3.2** (560.3 @20CID to 243.20, 344.29 at 8.46 min).

3.2.3 Washes of Ligand-Functionalized Media

The values of pH were determined using a benchtop pH meter (Accumet AE150, FisherScientific) or pH paper (MColorpHast, pH 0–14 universal indicator pH strips). For the pH 5.5 water wash, samples were prepared by mixing ligand-functionalized media prepared with **3.1** (252 ± 1 mg) or **3.2** (251 ± 1 mg) with water (8.5 mL, pH ~5–6 via pH strips). For the pH 0.9 wash, samples were prepared by mixing ligand-functionalized media prepared with **3.1** (251.4 ± 1.0 mg) or **3.2** (251.0 ± 0.4 mg) with acidic water (8.5 mL, HCl, pH 0.90 ± 0.01). For the methanol wash, samples were prepared by mixing ligand-functionalized media prepared with **3.1** (526.0 ± 0.9 mg) or **3.2** (526.3 ± 0.3 mg) with methanol (18 mL). The suspensions were rotated at 30 revolutions per minute for 1 h at ambient temperature and filtered using water-aspiration vacuum filtration with a Buchner funnel and filter paper (Qualitative 90 mm, Whatman). Filtrates were collected in 15 mL plastic screw-cap vials. The media was returned to the vial and residual solvent was removed under reduced pressure. Dilutions for LCMS analysis were by prepared by diluting the water filtrates to 25 mL using a 25 mL volumetric flask with purified water. Aliquots (2 mL) were removed from each sample and filtered into disposable glass test tubes using hydrophilic filters (0.2 µm, 4 mm PFTE, Millex-LG). Each filtered aliquot (1.6 mL of each filtered sample via pipet) was added to a 2 mL volumetric flask and diluted to 2 mL using methanol. The samples were added to 2 mL screw cap glass LCMS vials and sealed with septum caps. The collected methanol filtrates were each diluted to 25 mL using 25 mL volumetric flasks with methanol. Aliquots (1 mL) were removed from each sample and filtered into disposable glass test tubes using hydrophilic filters (0.2 µm, 4 mm PFTE, Millex-LG). Filtered aliquots (0.4 mL of each filtered sample) were added to a 4 mL screw cap vial using a glass syringe and diluted to 2 mL using purified water (1.6 mL via pipet). The resulting samples were filtered into 2 mL screw cap glass LCMS vials and sealed with septum caps. All diluted filtrate samples were quantified using the calibration curves described in Section 3.3.2.

3.4 Results and Discussion

3.4.1 Comparison of Amphiphalic Ligand Loadings

To measure the amount of ligand adsorbed to organosilica, techniques quantifying the prepared solid-phase media or the filtrate were performed. Attempts to quantify ligand loading on the solid-phase media by directly measuring the solid-phase media focused on the fact that the only source of nitrogen in the ligand-functionalized media is from the ligand. Thus, X-ray photoelectron spectroscopy (XPS) was used to analyze the relative percent nitrogen composition of the solid-phase media samples. The results from XPS analysis for both **3.1**-loaded media and **3.2**-loaded media showed results that were within the baseline and could not be fitted for quantification. Although the limit of detection for a nitrogen signal in XPS is ~0.1%, we determined that XPS was not compatible with quantification **3.1** or **3.2** on the solid-phase media. The next characterization technique used to measure percent nitrogen was combustion analysis. The values obtained for percent loading in the **3.1**-loaded media had deviation of ± 33% and the values obtained for percent loading in the **3.2**-loaded media had deviation of ± 51%. Again, nitrogen was observed in the samples above the limit of quantification, but after multiple attempts to troubleshoot the variability from the measured values, alternate characterization methods sought to obtain reliable results.

To quantify the amount of ligand bound to the resin, the amount of unbound ligand measured in the filtrate post-adsorption was measured using liquid-chromatography–mass spectrometry (LCMS). To prepare the solid-phase media, methanolic solutions of ligands **3.1** and **3.2** (0.51 mM) were rotated with organosilica for 1 h at room temperature. **3.1** resulted in a solid-phase media that had 6.0 ± 0.7% loading and **3.2** was measured to have 9.7 ± 0.7% loading (**Figure 3.6**). These data support the hypothesis that ligands featuring longer chains (**3.2**) exhibit stronger noncovalent interactions with the hydrophobic solid support than ligands featuring shorter chains (**3.1**), as evidenced by the difference in the amount of ligand bound to the solid support.

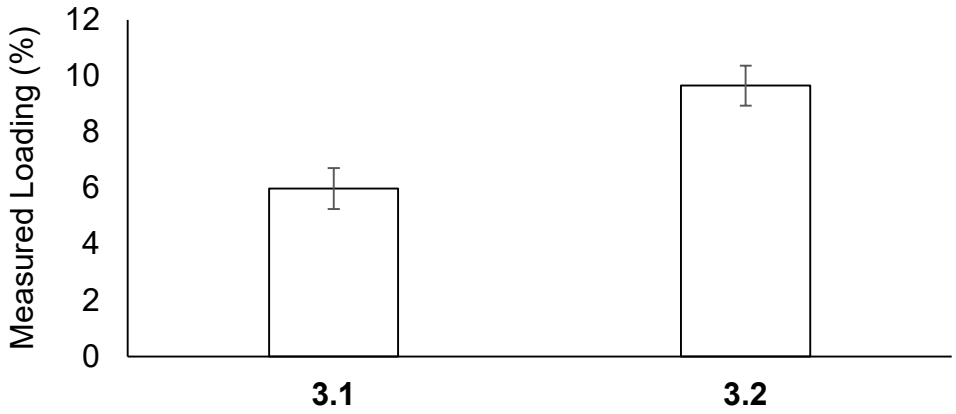

Figure 3.6. Ligand-functionalized media loadings where the ligand on the media is represented by the number below each set of data on the x-axis. Error bars for **3.1** indicate the standard error of the mean of five independently prepared samples, and error bars for **3.2** indicate the standard error of the mean of seven independently prepared samples.

3.4.2 Ligand-Functionalized Media Washes

Because one goal for solid-phase media is to reuse the material, it is important to characterize the stability of the ligand through changes in environment such as changes in pH to characterize the extent to which ligand washes off of the media. The prepared solid-phase media from Section 3.3.1 was used to analyze three different environments relevant to rare-earth element enrichment: methanol representative of ligand loading conditions; pH 5.5 water representative of the binding pH; and pH 0.9 water representative of the elution environment. To test wash off under these conditions, solid-phase media (525 mg) was added to methanol (18 mL), a second batch of solid-phase media (250 mg) was added to pH 5.5 purified water (8.5 mL), and a third batch of solid-phase media (250 mg) was added to pH 0.9 water adjusted with concentrated HCl (8.5 mL), and all samples were rotated for 1 hr at room temperature. Ligand **3.1** exhibited 0.02 ± 0.01% wash off in methanol, 0.28 ± 0.08% wash off in pH 5.5 water, and <0.01% wash off in pH 0.9 water (**Figure 3.7**). Ligand **3.2** exhibited 0.01% wash off in methanol, <0.01%

wash off in pH 5.5 water, and <0.01% wash off in pH 0.9 water (**Figure 3.7**). The increased wash-off of ligand **3.1** at pH 5.5 compared to ligand **3.2** is likely due to the solubility differences of **3.1** and **3.2**, where ligand **3.1** is more soluble in aqueous environments. Therefore, the data suggest that solid-phase media prepared with ligand **3.2** would be more stable over rounds of reuse compared to solid-phase media prepared with ligand **3.1**.

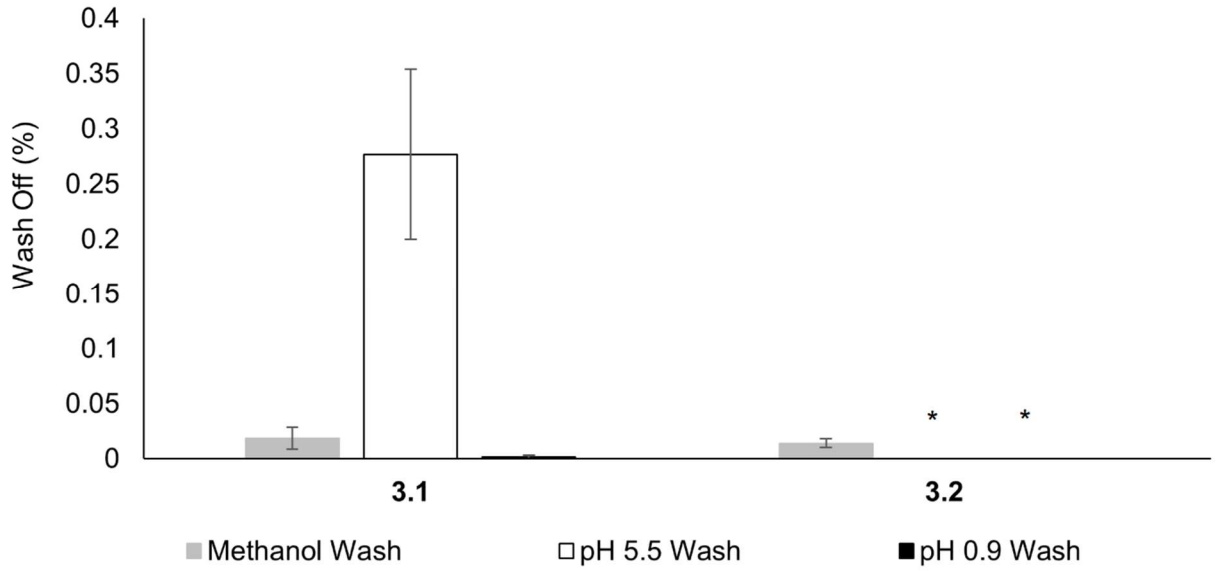

Figure 3.7. Washes of ligand-functionalized media. The ligand on the media is represented by the compound number below each set of data on the x-axis. Grey bars represent media washed in methanol; white bars represent media washed in pH 5.5 water; and black bars represent media washed in pH 0.9 water. Error bars indicate the standard error of the mean of three independently prepared samples for all data, except error bars for methanol wash for compound **3.1** represent the standard error of the mean of two independently prepared samples. A data point was removed by statistical analysis using a q test from the methanol wash for compound **3.1**. *Values measured for the pH 5.5 and pH 0.9 washes were below the limit of detection of LCMS (10 ppb).

3.5 Conclusions

Solid-phase materials were synthesized containing amphiphalic ligands differing in hydrophobic chain lengths were prepared to characterize the loading of the materials on

hydrophobic organically modified silica and to analyze the effects of increasing chain length on the stability of the solid-phase materials. The use of ligands **3.1** and **3.2**, support the hypothesis that ligands featuring longer chain lengths exhibit increased uptake onto the resin compared to ligands featuring shorter chain lengths. Future studies with ligands featuring longer hydrophobic chains are expected to show similar results, provided the solubility is compatible with the preparation of the solid-phase media. The data also show that solid-phase media prepared with ligand **3.1** exhibits ligand wash off at pH 5.5. Because of the stark differences in ligand wash off between ligands **3.1** and **3.2**, testing of ligands featuring longer chain lengths are expected to support many rounds of reuse and increase the efficiency of rare-earth element extraction. Future studies aim to test metal uptake by comparing the solid-phase media that exhibited the best uptake onto the solid support to the solid-phase media that had the least wash off.

CHAPTER 4

Luminescence Differences between Two Complexes of Divalent Europium

4.1 Permissions and Description of Author Contributions

This chapter was adapted with permission from Corbin, B. A.; Hovey, J. L.; Thapa, B.; Schlegel, H. B.; Allen, M. J. Luminescence Differences between Two Complexes of Divalent Europium. *J. Organomet. Chem.* **2018**, *857*, 88–93. The studies described in this chapter were performed in collaboration with Dr. Bishnu Thapa, Brooke A. Corbin, Dr. H. Bernhard Schlegel, and Dr. Matthew J. Allen. My contributions to the research included the UV–visible and fluorescence measurements for the two divalent europium complexes, optimization of the functional used in calculations using time-dependent density functional theory, and the calculations for the Eu^{II}-containing octaaza-cryptate. Within chapter 4, “we” and “our” refers to the authors of the manuscript Corbin, B. A.; Hovey, J. L.; Thapa, B.; Schlegel, H. B.; and Allen, M. J.

4.2 Introduction

In this chapter, studies analyzing one of the critically important rare-earth elements, europium, are described with respect to its use in photoredox chemistry and magnetic resonance imaging. Europium has been determined by the U.S. Department of Energy to be of critical importance because the demand of europium for fluorescent lighting, phosphors in the screens of electronic devices, and as a dopant for laser production outweighs the current accessible supply of europium.[2,7] The aforementioned uses of europium stem from the unique luminescent properties of trivalent europium featuring 4f–4f electronic transitions, but europium also has a redox-accessible divalent state where the luminescence is caused by a 5d–4f transition.

Divalent lanthanides have been a flourishing area of study, especially with the recent completion of the divalent series by Evans and co-workers.[288–309] Of the divalent lanthanides, europium is of specific interest due to the stability imparted by half-filled 4f orbitals making the divalent state relatively easy to access. Owing to the exceptional electronic stability and distinct magnetic properties, divalent europium has become prevalent in fields such as magnetic

resonance imaging,[274,301,306,310–313] photochemistry,[314,315] and lanthanide-activated phosphors.[303,316,317] Complexes of divalent europium, like **4.1** (**Figure 4.1**), generally absorb UV radiation, emit blue light, and have low quantum yields in solution[318] (0.1% quantum yield for **4.1** in 6:4 methanol/water [319]; ~9.3% quantum yield for **4.1** in methanol[320]). Recently, we reported a Eu^{II}-containing complex, **4.2**, that exhibits yellow luminescence with an exceptionally high quantum yield (26% in aqueous solution[300]). The stark difference in luminescence properties between **4.1** and **4.2** highlights the need to more thoroughly understand the energetics of **4.1** and **4.2** if new Eu-containing luminescent materials are to be designed and studied.

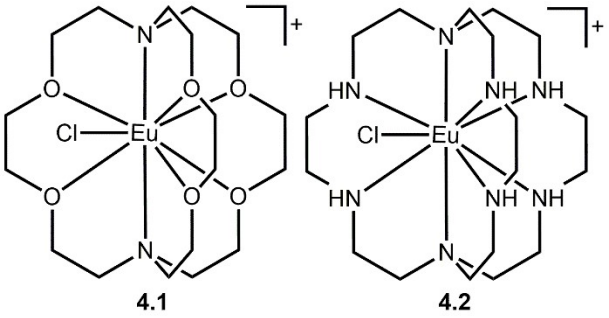

Figure 4.1. (left) Eu^{II}-containing 222-cryptate **4.1** and (right) Eu^{II}-containing octaaza-cryptate **4.2**.

Computational chemistry offers a unique way to investigate the molecular orbitals involved in electronic transitions and predict energies that can be applied to understanding ligand effects. There are few computational studies that report UV–visible spectral models for divalent lanthanide complexes in solution and examine excited states,[321–323] and to the best of our knowledge, calculated emission spectra of divalent europium complexes in solution have not been reported. This paucity is likely because a common computational method for lanthanides employs f-in-core pseudopotentials that enforce fixed $4f^n$ configurations.[324] While this enforcement minimizes convergence problems, it precludes studies of f–d luminescence. The lack of reported divalent europium emission studies could also be attributed to the anticipation that Eu^{II} complexes in solution have low quantum yields, similar to **1**.[318] However, given the bright luminescence of **4.2** and its excitation by visible light, along with other Eu^{II}-containing complexes demonstrating high

quantum yields,[325–328] the number of interesting systems that contain divalent europium that would benefit from computational analysis is expanding.

In the present study, we used density functional theory to examine the differences in luminescence between **4.1** and **4.2**. Our calculations reproduce the expected spin- and dipole-allowed transition from the Eu^{II} ground state ($4f^7$) to the excited state ($4f^65d^1$), and from excited state to ground state.[329] In these transitions, no spin flip is expected due to the strong exchange interaction of Eu^{II} (spin multiplicity = 8). We hypothesized, based on ligand field theory, the difference in electronic energies is likely due to the 5d orbitals that are influenced by the ligand field unlike the shielded 4f orbitals. In our computational study, we compare **4.1** and **4.2** because these complexes are structurally similar and have reported absorption, excitation, and emission spectra, with distinct excitation and emission characteristics.

4.2 Materials and Methods

4.2.1 UV–visible and fluorescence measurements

Commercially available chemicals were of reagent-grade purity or better and were used without further purification unless otherwise noted. Water was purified using a PURELAB Ultra Mk2 water purification system (ELGA). Anhydrous methanol was stored over activated molecular sieves (3 Å) and degassed under reduced pressure (0.2 Torr). The ligand for **4.1** (4,7,13,16,21,24-hexaoxa-1,10-diazabicyclo[8.8.8]hexacosane) was purchased from TCI chemicals. The ligand for **4.2** (1,4,7,10,13,16,21,24-octaazabicyclo[8.8.8]hexacosane) was prepared according to a reported procedure.[330,331] Concentrations of Eu were determined using energy-dispersive X-ray fluorescence spectroscopy with an EDX-7000 spectrometer (Shimadzu Scientific Instruments) at the Lumigen Instrument Center at Wayne State University. A calibration curve was used to determine the concentration of a stock solution of $EuCl_2$. The curve was created using the Eu fluorescence intensity at 5.485 keV for a 250–1000 ppm concentration range prepared using a standard solution of europium (Europium Standard for ICP 1000 mg/L Eu in nitric acid, Sigma) and dilutions with water.

Samples of **4.1** and **4.2** were complexed in a dry glove box under an atmosphere of N_2 in a 5 mL volumetric flask. Solutions of the complexes were transferred into quartz cuvettes with screw-top caps and sealed with electrical tape to maintain inert atmosphere. UV–visible spectra were recorded using a Shimadzu UVmini-1240 spectrophotometer. Emissions were recorded using a HORIBA Jobin Yvon Fluoromax–4 spectrophotometer. Slit widths of 1 and 0.5 nm were used for excitation and emission, respectively.

4.2.2 Computational Details

All calculations were carried out with the Gaussian 09 suite of programs.[332] Density-functional-theory (DFT) calculations employed the hybrid B3PW91 functional (optimized using energies and oscillator strengths outlined in **Table 4.1**),[333–335] the Stuttgardt–Dresden relativistic core potential (SDD)[336,337] basis set for europium, and the D95 basis set for the remaining elements[338]. Calculated structures were tested for self-consistent-field (SCF) stability[339,340]. Solvent effects were modeled using the SMD implicit solvation method[341] in methanol. The ground state geometries of both cryptates were optimized in solution starting from the reported crystal structures[300,312]. The absorption spectra were calculated with time-dependent density functional theory (TD-DFT, 80 states).[342–344] Spin-orbit effects broaden the 4f–5d transitions of Eu^{II} compounds by 6000 cm^{-1} or more[329] but were not taken into account in the present calculations. For the emission spectra, the lowest energy 4f–5d transition with the highest oscillator strength was chosen for optimization. Fluorescence energies were calculated with state-specific solvation[345,346] and the width of the Gaussian lineshape was adjusted to match experiment. Natural-transition-orbital[347] calculations were used to characterize the excitations. Molecular orbitals and spin densities were plotted with GaussView.[348]

Table 4.1: Optimization of the functional using experimental values for **4.1**.

Functional	Excitation (nm)	Emission (nm)	Oscillator Strength	Energy (kcal/mol)
Experimental	400	576	-	-
PBEPBE	616.01	-	0.0018	46.41395
B3PW91	427.49	582	0.0006	65.65336
ωB97XD	430.64	-	0.0017	66.39361
LC-BLYP	427.19	-	0.0020	83.49761

4.3 Results and Discussion

To augment the previously reported luminescence data for **4.1** and **4.2**,[300,319,320] we measured UV–visible and fluorescence spectra with similar concentrations (2–5 mM) in methanol at ambient temperature. Methanol was chosen as the solvent because the reported crystal structures of both **4.1** and **4.2** were obtained using crystals grown from methanol, and our calculations used the reported crystal structures as starting coordinates.[300,312] For **4.1**, our experimental data corresponded well to the reported spectra in methanol[320] and water[319]. We experimentally measured the absorbance maximum for **4.1** to be 259 nm (38,600 cm^{-1}) and the emission maximum to be 471 nm (21,200 cm^{-1}). For **4.2**, the reported absorption and emission experiments were run in pH 12 solutions of KOH, and the absorbance maximum was reported as 415 nm (24,100 cm^{-1}) with an emission maximum of 580 nm (17,200 cm^{-1}).[300] In methanol, we experimentally measured the absorbance maximum for **4.2** to be 400 nm (25,000 cm^{-1}) and the emission maximum to be 576 nm (17,400 cm^{-1}). Our experimental excitation and emission spectra in methanol differ from aqueous data by 4–15 nm,[300] suggesting that computations in methanol serve as good approximations for aqueous photophysical behaviors.

To calculate electronic properties of the divalent-europium-containing cryptates, we started by optimizing the ground-state structures of **4.1** and **4.2**. Although structurally comparable, the crystal structures have slightly different geometries: **4.1** has an eclipsed hula-hoop geometry and **4.2** has a distorted staggered hula-hoop geometry. Upon optimization with implicit solvation,

the structures show good agreement with the reported crystallographic data (**Tables 4.2** and **4.3**). For **4.1**, the calculated Eu^{II}–O bond lengths range from 2.750 to 2.843 Å compared to the experimental range of 2.659–2.707 Å, and the computed Eu^{II}–N bond lengths range from 2.936 to 3.084 Å compared to the experimental range of 2.838–2.859 Å. The Eu^{II}–Cl bond lengths for **4.1** computed and measured from crystallographic data are 2.962 and 2.837 Å, respectively. The overall trend for the bonds in **4.1** shows slightly longer computed bonds compared to crystallographically measured bond lengths, but the differences are in the range reported for the B3PW91 density functional and SDD basis set.[349] A similar lengthening is found for **4.2**, with the calculated Eu^{II}–N bond lengths ranging from 2.705 to 3.119 Å compared to the experimental values ranging from 2.675 to 2.958 Å. The calculated Eu^{II}–Cl bond for **4.2** is 3.286 Å, which is considerably longer than the bond length of 2.694 Å in the crystal structure.

Table 4.2: Bond lengths (Å) for **4.1** from crystallographic[312] and computational structures.

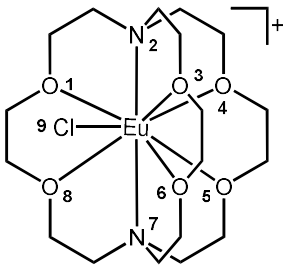

Complex	Eu–O_1	Eu–N_2	Eu–O_3	Eu–O_4	Eu–O_5	Eu–O_6	Eu–N_7	Eu–O_8	Eu–Cl_9
4.1$_{(crystallographic)}$*	2.681	2.838	2.659	2.707	2.701	2.678	2.859	2.686	2.837
4.1$_{(calculated, ground state)}$	2.810	2.936	2.750	2.772	2.843	2.832	3.084	2.784	2.962
4.1$_{(calculated, excited state)}$	2.683	2.806	2.735	2.690	2.768	2.833	3.037	2.767	2.924

Table 4.3: Bond lengths (Å) for **4.2** from crystallographic[300] and computational structures

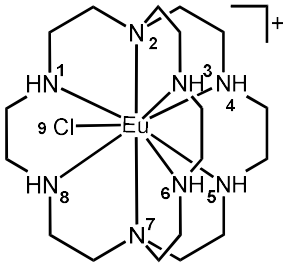

Complex	$Eu–N_1$	$Eu–N_2$	$Eu–N_3$	$Eu–N_4$	$Eu–N_5$	$Eu–N_6$	$Eu–N_7$	$Eu–N_8$	$Eu–Cl_9$
4.2$_{(crystallographic)}$*	2.895	2.845	2.795	2.696	2.675	2.958	2.922	2.774	2.964
4.2$_{(calculated, ground state)}$	2.933	2.923	2.835	2.725	2.720	3.072	3.005	2.806	3.293
4.2$_{(calculated, excited state)}$	2.640	2.757	2.679	2.653	2.655	2.640	2.758	2.682	4.537

Computational studies of lanthanide luminescence require careful consideration of how spin multiplicity is affected by excitation. For divalent europium in the ground state, the spin multiplicity is eight due to the seven unpaired 4f electrons. Because of strong exchange interactions, the 5d electron in the excited state aligns with the total spin vector, thus simplifying calculations and leaving the spin multiplicity of the system unchanged throughout the original optimization and subsequent calculations. Spin-density plots show that the seven unpaired electrons in the ground states of both **4.1** and **4.2** are localized on the metal (**Figure 4.2**).

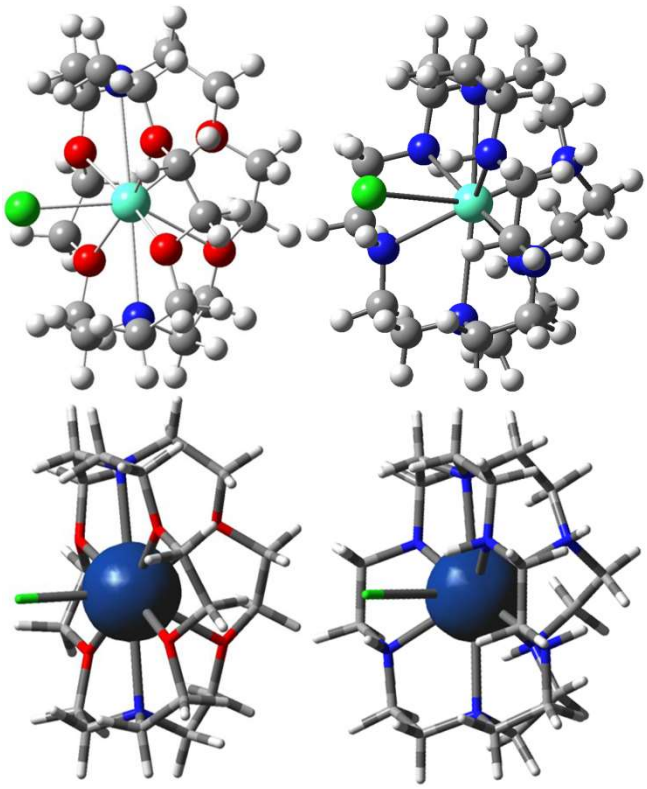

Figure 4.2. B3PW91/SDD optimized ground-state structures in SMD methanol: (top left) optimized structure of **4.1**; (top right) optimized structure of **4.2**; (bottom left) spin density (blue) mapped onto **4.1**; (bottom right) spin density (blue) mapped onto **4.2**.

The broad luminescence curves present in all spectra (**Figure 4.3**) are indicative of a Eu^{II}-containing complex, in part due to spin-orbit effects for the 4f–5d transitions. The TD-DFT calculated absorption spectrum for **4.1** (broad range of 200–400 nm; maximum absorbance = 277 nm, 36,100 cm^{-1}) reproduced the experimental values (broad range of 230–375 nm; maximum absorbance = 259 nm, 38,600 cm^{-1}). Similarly, the results for **4.2** are consistent with experiment; the calculated excitation (range of 380–600 nm; maximum absorbance = 427 nm, 23,400 cm^{-1}) are comparable to the experimental values (broad range of 350–550 nm; maximum absorbance = 400 nm, 25,000 cm^{-1}). Both experimental and calculated spectra for **4.2** showed the same broad higher-energy absorbance curve with the previously reported visible-light excitation curve. Interestingly, the higher-energy curve (experimental maximum absorbance = 265 nm, 37,200 cm^{-}

^{1}, calculated maximum absorbance = 260 nm, 38,500 cm^{-1}) is similar in energy to the absorbance curve for **4.1**.

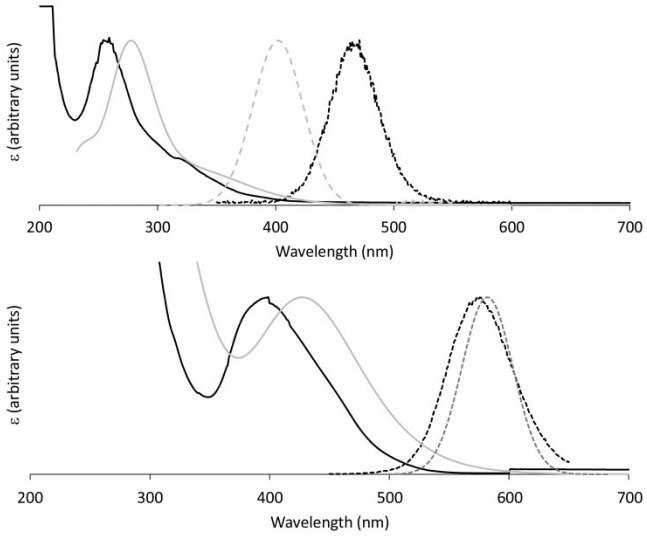

Figure 4.3. UV–visible spectra from experiment and TD-DFT B3PW91/SDD calculations in SMD methanol. Experimental absorption (—) and emission (---) and calculated absorption (—) and emission (---) of **4.1** (top) and **4.2** (bottom).

The excited states in the absorption spectra of **4.1** and **4.2** were interpreted by visualizing the natural-transition orbitals. The peak in the absorption spectrum for **4.1** corresponds to a Laporte-allowed $4f^7$–$4f^6 5d^1$ excitation. Natural-transition-orbital calculations for this state find that the electronic transition can be described as an excitation from $4f_{z^3}$ orbital to a $5d_{z^2}$ orbital (**Figure 4.4**). For **4.2**, natural-transition-orbital calculations reveal that the high-energy excited state (260 nm calculated) involves a transition from a $4f_{z^3}$ orbital to a $5d_{z^2}$ orbital. Structure **4.2** has the distinct visible-light absorbance (400 nm experimental) that initiated interest in the complex. Natural-transition-orbital calculations indicate that this peak corresponds to transition from 4f orbitals to a $5d_{xy}$ orbital. Closer inspection of the calculated absorption spectrum of **4.1** (**Figure 4.5**) reveals a set of weaker excitations than the maximum excitations for **4.1** forming a shoulder (around 365 nm, 27,400 cm^{-1} calculated) that also involves 4f–$5d_{xy}$ transitions. **Figures 4.6 and 4.7** show calculated transitions of the absorption and emission of **4.2** respectively.

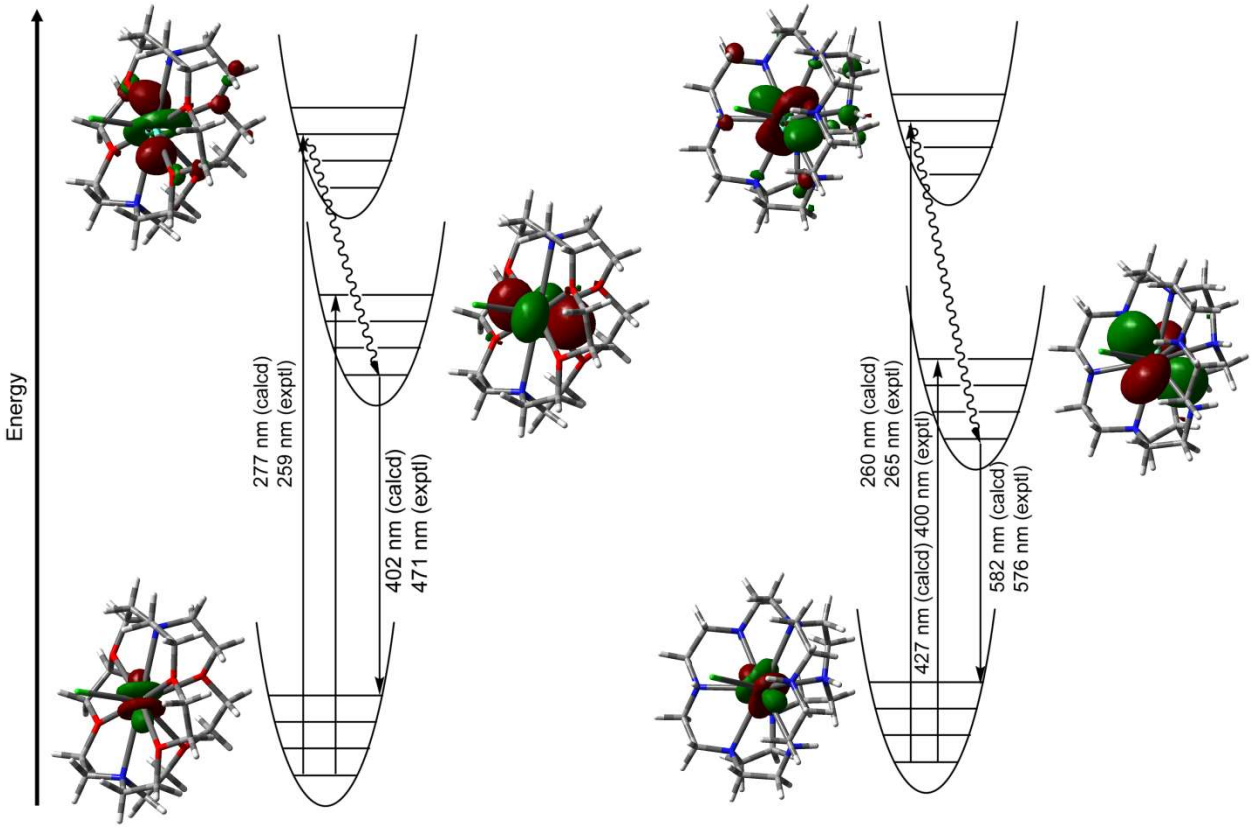

Figure 4.4. Energy diagram depicting 4f–5d transitions and the respective natural-transition orbitals involved based on TD-DFT B3PW91/SDD calculations of ground-state-to-excited-state and excited-state-to-ground-state transitions for (left) **4.1** and (right) **4.2**.

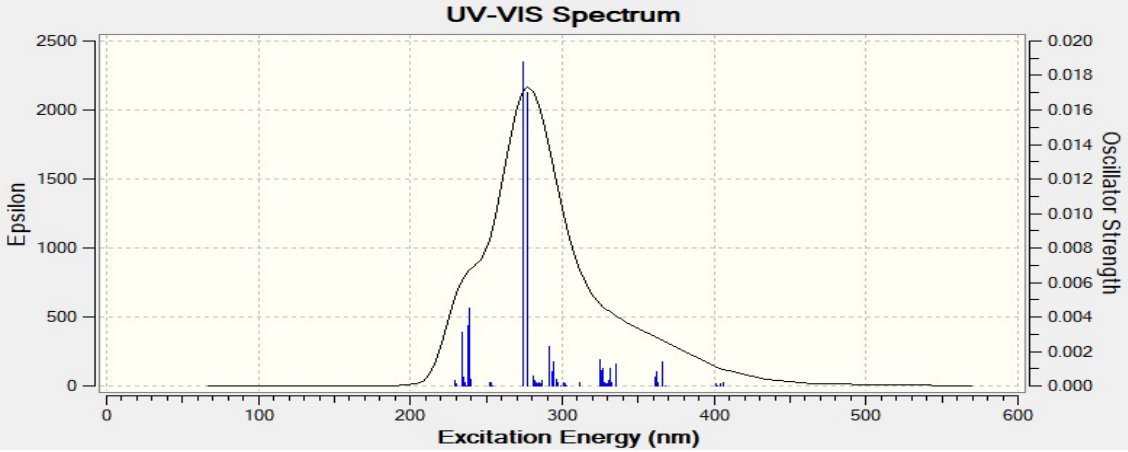

Figure 4.5. Spectrum depicting 80 calculated transitions of the absorption of **4.1**.

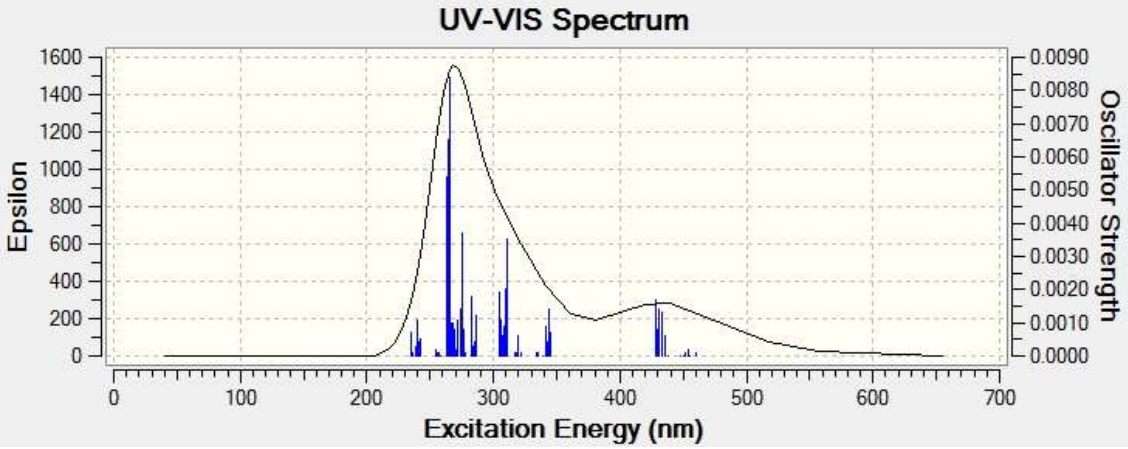

Figure 4.6. Spectrum depicting 80 calculated transitions of the absorption of **4.2**.

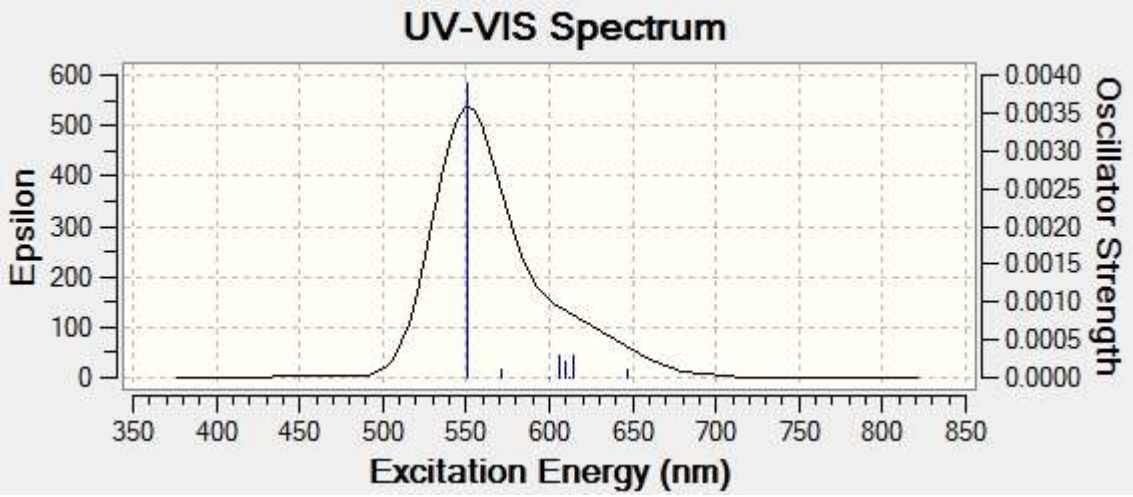

Figure 4.7. Spectrum depicting the lowest nine calculated transitions of the emission of **4.2**.

The changes in the energies of the 4f and 5d orbitals on going from **4.1** to **4.2**, and hence the changes in the excitation energies, can be understood qualitatively in terms of ligand field theory. Similar ligand-field arguments have been employed to explain 4f–5d transitions for Ce^{III}.[350] The strong-field character of the N-donors of **4.2** induces a larger energy splitting (Δ) between the $5d_{z^2}$ and $5d_{xy}$ orbitals compared to the O-donors of **4.1**, in agreement with the well-established trends of the spectrochemical series (**Figure 4.8**). Consequently, the energy difference between the $5d_{xy}$ and the $4f_{z^3}$ orbitals in **4.2** is smaller than in **4.1**; this transition experiences a bathochromic shift in the absorbance spectra with **4.2** compared to **4.1**, and this difference in energy moves the

transition far enough from the high-energy excitation to appear as a separate peak. While the 4f orbitals are generally shielded from direct interaction with the ligand orbitals, the greater electronegativity of the oxygens in **4.1** compared to the nitrogen atoms in **4.2** induces a small (0.40 eV) lowering of the f orbital energies through longer range electrostatic interactions relative to **2**. As a result, the 4f–5d_{z^2} energy difference is nearly the same in the two complexes, and both have strong absorbances near 270 nm.

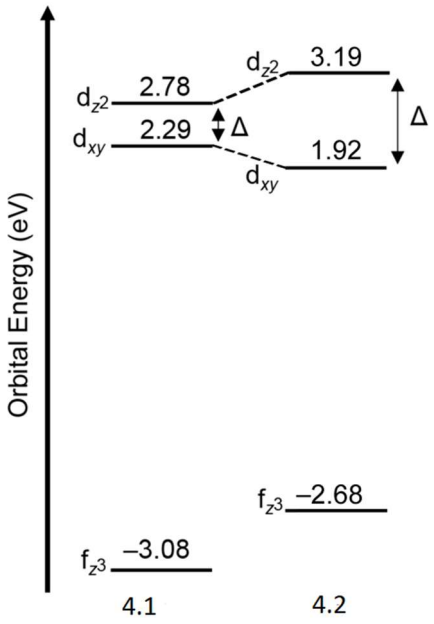

Figure 4.8. Orbital energy diagram of the 5d_{z^2}, 5d_{xy}, and 4f_{z^3} orbitals for **4.1** (left) and **4.2** (right). The relatively large splitting energy in **4.2** is due to the presence of strong-field amine donors in the octaaza-cryptate compared to ethers in **4.1**.

Emission occurs from the lowest vibrational levels of the lowest $4f^6 5d^1$ state that has significant oscillator strength for a transition to the ground state (**Figure 4.4**). Geometry optimization of the 4f–5d_{xy} transition of **4.1** using TD-DFT leads to an average shortening of the Eu^{II}–O and Eu^{II}–N bonds by 0.05 and 0.09 Å, respectively, and a 0.04 Å shortening of the Eu^{II}–Cl bond (**Table 4.2**). These changes stabilize the excited state by 1.23 kcal/mol, but the calculated emission maximum at 380 nm (26,300 cm^{-1}) differs considerably from the observed maximum at 471 nm (21,200 cm^{-1}). For **4.2**, geometry optimization of the emitting state resulted in an average

shortening of the Eu^{II}–N bonds by 0.2 Å (**Table 4.3**) and a stabilization of the excited state by 11.4 kcal/mol. Interestingly, the bond length of Eu^{II}–Cl extends to the point of full dissociation (4.54 Å), and subsequently the cryptand ligand geometry for **4.2** changes to become more symmetric, which did not occur for **4.1**. The emission maximum is calculated to be at 558 nm (17,900 cm^{-1}) and compares well with the observed emission maximum at 576 nm (17,400 cm^{-1}).

In the TD-DFT calculations, solvent effects for the absorption spectra are treated by linear response, which is adequate for states with large transition dipoles.[344] State-specific solvation calculations for the absorption maximum in **4.1** caused a shift of 11 nm; however, state-specific solvation calculations might be more important for emission because solvation accounts for solvent equilibration for the lowest-energy structure of the emitting state. Considering the state-specific solvation effects on emission, the calculated emission maximum for **4.1** is shifted to 402 nm, which is a relatively closer value to the experimental value than the original solvation method. For **4.2**, the emission maxima with and without state-specific solvation (582 nm and 558 nm) are both in good agreement with the observed value of 576 nm.

The experimental quantum yield for **4.1** is ~9.3% in methanol, but only 0.1% in water. This difference has been attributed to radiationless deactivation by water.[319] For **4.2**, the quantum yield in aqueous solution is 26%.[300] Because the absorption and emission involve the same electronic state, there is less opportunity for radiationless deactivation, resulting in a significantly higher quantum yield for **4.2** than for **4.1**.

4.4 Conclusions

We reported the use of TD-DFT calculations as a method to analyze the photophysical properties of divalent-europium-containing complexes. Structurally similar cryptates **4.1** and **4.2** were studied because of their different luminescence properties, and the results showed excitation and emission data that reflected experimental data. Natural-transition-orbital calculations provided visualizations of the orbitals of interest in the transition of one electron from the degenerate 4f orbitals to the 5d orbitals. State-specific solvation improved the calculated

values for the emission of both **4.1** and **4.2**. Based on the strong-field properties of the octaaza-cryptand ligand of **4.2**, we conclude that the difference in luminescence properties of **4.1** and **4.2** are due to a lowering in energy of the emissive state of **4.2**, resulting in a longer wavelength emission with greater quantum yield than **4.1**. The present study demonstrates the utility of computational methods in unraveling the complexities of photophysical properties of lanthanide complexes.

CHAPTER 5
SUMMARY AND FUTURE DIRECTIONS

5.1 Summary of Thesis

Differences in ligand donor atom polarizability impact both the selectivity for specific rare-earth elements and the luminescence properties of rare-earth element complexes. Within this thesis, **Chapter 1** provides important background in the use of coordination chemistry to adsorb rare-earth elements for enrichment and separation. Other than donor-atom polarizability, the main considerations discussed for solid–liquid extraction of rare-earth elements include metal charge density, ligand denticity, and the pK_a values of ligands. Although liquid–liquid extraction remains the most commonly used commercial technique for the extraction of rare-earth ions, solid–liquid extraction provides a pathway for a highly customizable, reusable, organic-solvent-free method of rare-earth element enrichment.

In **Chapter 2**, a pH-dependent solid-phase media is described that was developed using a multidentate chelator bis(ethyhexyl)amido DTPA noncovalently attached to a swellable, organically modified silica. The solid-phase media was used to enrich rare-earth elements and was found to show preference for the mid- to-heavy rare-earth elements. The monotonic trend between the complexation constants of unmodified DTPA and the uptake of rare-earth elements by the solid-phase media suggests that the binding mode of the solid-phase media was the same as the unmodified DTPA. The solid-phase media was found to bind Nd^{3+} above pH 3.3, elute Nd^{3+} below pH 1.0, and retain the binding and eluting trend for at least six cycles. When introduced to a solution of fly ash leachate containing rare-earth elements and competing ions including iron and aluminum, the ligand-associated media retained the preference toward mid and heavy rare-earth elements, even in the presence of large concentrations of Al and Fe (~700- to 90,000-fold excess with respect to the rare-earth ions). The results of this study outline the selectivity for mid-to-heavy rare-earth elements using a pH-dependent solid-phase media for rare-earth ion

enrichment, and provide details of the use of this media to enrich critical materials from fly ash leachate.

In **Chapter 3**, experiments are described that focus on the analysis of the chain length of DTPA derivatives in the solid-phase media. Because the solid-phase media described in **Chapter 2** is prepared from the hydrophobic interactions between ethylhexyl chains and the hydrophobic pockets in organically modified silica, we proposed that from ligands featuring butyl or hexyl, hydrophobic moieties, the ligands featuring longer chains would exhibit stronger noncovalent interactions to the solid support. To test this hypothesis, we prepared DTPA derivatives featuring butyl or hexyl hydrophobic moieties. The ligands were loaded onto organosilica, and we found that the ligand featuring butyl moieties adsorbed less than the ligand featuring hexyl moieties. The ligand featuring butyl moieties also exhibited less wash off than the ligand featuring hexyl moieties, providing preliminary data to suggest that the ligand featuring the hexyl moiety would lead to a solid-phase media that may be reused for rare-earth element enrichment without marked loss of efficiency. The results of this study provide insight into the effects of varying the binding modes of solid-phase media through noncovalent interactions and inform future solid-phase media design for the enrichment of rare-earth elements.

In **Chapter 4**, computational analyses were performed to determine the cause of observed differences in luminescence behavior between two complexes of divalent europium differing only in ligand donor atoms. After optimization of complexes **4.1** and **4.2**, the absorbance and emission spectra were calculated using TD-DFT with implicit solvation in methanol and found to be consistent with experimental spectra. Natural transition orbitals showed the absorbance of both **4.1** and **4.2** involved either a $4f_{z^3}$–$5d_{z^2}$-type transition or a 4f–$5d_{xy}$-type transition. After plotting the orbital energies for **4.1** and **4.2**, the bright yellow luminescence observed from complex **4.2** was determined to be due to a lowering in energy of the emissive state of **4.2**, resulting in a longer wavelength emission with greater quantum yield than **4.1**. The results of this study provide an

important tool by which the design of ligands for divalent lanthanides may be adjusted to regulate photophysical properties of rare-earth complexes.

5.2 Future Directions

Chapters 2 and **3** describe the development of a pH-dependent solid-phase media for the enrichment of rare-earth elements. Because the solid-phase media is likely compatible with most leachate materials, a logical extension of this research would be to experiment with leachate materials from different spent materials to further gauge the utility and efficiency of the system in the presence of different matrices. Future directions of this project include the analysis of loading and wash off of ligands with longer hydrophobic moieties—dodecyl or tetradecyl moieties— using the same experimental conditions as **Chapter 3** to fully characterize the properties of this family of solid-phase media. When designing a solid-phase media for the enrichment of rare-earth elements, both the solid support and the ligand can be adjusted to tune the selectivity and efficiency of rare-earth enrichment. Thus, further investigation into rare-earth element enrichment is likely to focus on analyzing solid-phase media with different solid supports, such as polymeric resins or inorganic materials, or by adjusting the ligand to tune rare-earth element selectivity. Toward the goal of increasing selectivity and productivity, the future of solid–liquid adsorption would benefit from creating a single column or set of columns with solid-phase materials designed to fully separate individual rare-earth ions. Although column-based separation has been shown to be an efficient technique for separating individual rare-earth elements from each other in bench scale analytical separations, one of the major obstacles that must be overcome is scaling to achieve sufficient productivity. Sorbents with fast sorption kinetics, high sorption capacities, and the ability to be cycled many times could provide an organic-solvent-free method to efficiently remove rare-earth ions from aqueous solutions.

Chapter 4 describes a computational method for the calculation of absorbance and luminescence data for two geometrically similar divalent europium cryptates. Since the publication of **Chapter 4**, the Allen research group has used the calculations to discern photophysical

differences in other geometrically similar complexes of divalent europium. Because adjusting ligand field can drastically change the photophysical effects of complexes of rare-earth elements, it is likely that these calculations will continue to provide details to discern energetic differences of new coordination complexes of divalent europium. Another possible use for these computational analyses could be to create a screening procedure from which light-promoted precatalyst candidates for photoredox chemistry might be chosen based on maximum calculated absorbances.

APPENDIX

PERMISSIONS

Permission to adapt Hovey, J. L.; Dittrich, T. M.; Allen, M. J. *J. Rare Earths* **2021**, https://doi.org/10.1016/j.jre.2022.05.012 for Chapter 1:

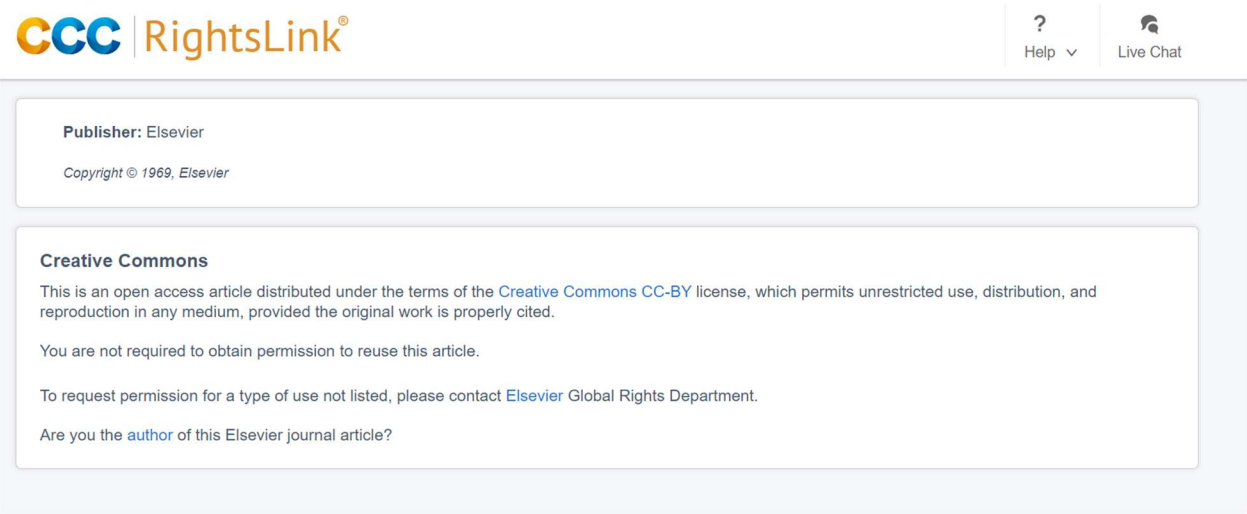

Permission to use Figure 2 from Van Nguyen, N.; Iizuka, A.; Shibata, E.; Nakamura, T. Study on adsorption behavior of a new synthesized resin containing glycol amic acid group for separation of scandium from aqueous solutions. *Hydrometallurgy*. **2016**, *165*, 51–56:

ELSEVIER LICENSE
TERMS AND CONDITIONS

Apr 20, 2022

This Agreement between Wayne State University -- Jessica Hovey ("You") and Elsevier ("Elsevier") consists of your license details and the terms and conditions provided by Elsevier and Copyright Clearance Center.

License Number	5293111233789
License date	Apr 20, 2022
Licensed Content Publisher	Elsevier
Licensed Content Publication	Hydrometallurgy
Licensed Content Title	Study of adsorption behavior of a new synthesized resin containing glycol amic acid group for separation of scandium from aqueous solutions

Licensed Content Author	Nghiem Van Nguyen,Atsushi Iizuka,Etsuro Shibata,Takashi Nakamura
Licensed Content Date	Oct 1, 2016
Licensed Content Volume	165
Licensed Content Issue	n/a
Licensed Content Pages	6
Start Page	51
End Page	56
Type of Use	reuse in a thesis/dissertation
Portion	figures/tables/illustrations
Number of figures/tables/illustrations	1

Format	both print and electronic
Are you the author of this Elsevier article?	No
Will you be translating?	No
Title	LANTHANIDE COORDINATION CHEMISTRY IN RARE-EARTH ELEMENT EXTRACTION AND PHOTOCATALYSIS
Institution name	Wayne State University
Expected presentation date	May 2022
Portions	Figure 2, page 53: Speciation diagram of scandium in chloride medium.
	Wayne State University 5101 Cass Avenue CHM 230

Requestor Location	DETROIT, MI 48202 United States Attn: Wayne State University
Publisher Tax ID	98-0397604
Total	0.00 USD

Terms and Conditions

INTRODUCTION

1. The publisher for this copyrighted material is Elsevier. By clicking "accept" in connection with completing this licensing transaction, you agree that the following terms and conditions apply to this transaction (along with the Billing and Payment terms and conditions established by Copyright Clearance Center, Inc. ("CCC"), at the time that you opened your Rightslink account and that are available at any time at http://myaccount.copyright.com).

GENERAL TERMS

2. Elsevier hereby grants you permission to reproduce the aforementioned material subject to the terms and conditions indicated.

3. Acknowledgement: If any part of the material to be used (for example, figures) has appeared in our publication with credit or acknowledgement to another source, permission must also be sought from that source. If such permission is not obtained then that material

may not be included in your publication/copies. Suitable acknowledgement to the source must be made, either as a footnote or in a reference list at the end of your publication, as follows:

"Reprinted from Publication title, Vol /edition number, Author(s), Title of article / title of chapter, Pages No., Copyright (Year), with permission from Elsevier [OR APPLICABLE SOCIETY COPYRIGHT OWNER]." Also Lancet special credit - "Reprinted from The Lancet, Vol. number, Author(s), Title of article, Pages No., Copyright (Year), with permission from Elsevier."

4. Reproduction of this material is confined to the purpose and/or media for which permission is hereby given.

5. Altering/Modifying Material: Not Permitted. However figures and illustrations may be altered/adapted minimally to serve your work. Any other abbreviations, additions, deletions and/or any other alterations shall be made only with prior written authorization of Elsevier Ltd. (Please contact Elsevier's permissions helpdesk here). No modifications can be made to any Lancet figures/tables and they must be reproduced in full.

6. If the permission fee for the requested use of our material is waived in this instance, please be advised that your future requests for Elsevier materials may attract a fee.

7. Reservation of Rights: Publisher reserves all rights not specifically granted in the combination of (i) the license details provided by you and accepted in the course of this licensing transaction, (ii) these terms and conditions and (iii) CCC's Billing and Payment terms and conditions.

8. License Contingent Upon Payment: While you may exercise the rights licensed immediately upon issuance of the license at the end of the licensing process for the transaction, provided that you have disclosed complete and accurate details of your proposed use, no license is finally effective unless and until full payment is received from you (either by publisher or by CCC) as provided in CCC's Billing and Payment terms and conditions. If

full payment is not received on a timely basis, then any license preliminarily granted shall be deemed automatically revoked and shall be void as if never granted. Further, in the event that you breach any of these terms and conditions or any of CCC's Billing and Payment terms and conditions, the license is automatically revoked and shall be void as if never granted. Use of materials as described in a revoked license, as well as any use of the materials beyond the scope of an unrevoked license, may constitute copyright infringement and publisher reserves the right to take any and all action to protect its copyright in the materials.

9. Warranties: Publisher makes no representations or warranties with respect to the licensed material.

10. Indemnity: You hereby indemnify and agree to hold harmless publisher and CCC, and their respective officers, directors, employees and agents, from and against any and all claims arising out of your use of the licensed material other than as specifically authorized pursuant to this license.

11. No Transfer of License: This license is personal to you and may not be sublicensed, assigned, or transferred by you to any other person without publisher's written permission.

12. No Amendment Except in Writing: This license may not be amended except in a writing signed by both parties (or, in the case of publisher, by CCC on publisher's behalf).

13. Objection to Contrary Terms: Publisher hereby objects to any terms contained in any purchase order, acknowledgment, check endorsement or other writing prepared by you, which terms are inconsistent with these terms and conditions or CCC's Billing and Payment terms and conditions. These terms and conditions, together with CCC's Billing and Payment terms and conditions (which are incorporated herein), comprise the entire agreement between you and publisher (and CCC) concerning this licensing transaction. In the event of any conflict between your obligations established by these terms and conditions and those established by CCC's Billing and Payment terms and conditions, these terms and conditions shall control.

14. Revocation: Elsevier or Copyright Clearance Center may deny the permissions described in this License at their sole discretion, for any reason or no reason, with a full refund payable to you. Notice of such denial will be made using the contact information provided by you. Failure to receive such notice will not alter or invalidate the denial. In no event will Elsevier or Copyright Clearance Center be responsible or liable for any costs, expenses or damage incurred by you as a result of a denial of your permission request, other than a refund of the amount(s) paid by you to Elsevier and/or Copyright Clearance Center for denied permissions.

LIMITED LICENSE

The following terms and conditions apply only to specific license types:

15. **Translation**: This permission is granted for non-exclusive world **English** rights only unless your license was granted for translation rights. If you licensed translation rights you may only translate this content into the languages you requested. A professional translator must perform all translations and reproduce the content word for word preserving the integrity of the article.

16. **Posting licensed content on any Website**: The following terms and conditions apply as follows: Licensing material from an Elsevier journal: All content posted to the web site must maintain the copyright information line on the bottom of each image; A hyper-text must be included to the Homepage of the journal from which you are licensing at http://www.sciencedirect.com/science/journal/xxxxx or the Elsevier homepage for books at http://www.elsevier.com; Central Storage: This license does not include permission for a scanned version of the material to be stored in a central repository such as that provided by Heron/XanEdu.

Licensing material from an Elsevier book: A hyper-text link must be included to the Elsevier homepage at http://www.elsevier.com . All content posted to the web site must maintain the copyright information line on the bottom of each image.

Posting licensed content on Electronic reserve: In addition to the above the following clauses are applicable: The web site must be password-protected and made available only to bona fide students registered on a relevant course. This permission is granted for 1 year only. You may obtain a new license for future website posting.

17. **For journal authors:** the following clauses are applicable in addition to the above:

Preprints:

A preprint is an author's own write-up of research results and analysis, it has not been peer-reviewed, nor has it had any other value added to it by a publisher (such as formatting, copyright, technical enhancement etc.).

Authors can share their preprints anywhere at any time. Preprints should not be added to or enhanced in any way in order to appear more like, or to substitute for, the final versions of articles however authors can update their preprints on arXiv or RePEc with their Accepted Author Manuscript (see below).

If accepted for publication, we encourage authors to link from the preprint to their formal publication via its DOI. Millions of researchers have access to the formal publications on ScienceDirect, and so links will help users to find, access, cite and use the best available version. Please note that Cell Press, The Lancet and some society-owned have different preprint policies. Information on these policies is available on the journal homepage.

Accepted Author Manuscripts: An accepted author manuscript is the manuscript of an article that has been accepted for publication and which typically includes author-incorporated changes suggested during submission, peer review and editor-author communications.

Authors can share their accepted author manuscript:

- immediately

- via their non-commercial person homepage or blog
- by updating a preprint in arXiv or RePEc with the accepted manuscript
- via their research institute or institutional repository for internal institutional uses or as part of an invitation-only research collaboration work-group
- directly by providing copies to their students or to research collaborators for their personal use
- for private scholarly sharing as part of an invitation-only work group on commercial sites with which Elsevier has an agreement

- After the embargo period
  - via non-commercial hosting platforms such as their institutional repository
  - via commercial sites with which Elsevier has an agreement

In all cases accepted manuscripts should:

- link to the formal publication via its DOI
- bear a CC-BY-NC-ND license - this is easy to do
- if aggregated with other manuscripts, for example in a repository or other site, be shared in alignment with our hosting policy not be added to or enhanced in any way to appear more like, or to substitute for, the published journal article.

Published journal article (JPA): A published journal article (PJA) is the definitive final record of published research that appears or will appear in the journal and embodies all value-adding publishing activities including peer review co-ordination, copy-editing, formatting, (if relevant) pagination and online enrichment.

Policies for sharing publishing journal articles differ for subscription and gold open access articles:

Subscription Articles: If you are an author, please share a link to your article rather than the full-text. Millions of researchers have access to the formal publications on ScienceDirect, and so links will help your users to find, access, cite, and use the best available version.

Theses and dissertations which contain embedded PJAs as part of the formal submission can be posted publicly by the awarding institution with DOI links back to the formal publications on ScienceDirect.

If you are affiliated with a library that subscribes to ScienceDirect you have additional private sharing rights for others' research accessed under that agreement. This includes use for classroom teaching and internal training at the institution (including use in course packs and courseware programs), and inclusion of the article for grant funding purposes.

Gold Open Access Articles: May be shared according to the author-selected end-user license and should contain a CrossMark logo, the end user license, and a DOI link to the formal publication on ScienceDirect.

Please refer to Elsevier's posting policy for further information.

18. **For book authors** the following clauses are applicable in addition to the above: Authors are permitted to place a brief summary of their work online only. You are not allowed to download and post the published electronic version of your chapter, nor may you scan the printed edition to create an electronic version. **Posting to a repository:** Authors are permitted to post a summary of their chapter only in their institution's repository.

19. **Thesis/Dissertation**: If your license is for use in a thesis/dissertation your thesis may be submitted to your institution in either print or electronic form. Should your thesis be published commercially, please reapply for permission. These requirements include permission for the Library and Archives of Canada to supply single copies, on demand, of the complete thesis and include permission for Proquest/UMI to supply single copies, on demand, of the complete thesis. Should your thesis be published commercially, please reapply for permission. Theses and dissertations which contain embedded PJAs as part of the formal submission can be posted publicly by the awarding institution with DOI links back to the formal publications on ScienceDirect.

Permission to adapt Scheme 1 and Figure 5 from Zheng, X.; Wang, C.; Dai, J.; Shi, W.; Yan, Y. Design of mesoporous silica hybrid materials as sorbents for the selective recovery of rare earth metals. J. Mater. Chem. A. **2015**, *3*,10327–10335:

CCC Marketplace™

Order Date	20-Apr-2022	Type of Use	Republish in a thesis/dissertation
Order License ID	1212988-1	Publisher	Royal Society of Chemistry
ISSN	2050-7488	Portion	Chart/graph/table/figure

LICENSED CONTENT

Publication Title	Journal of materials chemistry	Rightsholder	Royal Society of Chemistry
Article Title	Design of mesoporous silica hybrid materials as sorbents for the selective recovery of rare earth metals	Publication Type	Journal
		Start Page	10327
Author/Editor	Royal Society of Chemistry (Great Britain)	End Page	10335
Date	01/01/2012	Issue	19
Language	English	Volume	3
Country	United Kingdom of Great Britain and Northern Ireland		

REQUEST DETAILS

Portion Type	Chart/graph/table/figure	Distribution	Worldwide
Number of charts / graphs / tables / figures requested	2	Translation	Original language of publication
		Copies for the disabled?	No

Format (select all that apply)	Print, Electronic	Minor editing privileges?	Yes
Who will republish the content?	Academic institution	Incidental promotional use?	No
Duration of Use	Life of current edition	Currency	USD
Lifetime Unit Quantity	Up to 499		
Rights Requested	Main product		

NEW WORK DETAILS

Title	LANTHANIDE COORDINATION CHEMISTRY IN RARE-EARTH ELEMENT EXTRACTION AND PHOTOCATALYSIS	Institution name	Wayne State University
		Expected presentation date	2022-05-20
Instructor name	Jessica L. Hovey		

ADDITIONAL DETAILS

Order reference number	N/A	The requesting person / organization to appear on the license	Jessica Hovey

REUSE CONTENT DETAILS

Title, description or numeric reference of the portion(s)	Scheme 1, page 10329 and Figure 5, page 10332	Title of the article/chapter the portion is from	Design of mesoporous silica hybrid materials as sorbents for the selective recovery of rare earth metals
Editor of portion(s)	Zheng, Xudong; Wang, Chun; Dai, Jiangdong; Shi, Weidong; Yan, Yongsheng	Author of portion(s)	Zheng, Xudong; Wang, Chun; Dai, Jiangdong; Shi, Weidong; Yan, Yongsheng
Volume of serial or monograph	3	Issue, if republishing an article from a serial	19
Page or page range of portion	10327-10335	Publication date of portion	2015-01-01

CCC Terms and Conditions

1. Description of Service; Defined Terms. This Republication License enables the User to obtain licenses for republication of one or more copyrighted works as described in detail on the relevant Order Confirmation (the "Work(s)"). Copyright Clearance Center, Inc. ("CCC") grants licenses through the Service on behalf of the rightsholder identified on the Order Confirmation (the "Rightsholder"). "Republication", as used herein, generally means the inclusion of a Work, in whole or in part, in a new work or works, also as described on the Order Confirmation. "User", as used herein, means the person or entity making such republication.

2. The terms set forth in the relevant Order Confirmation, and any terms set by the Rightsholder with respect to a particular Work, govern the terms of use of Works in connection with the Service. By using the Service, the person transacting for a republication license on behalf of the User represents and warrants that he/she/it (a) has been duly authorized by the User to accept, and hereby does accept, all such terms and conditions on behalf of User, and (b) shall inform User of all such terms and conditions. In the event such person is a "freelancer" or other third party independent of User and CCC, such party shall be deemed jointly a "User" for purposes of these terms and conditions. In any event, User shall be deemed to have accepted and agreed to all such terms and conditions if User republishes the Work in any fashion.

3. Scope of License; Limitations and Obligations.

    3.1. All Works and all rights therein, including copyright rights, remain the sole and exclusive property of the Rightsholder. The license created by the exchange of an Order Confirmation (and/or any invoice) and payment by User of the full amount set forth on that document includes only those rights expressly set forth in the Order Confirmation and in these terms and conditions, and conveys no other rights in the Work(s) to User. All rights not expressly granted are hereby reserved.

    3.2. General Payment Terms: You may pay by credit card or through an account with us payable at the end of the month. If you and we agree that you may establish a standing account with CCC, then the following terms apply: Remit Payment to: Copyright Clearance Center, 29118 Network Place, Chicago, IL 60673-1291. Payments Due: Invoices are payable upon their delivery to you (or upon our notice to you that they are available to you for downloading). After 30 days, outstanding amounts will be subject to a service charge of 1-1/2% per month or, if less, the maximum rate allowed by applicable law. Unless otherwise specifically set forth in the Order Confirmation or in a separate written agreement signed by CCC, invoices are due and payable on "net 30" terms. While User may exercise the rights licensed immediately upon issuance of the Order Confirmation, the license is automatically revoked and is null and void, as if it had never been issued, if complete payment for the license is not received on a timely basis either from User directly or through a payment agent, such as a credit card company.

    3.3. Unless otherwise provided in the Order Confirmation, any grant of rights to User (i) is "one-time" (including the editions and product family specified in the license), (ii) is non-exclusive and non-transferable and (iii) is subject to any and all limitations and restrictions (such as, but not limited to, limitations on duration of use or circulation) included in the Order Confirmation or invoice and/or in these terms and conditions. Upon completion of the licensed use, User shall either secure a new permission for further use of the Work(s) or immediately cease any new use of the Work(s) and shall render inaccessible (such as by deleting or by removing or severing links or other locators) any further copies of the Work (except for copies printed on paper in accordance with this license and still in User's stock at the end of such period).

    3.4. In the event that the material for which a republication license is sought includes third party materials (such as photographs, illustrations, graphs, inserts and similar materials) which are identified in such material as having been used by permission, User is responsible for identifying, and seeking separate licenses (under this Service or otherwise) for, any of such third party materials; without a separate license, such third party materials may not be used.

    3.5. Use of proper copyright notice for a Work is required as a condition of any license granted under the Service. Unless otherwise provided in the Order Confirmation, a proper copyright notice will read substantially as follows: "Republished with permission of [Rightsholder's name], from [Work's title, author, volume, edition number and year of copyright]; permission conveyed through Copyright Clearance Center, Inc. " Such notice must be provided in a reasonably legible font size and must be placed either immediately adjacent to the Work as used (for example, as part of a by-line or footnote but not as a separate electronic link) or in the place where substantially all other credits or notices for the new work containing the republished Work are located. Failure to include the required notice results in loss to the Rightsholder and CCC, and the User shall be liable to pay liquidated damages for each such failure equal to twice the use fee specified in the Order Confirmation, in addition to the use fee itself and any other fees and charges specified.

    3.6. User may only make alterations to the Work if and as expressly set forth in the Order Confirmation. No Work may be used in any way that is defamatory, violates the rights of third parties (including such third parties' rights of copyright, privacy, publicity, or other tangible or intangible property), or is otherwise illegal, sexually explicit or obscene. In addition, User may not conjoin a Work with any other material that may result in damage to the reputation of the Rightsholder. User agrees to inform CCC if it becomes aware of any infringement of any rights in a Work and to cooperate with any reasonable request of CCC or the Rightsholder in connection therewith.

4. Indemnity. User hereby indemnifies and agrees to defend the Rightsholder and CCC, and their respective employees and directors, against all claims, liability, damages, costs and expenses, including legal fees and expenses, arising out of any use of a Work beyond the scope of the rights granted herein, or any use of a Work which has been altered in any unauthorized way by User, including claims of defamation or infringement of rights of copyright, publicity, privacy or other tangible or intangible property.

5. Limitation of Liability. UNDER NO CIRCUMSTANCES WILL CCC OR THE RIGHTSHOLDER BE LIABLE FOR ANY DIRECT, INDIRECT, CONSEQUENTIAL OR INCIDENTAL DAMAGES (INCLUDING WITHOUT LIMITATION DAMAGES FOR LOSS OF BUSINESS PROFITS OR INFORMATION, OR FOR BUSINESS INTERRUPTION) ARISING OUT OF THE USE OR INABILITY TO USE A WORK, EVEN IF ONE OF THEM HAS BEEN ADVISED OF THE POSSIBILITY OF SUCH DAMAGES. In any event, the total liability of the Rightsholder and CCC (including their respective employees and directors) shall not exceed the total amount actually paid by User for this license. User assumes full liability for the actions and omissions of its principals, employees, agents, affiliates, successors and assigns.

Permission to reprint TOC graphic from Hu, Y.; Drouin, E.; Larivière, D.; Kleitz, F.; Fontaine, F-G. Highly efficient and selective recovery of rare earth elements using mesoporous silica functionalized by preorganized chelating ligands. *ACS Appl. Mater. Interfaces.* **2017**, *9*, 38584:

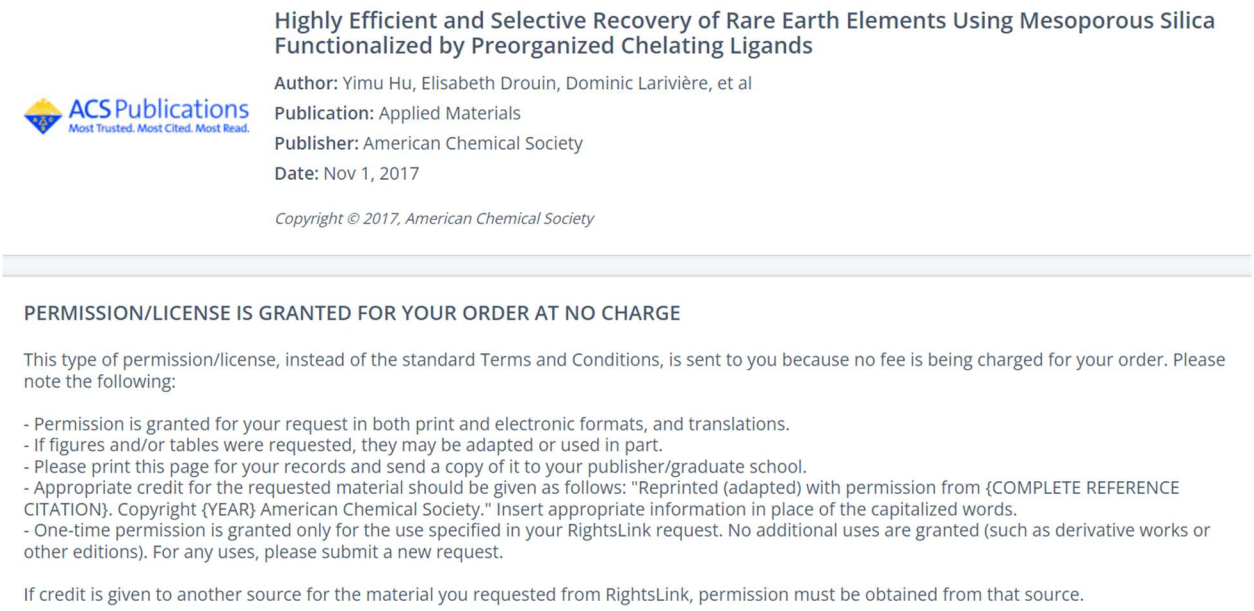

Highly Efficient and Selective Recovery of Rare Earth Elements Using Mesoporous Silica Functionalized by Preorganized Chelating Ligands

Author: Yimu Hu, Elisabeth Drouin, Dominic Larivière, et al

Publication: Applied Materials

Publisher: American Chemical Society

Date: Nov 1, 2017

Copyright © 2017, American Chemical Society

PERMISSION/LICENSE IS GRANTED FOR YOUR ORDER AT NO CHARGE

This type of permission/license, instead of the standard Terms and Conditions, is sent to you because no fee is being charged for your order. Please note the following:

- Permission is granted for your request in both print and electronic formats, and translations.
- If figures and/or tables were requested, they may be adapted or used in part.
- Please print this page for your records and send a copy of it to your publisher/graduate school.
- Appropriate credit for the requested material should be given as follows: "Reprinted (adapted) with permission from {COMPLETE REFERENCE CITATION}. Copyright {YEAR} American Chemical Society." Insert appropriate information in place of the capitalized words.
- One-time permission is granted only for the use specified in your RightsLink request. No additional uses are granted (such as derivative works or other editions). For any uses, please submit a new request.

If credit is given to another source for the material you requested from RightsLink, permission must be obtained from that source.

Permission to adapt Ramzan, M.; Kifle, D.; Wibetoe, G. Comparitive study of stationary phases impregnated with acidic organophosphorous extractants for HPLC separation of rare earth elements. Sep. Sci. Technol. **2016**, *51*, 494–501:

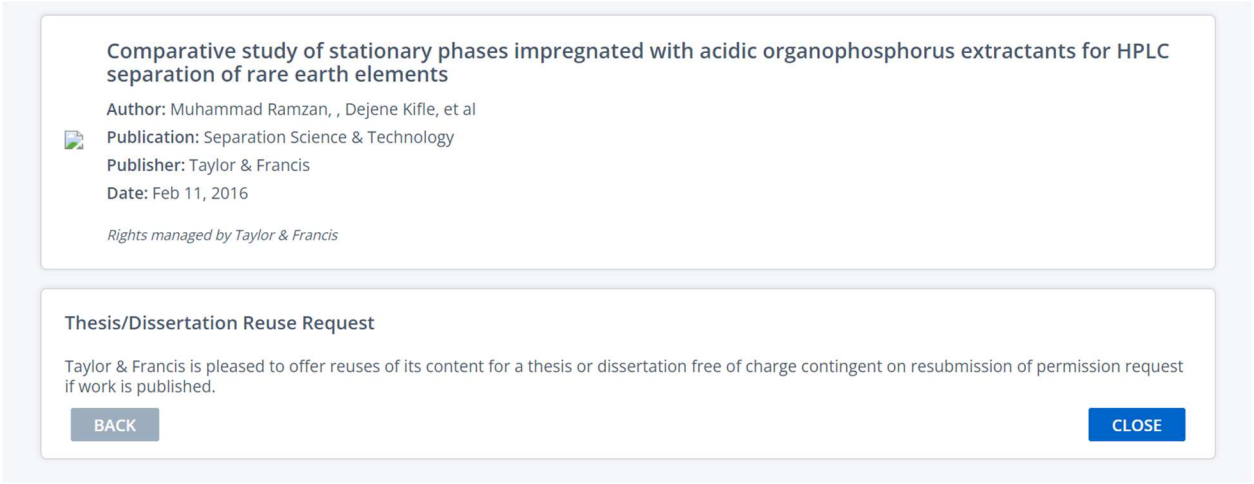

Comparative study of stationary phases impregnated with acidic organophosphorus extractants for HPLC separation of rare earth elements

Author: Muhammad Ramzan, , Dejene Kifle, et al

Publication: Separation Science & Technology

Publisher: Taylor & Francis

Date: Feb 11, 2016

Rights managed by Taylor & Francis

Thesis/Dissertation Reuse Request

Taylor & Francis is pleased to offer reuses of its content for a thesis or dissertation free of charge contingent on resubmission of permission request if work is published.

BACK CLOSE

Permission to adapt Figure 4 from Roosen, J.; Spooren, J.; Binnemans, K. Adsorption performance of functionalized chitosan–silica hybrid materials toward rare earths. *J. Mater. Chem. A*. **2014**, *2*, 19415–19426:

CCC Marketplace™

Order Date	20-Apr-2022	Type of Use	Republish in a thesis/dissertation
Order License ID	1213005-1	Publisher	Royal Society of Chemistry
ISSN	2050-7488	Portion	Chart/graph/table/figure

LICENSED CONTENT

Publication Title	Journal of materials chemistry	Rightsholder	Royal Society of Chemistry
Article Title	Adsorption performance of functionalized chitosan–silica hybrid materials toward rare earths	Publication Type	Journal
		Start Page	19415
Author/Editor	Royal Society of Chemistry (Great Britain)	End Page	19426
Date	01/01/2012	Issue	45
Language	English	Volume	2
Country	United Kingdom of Great Britain and Northern Ireland		

REQUEST DETAILS

Portion Type	Chart/graph/table/figure	Distribution	Worldwide
Number of charts / graphs / tables / figures requested	1	Translation	Original language of publication
		Copies for the disabled?	No

Format (select all that apply)	Print, Electronic	Minor editing privileges?	Yes
Who will republish the content?	Academic institution	Incidental promotional use?	No
Duration of Use	Life of current edition	Currency	USD
Lifetime Unit Quantity	Up to 499		
Rights Requested	Main product		

NEW WORK DETAILS

Title	LANTHANIDE COORDINATION CHEMISTRY IN RARE-EARTH ELEMENT EXTRACTION AND PHOTOCATALYSIS	Institution name	Wayne State University
		Expected presentation date	2022-05-20
Instructor name	Jessica L. Hovey		

ADDITIONAL DETAILS

Order reference number	N/A	The requesting person / organization to appear on the license	Jessica Hovey

REUSE CONTENT DETAILS

Title, description or numeric reference of the portion(s)	Fig. 4, page 19421	Title of the article/chapter the portion is from	Adsorption performance of functionalized chitosan–silica hybrid materials toward rare earths
Editor of portion(s)	Roosen, Joris; Spooren, Jeroen; Binnemans, Koen	Author of portion(s)	Roosen, Joris; Spooren, Jeroen; Binnemans, Koen
Volume of serial or monograph	2		
Page or page range of portion	19415-19426	Issue, if republishing an article from a serial	45

Publication date of portion	2014-09-16

CCC Terms and Conditions

1. Description of Service; Defined Terms. This Republication License enables the User to obtain licenses for republication of one or more copyrighted works as described in detail on the relevant Order Confirmation (the "Work(s)"). Copyright Clearance Center, Inc. ("CCC") grants licenses through the Service on behalf of the rightsholder identified on the Order Confirmation (the "Rightsholder"). "Republication", as used herein, generally means the inclusion of a Work, in whole or in part, in a new work or works, also as described on the Order Confirmation. "User", as used herein, means the person or entity making such republication.

2. The terms set forth in the relevant Order Confirmation, and any terms set by the Rightsholder with respect to a particular Work, govern the terms of use of Works in connection with the Service. By using the Service, the person transacting for a republication license on behalf of the User represents and warrants that he/she/it (a) has been duly authorized by the User to accept, and hereby does accept, all such terms and conditions on behalf of User, and (b) shall inform User of all such terms and conditions. In the event such person is a "freelancer" or other third party independent of User and CCC, such party shall be deemed jointly a "User" for purposes of these terms and conditions. In any event, User shall be deemed to have accepted and agreed to all such terms and conditions if User republishes the Work in any fashion.

3. Scope of License; Limitations and Obligations.

    3.1. All Works and all rights therein, including copyright rights, remain the sole and exclusive property of the Rightsholder. The license created by the exchange of an Order Confirmation (and/or any invoice) and payment by User of the full amount set forth on that document includes only those rights expressly set forth in the Order Confirmation and in these terms and conditions, and conveys no other rights in the Work(s) to User. All rights not expressly granted are hereby reserved.

    3.2. General Payment Terms: You may pay by credit card or through an account with us payable at the end of the month. If you and we agree that you may establish a standing account with CCC, then the following terms apply: Remit Payment to: Copyright Clearance Center, 29118 Network Place, Chicago, IL 60673-1291. Payments Due: Invoices are payable upon their delivery to you (or upon our notice to you that they are available to you for downloading). After 30 days, outstanding amounts will be subject to a service charge of 1-1/2% per month or, if less, the maximum rate allowed by applicable law. Unless otherwise specifically set forth in the Order Confirmation or in a separate written agreement signed by CCC, invoices are due and payable on "net 30" terms. While User may exercise the rights licensed immediately upon issuance of the Order Confirmation, the license is automatically revoked and is null and void, as if it had never been issued, if complete payment for the license is not received on a timely basis either from User directly or through a payment agent, such as a credit card company.

    3.3. Unless otherwise provided in the Order Confirmation, any grant of rights to User (i) is "one-time" (including the editions and product family specified in the license), (ii) is non-exclusive and non-transferable and (iii) is subject to any and all limitations and restrictions (such as, but not limited to, limitations on duration of use or circulation) included in the Order Confirmation or invoice and/or in these terms and conditions. Upon completion of the licensed use, User shall either secure a new permission for further use of the Work(s) or immediately cease any new use of the Work(s) and shall render inaccessible (such as by deleting or by removing or severing links or other locators) any further copies of the Work (except for copies printed on paper in accordance with this license and still in User's stock at the end of such period).

    3.4. In the event that the material for which a republication license is sought includes third party materials (such as photographs, illustrations, graphs, inserts and similar materials) which are identified in such material as having been used by permission, User is responsible for identifying, and seeking separate licenses (under this Service or otherwise) for, any of such third party materials; without a separate license, such third party materials may not be used.

    3.5. Use of proper copyright notice for a Work is required as a condition of any license granted under the Service. Unless otherwise provided in the Order Confirmation, a proper copyright notice will read substantially as follows: "Republished with permission of [Rightsholder's name], from [Work's title, author, volume, edition number and year of copyright]; permission conveyed through Copyright Clearance Center, Inc. " Such notice must be provided in a reasonably legible font size and must be placed either immediately adjacent to the Work as used (for example, as part of a by-line or footnote but not as a separate electronic link) or in the place where substantially all other credits or notices for the new work containing the republished Work are located. Failure to include the required notice results in loss to the Rightsholder and CCC, and the User shall be liable to pay liquidated damages for each such failure equal to twice the use fee specified in the Order Confirmation, in addition to the use fee itself and any other fees and charges specified.

    3.6. User may only make alterations to the Work if and as expressly set forth in the Order Confirmation. No Work may be used in any way that is defamatory, violates the rights of third parties (including such third parties' rights of copyright, privacy, publicity, or other tangible or intangible property), or is otherwise illegal, sexually explicit or obscene. In addition, User may not conjoin a Work with any other material that may result in damage to the reputation of the Rightsholder. User agrees to inform CCC if it becomes aware of any infringement of any rights in a Work and to cooperate with any reasonable request of CCC or the Rightsholder in connection therewith.

4. Indemnity. User hereby indemnifies and agrees to defend the Rightsholder and CCC, and their respective employees and directors, against all claims, liability, damages, costs and expenses, including legal fees and expenses, arising out of any use of a Work beyond the scope of the rights granted herein, or any use of a Work which has been altered in any unauthorized way by User, including claims of defamation or infringement of rights of copyright, publicity, privacy or other tangible or intangible property.

5. Limitation of Liability. UNDER NO CIRCUMSTANCES WILL CCC OR THE RIGHTSHOLDER BE LIABLE FOR ANY DIRECT, INDIRECT, CONSEQUENTIAL OR INCIDENTAL DAMAGES (INCLUDING WITHOUT LIMITATION DAMAGES FOR LOSS OF BUSINESS PROFITS OR INFORMATION, OR FOR BUSINESS INTERRUPTION) ARISING OUT OF THE USE OR INABILITY TO USE A WORK, EVEN IF ONE OF THEM HAS BEEN ADVISED OF THE POSSIBILITY OF SUCH DAMAGES. In any event, the total liability of the Rightsholder and CCC (including their respective employees and directors) shall not exceed the total amount actually paid by User for this license. User assumes full liability for the actions and omissions of its principals, employees,

Permission to adapt Figure 14 from Artiushenko, O.; Ávila, E. P.; Nazarkovsky, M.; Zaitsev, V. Reusable hydroxamate immobilized silica adsorbent for dispersive solid phase extraction and separation of rare earth metal ions. *Sep. Purif. Technol.* **2020**, *231*, 1–10:

ELSEVIER LICENSE
TERMS AND CONDITIONS

Apr 20, 2022

This Agreement between Wayne State University -- Jessica Hovey ("You") and Elsevier ("Elsevier") consists of your license details and the terms and conditions provided by Elsevier and Copyright Clearance Center.

License Number	5293131264315
License date	Apr 20, 2022
Licensed Content Publisher	Elsevier
Licensed Content Publication	Separation and Purification Technology
Licensed Content Title	Reusable hydroxamate immobilized silica adsorbent for dispersive solid phase extraction and separation of rare earth metal ions

Licensed Content Author	Olena Artiushenko,Eloah Pereira Avila,Michael Nazarkovsky,Vladimir Zaitsev
Licensed Content Date	Jan 16, 2020
Licensed Content Volume	231
Licensed Content Issue	n/a
Licensed Content Pages	1
Start Page	115934
End Page	0
Type of Use	reuse in a thesis/dissertation
Portion	figures/tables/illustrations
Number of figures/tables/illustrations	1

Format	both print and electronic
Are you the author of this Elsevier article?	No
Will you be translating?	No
Title	LANTHANIDE COORDINATION CHEMISTRY IN RARE-EARTH ELEMENT EXTRACTION AND PHOTOCATALYSIS
Institution name	Wayne State University
Expected presentation date	May 2022
Portions	Figure 14, page 9
Requestor Location	Wayne State University 5101 Cass Avenue CHM 230 DETROIT, MI 48202 United States Attn: Wayne State University

Publisher Tax ID	98-0397604
Total	0.00 USD

Terms and Conditions

INTRODUCTION

1. The publisher for this copyrighted material is Elsevier. By clicking "accept" in connection with completing this licensing transaction, you agree that the following terms and conditions apply to this transaction (along with the Billing and Payment terms and conditions established by Copyright Clearance Center, Inc. ("CCC"), at the time that you opened your Rightslink account and that are available at any time at http://myaccount.copyright.com).

GENERAL TERMS

2. Elsevier hereby grants you permission to reproduce the aforementioned material subject to the terms and conditions indicated.

3. Acknowledgement: If any part of the material to be used (for example, figures) has appeared in our publication with credit or acknowledgement to another source, permission must also be sought from that source. If such permission is not obtained then that material may not be included in your publication/copies. Suitable acknowledgement to the source must be made, either as a footnote or in a reference list at the end of your publication, as follows:

"Reprinted from Publication title, Vol /edition number, Author(s), Title of article / title of chapter, Pages No., Copyright (Year), with permission from Elsevier [OR APPLICABLE

SOCIETY COPYRIGHT OWNER]." Also Lancet special credit - "Reprinted from The Lancet, Vol. number, Author(s), Title of article, Pages No., Copyright (Year), with permission from Elsevier."

4. Reproduction of this material is confined to the purpose and/or media for which permission is hereby given.

5. Altering/Modifying Material: Not Permitted. However figures and illustrations may be altered/adapted minimally to serve your work. Any other abbreviations, additions, deletions and/or any other alterations shall be made only with prior written authorization of Elsevier Ltd. (Please contact Elsevier's permissions helpdesk here). No modifications can be made to any Lancet figures/tables and they must be reproduced in full.

6. If the permission fee for the requested use of our material is waived in this instance, please be advised that your future requests for Elsevier materials may attract a fee.

7. Reservation of Rights: Publisher reserves all rights not specifically granted in the combination of (i) the license details provided by you and accepted in the course of this licensing transaction, (ii) these terms and conditions and (iii) CCC's Billing and Payment terms and conditions.

8. License Contingent Upon Payment: While you may exercise the rights licensed immediately upon issuance of the license at the end of the licensing process for the transaction, provided that you have disclosed complete and accurate details of your proposed use, no license is finally effective unless and until full payment is received from you (either by publisher or by CCC) as provided in CCC's Billing and Payment terms and conditions. If full payment is not received on a timely basis, then any license preliminarily granted shall be deemed automatically revoked and shall be void as if never granted. Further, in the event that you breach any of these terms and conditions or any of CCC's Billing and Payment terms and conditions, the license is automatically revoked and shall be void as if never granted. Use of materials as described in a revoked license, as well as any use of the materials beyond the scope of an unrevoked license, may constitute copyright infringement

and publisher reserves the right to take any and all action to protect its copyright in the materials.

9. Warranties: Publisher makes no representations or warranties with respect to the licensed material.

10. Indemnity: You hereby indemnify and agree to hold harmless publisher and CCC, and their respective officers, directors, employees and agents, from and against any and all claims arising out of your use of the licensed material other than as specifically authorized pursuant to this license.

11. No Transfer of License: This license is personal to you and may not be sublicensed, assigned, or transferred by you to any other person without publisher's written permission.

12. No Amendment Except in Writing: This license may not be amended except in a writing signed by both parties (or, in the case of publisher, by CCC on publisher's behalf).

13. Objection to Contrary Terms: Publisher hereby objects to any terms contained in any purchase order, acknowledgment, check endorsement or other writing prepared by you, which terms are inconsistent with these terms and conditions or CCC's Billing and Payment terms and conditions. These terms and conditions, together with CCC's Billing and Payment terms and conditions (which are incorporated herein), comprise the entire agreement between you and publisher (and CCC) concerning this licensing transaction. In the event of any conflict between your obligations established by these terms and conditions and those established by CCC's Billing and Payment terms and conditions, these terms and conditions shall control.

14. Revocation: Elsevier or Copyright Clearance Center may deny the permissions described in this License at their sole discretion, for any reason or no reason, with a full refund payable to you. Notice of such denial will be made using the contact information provided by you. Failure to receive such notice will not alter or invalidate the denial. In no event will Elsevier or Copyright Clearance Center be responsible or liable for any costs, expenses or damage

incurred by you as a result of a denial of your permission request, other than a refund of the amount(s) paid by you to Elsevier and/or Copyright Clearance Center for denied permissions.

LIMITED LICENSE

The following terms and conditions apply only to specific license types:

15. **Translation**: This permission is granted for non-exclusive world **English** rights only unless your license was granted for translation rights. If you licensed translation rights you may only translate this content into the languages you requested. A professional translator must perform all translations and reproduce the content word for word preserving the integrity of the article.

16. **Posting licensed content on any Website**: The following terms and conditions apply as follows: Licensing material from an Elsevier journal: All content posted to the web site must maintain the copyright information line on the bottom of each image; A hyper-text must be included to the Homepage of the journal from which you are licensing at http://www.sciencedirect.com/science/journal/xxxxx or the Elsevier homepage for books at http://www.elsevier.com; Central Storage: This license does not include permission for a scanned version of the material to be stored in a central repository such as that provided by Heron/XanEdu.

Licensing material from an Elsevier book: A hyper-text link must be included to the Elsevier homepage at http://www.elsevier.com . All content posted to the web site must maintain the copyright information line on the bottom of each image.

Posting licensed content on Electronic reserve: In addition to the above the following clauses are applicable: The web site must be password-protected and made available only to bona fide students registered on a relevant course. This permission is granted for 1 year only. You may obtain a new license for future website posting.

17. **For journal authors:** the following clauses are applicable in addition to the above:

Preprints:

A preprint is an author's own write-up of research results and analysis, it has not been peer-reviewed, nor has it had any other value added to it by a publisher (such as formatting, copyright, technical enhancement etc.).

Authors can share their preprints anywhere at any time. Preprints should not be added to or enhanced in any way in order to appear more like, or to substitute for, the final versions of articles however authors can update their preprints on arXiv or RePEc with their Accepted Author Manuscript (see below).

If accepted for publication, we encourage authors to link from the preprint to their formal publication via its DOI. Millions of researchers have access to the formal publications on ScienceDirect, and so links will help users to find, access, cite and use the best available version. Please note that Cell Press, The Lancet and some society-owned have different preprint policies. Information on these policies is available on the journal homepage.

Accepted Author Manuscripts: An accepted author manuscript is the manuscript of an article that has been accepted for publication and which typically includes author-incorporated changes suggested during submission, peer review and editor-author communications.

Authors can share their accepted author manuscript:

- immediately
    - via their non-commercial person homepage or blog
    - by updating a preprint in arXiv or RePEc with the accepted manuscript
    - via their research institute or institutional repository for internal institutional uses or as part of an invitation-only research collaboration work-group
    - directly by providing copies to their students or to research collaborators for

their personal use
    - for private scholarly sharing as part of an invitation-only work group on commercial sites with which Elsevier has an agreement
- After the embargo period
    - via non-commercial hosting platforms such as their institutional repository
    - via commercial sites with which Elsevier has an agreement

In all cases accepted manuscripts should:

- link to the formal publication via its DOI
- bear a CC-BY-NC-ND license - this is easy to do
- if aggregated with other manuscripts, for example in a repository or other site, be shared in alignment with our hosting policy not be added to or enhanced in any way to appear more like, or to substitute for, the published journal article.

Published journal article (JPA): A published journal article (PJA) is the definitive final record of published research that appears or will appear in the journal and embodies all value-adding publishing activities including peer review co-ordination, copy-editing, formatting, (if relevant) pagination and online enrichment.

Policies for sharing publishing journal articles differ for subscription and gold open access articles:

Subscription Articles: If you are an author, please share a link to your article rather than the full-text. Millions of researchers have access to the formal publications on ScienceDirect, and so links will help your users to find, access, cite, and use the best available version.

Theses and dissertations which contain embedded PJAs as part of the formal submission can be posted publicly by the awarding institution with DOI links back to the formal publications on ScienceDirect.

If you are affiliated with a library that subscribes to ScienceDirect you have additional

private sharing rights for others' research accessed under that agreement. This includes use for classroom teaching and internal training at the institution (including use in course packs and courseware programs), and inclusion of the article for grant funding purposes.

Gold Open Access Articles: May be shared according to the author-selected end-user license and should contain a CrossMark logo, the end user license, and a DOI link to the formal publication on ScienceDirect.

Please refer to Elsevier's posting policy for further information.

18. **For book authors** the following clauses are applicable in addition to the above: Authors are permitted to place a brief summary of their work online only. You are not allowed to download and post the published electronic version of your chapter, nor may you scan the printed edition to create an electronic version. **Posting to a repository:** Authors are permitted to post a summary of their chapter only in their institution's repository.

19. **Thesis/Dissertation**: If your license is for use in a thesis/dissertation your thesis may be submitted to your institution in either print or electronic form. Should your thesis be published commercially, please reapply for permission. These requirements include permission for the Library and Archives of Canada to supply single copies, on demand, of the complete thesis and include permission for Proquest/UMI to supply single copies, on demand, of the complete thesis. Should your thesis be published commercially, please reapply for permission. Theses and dissertations which contain embedded PJAs as part of the formal submission can be posted publicly by the awarding institution with DOI links back to the formal publications on ScienceDirect.

Elsevier Open Access Terms and Conditions

You can publish open access with Elsevier in hundreds of open access journals or in nearly 2000 established subscription journals that support open access publishing. Permitted third

Permission to adapt Figure 4 from Ashour, R. M.; Abdel-Magied, A. F.; Abdel-khalek, A. A.; Helaly, O. S.; Ali, M. M. Preparation and characterization of magnetic iron oxide nanoparticles

functionalized by L-cysteine: adsorption and desorption behavior for rare earth metal ions. *J. Environ. Chem. Eng.* **2016**, *4*, 3114–3121:

ELSEVIER LICENSE
TERMS AND CONDITIONS

Apr 20, 2022

This Agreement between Wayne State University -- Jessica Hovey ("You") and Elsevier ("Elsevier") consists of your license details and the terms and conditions provided by Elsevier and Copyright Clearance Center.

License Number	5293150167502
License date	Apr 20, 2022
Licensed Content Publisher	Elsevier
Licensed Content Publication	Journal of Environmental Chemical Engineering
Licensed Content Title	Preparation and characterization of magnetic iron oxide nanoparticles functionalized by l-cysteine: Adsorption and desorption behavior for rare earth metal ions

Licensed Content Author	Radwa M. Ashour,Ahmed F. Abdel-Magied,Ahmed A. Abdel-khalek,O.S. Helaly,M.M. Ali
Licensed Content Date	Sep 1, 2016
Licensed Content Volume	4
Licensed Content Issue	3
Licensed Content Pages	8
Start Page	3114
End Page	3121
Type of Use	reuse in a thesis/dissertation
Portion	figures/tables/illustrations
Number of figures/tables/illustrations	1

Format	both print and electronic
Are you the author of this Elsevier article?	No
Will you be translating?	No
Title	LANTHANIDE COORDINATION CHEMISTRY IN RARE-EARTH ELEMENT EXTRACTION AND PHOTOCATALYSIS
Institution name	Wayne State University
Expected presentation date	May 2022
Portions	Fig. 4, page 3117
Requestor Location	Wayne State University 5101 Cass Avenue CHM 230 DETROIT, MI 48202 United States Attn: Wayne State University

Publisher Tax ID	98-0397604
Total	0.00 USD

Terms and Conditions

INTRODUCTION

1. The publisher for this copyrighted material is Elsevier. By clicking "accept" in connection with completing this licensing transaction, you agree that the following terms and conditions apply to this transaction (along with the Billing and Payment terms and conditions established by Copyright Clearance Center, Inc. ("CCC"), at the time that you opened your Rightslink account and that are available at any time at http://myaccount.copyright.com).

GENERAL TERMS

2. Elsevier hereby grants you permission to reproduce the aforementioned material subject to the terms and conditions indicated.

3. Acknowledgement: If any part of the material to be used (for example, figures) has appeared in our publication with credit or acknowledgement to another source, permission must also be sought from that source. If such permission is not obtained then that material may not be included in your publication/copies. Suitable acknowledgement to the source must be made, either as a footnote or in a reference list at the end of your publication, as follows:

"Reprinted from Publication title, Vol /edition number, Author(s), Title of article / title of chapter, Pages No., Copyright (Year), with permission from Elsevier [OR APPLICABLE SOCIETY COPYRIGHT OWNER]." Also Lancet special credit - "Reprinted from The

Lancet, Vol. number, Author(s), Title of article, Pages No., Copyright (Year), with permission from Elsevier."

4. Reproduction of this material is confined to the purpose and/or media for which permission is hereby given.

5. Altering/Modifying Material: Not Permitted. However figures and illustrations may be altered/adapted minimally to serve your work. Any other abbreviations, additions, deletions and/or any other alterations shall be made only with prior written authorization of Elsevier Ltd. (Please contact Elsevier's permissions helpdesk here). No modifications can be made to any Lancet figures/tables and they must be reproduced in full.

6. If the permission fee for the requested use of our material is waived in this instance, please be advised that your future requests for Elsevier materials may attract a fee.

7. Reservation of Rights: Publisher reserves all rights not specifically granted in the combination of (i) the license details provided by you and accepted in the course of this licensing transaction, (ii) these terms and conditions and (iii) CCC's Billing and Payment terms and conditions.

8. License Contingent Upon Payment: While you may exercise the rights licensed immediately upon issuance of the license at the end of the licensing process for the transaction, provided that you have disclosed complete and accurate details of your proposed use, no license is finally effective unless and until full payment is received from you (either by publisher or by CCC) as provided in CCC's Billing and Payment terms and conditions. If full payment is not received on a timely basis, then any license preliminarily granted shall be deemed automatically revoked and shall be void as if never granted. Further, in the event that you breach any of these terms and conditions or any of CCC's Billing and Payment terms and conditions, the license is automatically revoked and shall be void as if never granted. Use of materials as described in a revoked license, as well as any use of the materials beyond the scope of an unrevoked license, may constitute copyright infringement and publisher reserves the right to take any and all action to protect its copyright in the

materials.

9. Warranties: Publisher makes no representations or warranties with respect to the licensed material.

10. Indemnity: You hereby indemnify and agree to hold harmless publisher and CCC, and their respective officers, directors, employees and agents, from and against any and all claims arising out of your use of the licensed material other than as specifically authorized pursuant to this license.

11. No Transfer of License: This license is personal to you and may not be sublicensed, assigned, or transferred by you to any other person without publisher's written permission.

12. No Amendment Except in Writing: This license may not be amended except in a writing signed by both parties (or, in the case of publisher, by CCC on publisher's behalf).

13. Objection to Contrary Terms: Publisher hereby objects to any terms contained in any purchase order, acknowledgment, check endorsement or other writing prepared by you, which terms are inconsistent with these terms and conditions or CCC's Billing and Payment terms and conditions. These terms and conditions, together with CCC's Billing and Payment terms and conditions (which are incorporated herein), comprise the entire agreement between you and publisher (and CCC) concerning this licensing transaction. In the event of any conflict between your obligations established by these terms and conditions and those established by CCC's Billing and Payment terms and conditions, these terms and conditions shall control.

14. Revocation: Elsevier or Copyright Clearance Center may deny the permissions described in this License at their sole discretion, for any reason or no reason, with a full refund payable to you. Notice of such denial will be made using the contact information provided by you. Failure to receive such notice will not alter or invalidate the denial. In no event will Elsevier or Copyright Clearance Center be responsible or liable for any costs, expenses or damage incurred by you as a result of a denial of your permission request, other than a refund of the

amount(s) paid by you to Elsevier and/or Copyright Clearance Center for denied permissions.

LIMITED LICENSE

The following terms and conditions apply only to specific license types:

15. **Translation**: This permission is granted for non-exclusive world **English** rights only unless your license was granted for translation rights. If you licensed translation rights you may only translate this content into the languages you requested. A professional translator must perform all translations and reproduce the content word for word preserving the integrity of the article.

16. **Posting licensed content on any Website**: The following terms and conditions apply as follows: Licensing material from an Elsevier journal: All content posted to the web site must maintain the copyright information line on the bottom of each image; A hyper-text must be included to the Homepage of the journal from which you are licensing at http://www.sciencedirect.com/science/journal/xxxxx or the Elsevier homepage for books at http://www.elsevier.com; Central Storage: This license does not include permission for a scanned version of the material to be stored in a central repository such as that provided by Heron/XanEdu.

Licensing material from an Elsevier book: A hyper-text link must be included to the Elsevier homepage at http://www.elsevier.com . All content posted to the web site must maintain the copyright information line on the bottom of each image.

Posting licensed content on Electronic reserve: In addition to the above the following clauses are applicable: The web site must be password-protected and made available only to bona fide students registered on a relevant course. This permission is granted for 1 year only. You may obtain a new license for future website posting.

17. **For journal authors:** the following clauses are applicable in addition to the above:

Preprints:

A preprint is an author's own write-up of research results and analysis, it has not been peer-reviewed, nor has it had any other value added to it by a publisher (such as formatting, copyright, technical enhancement etc.).

Authors can share their preprints anywhere at any time. Preprints should not be added to or enhanced in any way in order to appear more like, or to substitute for, the final versions of articles however authors can update their preprints on arXiv or RePEc with their Accepted Author Manuscript (see below).

If accepted for publication, we encourage authors to link from the preprint to their formal publication via its DOI. Millions of researchers have access to the formal publications on ScienceDirect, and so links will help users to find, access, cite and use the best available version. Please note that Cell Press, The Lancet and some society-owned have different preprint policies. Information on these policies is available on the journal homepage.

Accepted Author Manuscripts: An accepted author manuscript is the manuscript of an article that has been accepted for publication and which typically includes author-incorporated changes suggested during submission, peer review and editor-author communications.

Authors can share their accepted author manuscript:

- immediately
    - via their non-commercial person homepage or blog
    - by updating a preprint in arXiv or RePEc with the accepted manuscript
    - via their research institute or institutional repository for internal institutional uses or as part of an invitation-only research collaboration work-group
    - directly by providing copies to their students or to research collaborators for

their personal use
    - for private scholarly sharing as part of an invitation-only work group on commercial sites with which Elsevier has an agreement
- After the embargo period
    - via non-commercial hosting platforms such as their institutional repository
    - via commercial sites with which Elsevier has an agreement

In all cases accepted manuscripts should:

- link to the formal publication via its DOI
- bear a CC-BY-NC-ND license - this is easy to do
- if aggregated with other manuscripts, for example in a repository or other site, be shared in alignment with our hosting policy not be added to or enhanced in any way to appear more like, or to substitute for, the published journal article.

Published journal article (JPA): A published journal article (PJA) is the definitive final record of published research that appears or will appear in the journal and embodies all value-adding publishing activities including peer review co-ordination, copy-editing, formatting, (if relevant) pagination and online enrichment.

Policies for sharing publishing journal articles differ for subscription and gold open access articles:

Subscription Articles: If you are an author, please share a link to your article rather than the full-text. Millions of researchers have access to the formal publications on ScienceDirect, and so links will help your users to find, access, cite, and use the best available version.

Theses and dissertations which contain embedded PJAs as part of the formal submission can be posted publicly by the awarding institution with DOI links back to the formal publications on ScienceDirect.

If you are affiliated with a library that subscribes to ScienceDirect you have additional

private sharing rights for others' research accessed under that agreement. This includes use for classroom teaching and internal training at the institution (including use in course packs and courseware programs), and inclusion of the article for grant funding purposes.

Gold Open Access Articles: May be shared according to the author-selected end-user license and should contain a CrossMark logo, the end user license, and a DOI link to the formal publication on ScienceDirect.

Please refer to Elsevier's posting policy for further information.

18. **For book authors** the following clauses are applicable in addition to the above: Authors are permitted to place a brief summary of their work online only. You are not allowed to download and post the published electronic version of your chapter, nor may you scan the printed edition to create an electronic version. **Posting to a repository:** Authors are permitted to post a summary of their chapter only in their institution's repository.

19. **Thesis/Dissertation**: If your license is for use in a thesis/dissertation your thesis may be submitted to your institution in either print or electronic form. Should your thesis be published commercially, please reapply for permission. These requirements include permission for the Library and Archives of Canada to supply single copies, on demand, of the complete thesis and include permission for Proquest/UMI to supply single copies, on demand, of the complete thesis. Should your thesis be published commercially, please reapply for permission. Theses and dissertations which contain embedded PJAs as part of the formal submission can be posted publicly by the awarding institution with DOI links back to the formal publications on ScienceDirect.

Elsevier Open Access Terms and Conditions

You can publish open access with Elsevier in hundreds of open access journals or in nearly 2000 established subscription journals that support open access publishing. Permitted third

Permission to reprint Figure 1 from Alizadeh, T.; Amjadi, S. Synthesis of Eu^{3+}-imprinted polymer and its application for indirect voltametric determination of europium. *Talanta.* **2013**, *106*, 431–439:

ELSEVIER LICENSE
TERMS AND CONDITIONS

Apr 20, 2022

This Agreement between Wayne State University -- Jessica Hovey ("You") and Elsevier ("Elsevier") consists of your license details and the terms and conditions provided by Elsevier and Copyright Clearance Center.

License Number	5293150783520
License date	Apr 20, 2022
Licensed Content Publisher	Elsevier
Licensed Content Publication	Talanta
Licensed Content Title	Synthesis of nano-sized Eu3+-imprinted polymer and its application for indirect voltammetric determination of europium

Licensed Content Author	Taher Alizadeh,Somaye Amjadi
Licensed Content Date	Mar 15, 2013
Licensed Content Volume	106
Licensed Content Issue	n/a
Licensed Content Pages	9
Start Page	431
End Page	439
Type of Use	reuse in a thesis/dissertation
Portion	figures/tables/illustrations
Number of figures/tables/illustrations	1

Format	both print and electronic
Are you the author of this Elsevier article?	No
Will you be translating?	No
Title	LANTHANIDE COORDINATION CHEMISTRY IN RARE-EARTH ELEMENT EXTRACTION AND PHOTOCATALYSIS
Institution name	Wayne State University
Expected presentation date	May 2022
Portions	Figure 1, page 433
Requestor Location	Wayne State University 5101 Cass Avenue CHM 230 DETROIT, MI 48202 United States Attn: Wayne State University

Publisher Tax ID	98-0397604
Total	0.00 USD

Terms and Conditions

INTRODUCTION

1. The publisher for this copyrighted material is Elsevier. By clicking "accept" in connection with completing this licensing transaction, you agree that the following terms and conditions apply to this transaction (along with the Billing and Payment terms and conditions established by Copyright Clearance Center, Inc. ("CCC"), at the time that you opened your Rightslink account and that are available at any time at http://myaccount.copyright.com).

GENERAL TERMS

2. Elsevier hereby grants you permission to reproduce the aforementioned material subject to the terms and conditions indicated.

3. Acknowledgement: If any part of the material to be used (for example, figures) has appeared in our publication with credit or acknowledgement to another source, permission must also be sought from that source. If such permission is not obtained then that material may not be included in your publication/copies. Suitable acknowledgement to the source must be made, either as a footnote or in a reference list at the end of your publication, as follows:

"Reprinted from Publication title, Vol /edition number, Author(s), Title of article / title of chapter, Pages No., Copyright (Year), with permission from Elsevier [OR APPLICABLE SOCIETY COPYRIGHT OWNER]." Also Lancet special credit - "Reprinted from The

Lancet, Vol. number, Author(s), Title of article, Pages No., Copyright (Year), with permission from Elsevier."

4. Reproduction of this material is confined to the purpose and/or media for which permission is hereby given.

5. Altering/Modifying Material: Not Permitted. However figures and illustrations may be altered/adapted minimally to serve your work. Any other abbreviations, additions, deletions and/or any other alterations shall be made only with prior written authorization of Elsevier Ltd. (Please contact Elsevier's permissions helpdesk here). No modifications can be made to any Lancet figures/tables and they must be reproduced in full.

6. If the permission fee for the requested use of our material is waived in this instance, please be advised that your future requests for Elsevier materials may attract a fee.

7. Reservation of Rights: Publisher reserves all rights not specifically granted in the combination of (i) the license details provided by you and accepted in the course of this licensing transaction, (ii) these terms and conditions and (iii) CCC's Billing and Payment terms and conditions.

8. License Contingent Upon Payment: While you may exercise the rights licensed immediately upon issuance of the license at the end of the licensing process for the transaction, provided that you have disclosed complete and accurate details of your proposed use, no license is finally effective unless and until full payment is received from you (either by publisher or by CCC) as provided in CCC's Billing and Payment terms and conditions. If full payment is not received on a timely basis, then any license preliminarily granted shall be deemed automatically revoked and shall be void as if never granted. Further, in the event that you breach any of these terms and conditions or any of CCC's Billing and Payment terms and conditions, the license is automatically revoked and shall be void as if never granted. Use of materials as described in a revoked license, as well as any use of the materials beyond the scope of an unrevoked license, may constitute copyright infringement and publisher reserves the right to take any and all action to protect its copyright in the

materials.

9. Warranties: Publisher makes no representations or warranties with respect to the licensed material.

10. Indemnity: You hereby indemnify and agree to hold harmless publisher and CCC, and their respective officers, directors, employees and agents, from and against any and all claims arising out of your use of the licensed material other than as specifically authorized pursuant to this license.

11. No Transfer of License: This license is personal to you and may not be sublicensed, assigned, or transferred by you to any other person without publisher's written permission.

12. No Amendment Except in Writing: This license may not be amended except in a writing signed by both parties (or, in the case of publisher, by CCC on publisher's behalf).

13. Objection to Contrary Terms: Publisher hereby objects to any terms contained in any purchase order, acknowledgment, check endorsement or other writing prepared by you, which terms are inconsistent with these terms and conditions or CCC's Billing and Payment terms and conditions. These terms and conditions, together with CCC's Billing and Payment terms and conditions (which are incorporated herein), comprise the entire agreement between you and publisher (and CCC) concerning this licensing transaction. In the event of any conflict between your obligations established by these terms and conditions and those established by CCC's Billing and Payment terms and conditions, these terms and conditions shall control.

14. Revocation: Elsevier or Copyright Clearance Center may deny the permissions described in this License at their sole discretion, for any reason or no reason, with a full refund payable to you. Notice of such denial will be made using the contact information provided by you. Failure to receive such notice will not alter or invalidate the denial. In no event will Elsevier or Copyright Clearance Center be responsible or liable for any costs, expenses or damage incurred by you as a result of a denial of your permission request, other than a refund of the

amount(s) paid by you to Elsevier and/or Copyright Clearance Center for denied permissions.

LIMITED LICENSE

The following terms and conditions apply only to specific license types:

15. **Translation**: This permission is granted for non-exclusive world **English** rights only unless your license was granted for translation rights. If you licensed translation rights you may only translate this content into the languages you requested. A professional translator must perform all translations and reproduce the content word for word preserving the integrity of the article.

16. **Posting licensed content on any Website**: The following terms and conditions apply as follows: Licensing material from an Elsevier journal: All content posted to the web site must maintain the copyright information line on the bottom of each image; A hyper-text must be included to the Homepage of the journal from which you are licensing at http://www.sciencedirect.com/science/journal/xxxxx or the Elsevier homepage for books at http://www.elsevier.com; Central Storage: This license does not include permission for a scanned version of the material to be stored in a central repository such as that provided by Heron/XanEdu.

Licensing material from an Elsevier book: A hyper-text link must be included to the Elsevier homepage at http://www.elsevier.com . All content posted to the web site must maintain the copyright information line on the bottom of each image.

Posting licensed content on Electronic reserve: In addition to the above the following clauses are applicable: The web site must be password-protected and made available only to bona fide students registered on a relevant course. This permission is granted for 1 year only. You may obtain a new license for future website posting.

17. **For journal authors:** the following clauses are applicable in addition to the above:

Preprints:

A preprint is an author's own write-up of research results and analysis, it has not been peer-reviewed, nor has it had any other value added to it by a publisher (such as formatting, copyright, technical enhancement etc.).

Authors can share their preprints anywhere at any time. Preprints should not be added to or enhanced in any way in order to appear more like, or to substitute for, the final versions of articles however authors can update their preprints on arXiv or RePEc with their Accepted Author Manuscript (see below).

If accepted for publication, we encourage authors to link from the preprint to their formal publication via its DOI. Millions of researchers have access to the formal publications on ScienceDirect, and so links will help users to find, access, cite and use the best available version. Please note that Cell Press, The Lancet and some society-owned have different preprint policies. Information on these policies is available on the journal homepage.

Accepted Author Manuscripts: An accepted author manuscript is the manuscript of an article that has been accepted for publication and which typically includes author-incorporated changes suggested during submission, peer review and editor-author communications.

Authors can share their accepted author manuscript:

- immediately
    - via their non-commercial person homepage or blog
    - by updating a preprint in arXiv or RePEc with the accepted manuscript
    - via their research institute or institutional repository for internal institutional uses or as part of an invitation-only research collaboration work-group
    - directly by providing copies to their students or to research collaborators for

their personal use
    - for private scholarly sharing as part of an invitation-only work group on commercial sites with which Elsevier has an agreement
- After the embargo period
    - via non-commercial hosting platforms such as their institutional repository
    - via commercial sites with which Elsevier has an agreement

In all cases accepted manuscripts should:

- link to the formal publication via its DOI
- bear a CC-BY-NC-ND license - this is easy to do
- if aggregated with other manuscripts, for example in a repository or other site, be shared in alignment with our hosting policy not be added to or enhanced in any way to appear more like, or to substitute for, the published journal article.

Published journal article (JPA): A published journal article (PJA) is the definitive final record of published research that appears or will appear in the journal and embodies all value-adding publishing activities including peer review co-ordination, copy-editing, formatting, (if relevant) pagination and online enrichment.

Policies for sharing publishing journal articles differ for subscription and gold open access articles:

Subscription Articles: If you are an author, please share a link to your article rather than the full-text. Millions of researchers have access to the formal publications on ScienceDirect, and so links will help your users to find, access, cite, and use the best available version.

Theses and dissertations which contain embedded PJAs as part of the formal submission can be posted publicly by the awarding institution with DOI links back to the formal publications on ScienceDirect.

If you are affiliated with a library that subscribes to ScienceDirect you have additional

private sharing rights for others' research accessed under that agreement. This includes use for classroom teaching and internal training at the institution (including use in course packs and courseware programs), and inclusion of the article for grant funding purposes.

Gold Open Access Articles: May be shared according to the author-selected end-user license and should contain a CrossMark logo, the end user license, and a DOI link to the formal publication on ScienceDirect.

Please refer to Elsevier's posting policy for further information.

18. **For book authors** the following clauses are applicable in addition to the above: Authors are permitted to place a brief summary of their work online only. You are not allowed to download and post the published electronic version of your chapter, nor may you scan the printed edition to create an electronic version. **Posting to a repository:** Authors are permitted to post a summary of their chapter only in their institution's repository.

19. **Thesis/Dissertation**: If your license is for use in a thesis/dissertation your thesis may be submitted to your institution in either print or electronic form. Should your thesis be published commercially, please reapply for permission. These requirements include permission for the Library and Archives of Canada to supply single copies, on demand, of the complete thesis and include permission for Proquest/UMI to supply single copies, on demand, of the complete thesis. Should your thesis be published commercially, please reapply for permission. Theses and dissertations which contain embedded PJAs as part of the formal submission can be posted publicly by the awarding institution with DOI links back to the formal publications on ScienceDirect.

Elsevier Open Access Terms and Conditions

You can publish open access with Elsevier in hundreds of open access journals or in nearly 2000 established subscription journals that support open access publishing. Permitted third

party re-use of these open access articles is defined by the author's choice of Creative Commons user license. See our open access license policy for more information.

Terms & Conditions applicable to all Open Access articles published with Elsevier:

Any reuse of the article must not represent the author as endorsing the adaptation of the article nor should the article be modified in such a way as to damage the author's honour or reputation. If any changes have been made, such changes must be clearly indicated.

The author(s) must be appropriately credited and we ask that you include the end user license and a DOI link to the formal publication on ScienceDirect.

If any part of the material to be used (for example, figures) has appeared in our publication with credit or acknowledgement to another source it is the responsibility of the user to ensure their reuse complies with the terms and conditions determined by the rights holder.

Additional Terms & Conditions applicable to each Creative Commons user license:

CC BY: The CC-BY license allows users to copy, to create extracts, abstracts and new works from the Article, to alter and revise the Article and to make commercial use of the Article (including reuse and/or resale of the Article by commercial entities), provided the user gives appropriate credit (with a link to the formal publication through the relevant DOI), provides a link to the license, indicates if changes were made and the licensor is not represented as endorsing the use made of the work. The full details of the license are available at http://creativecommons.org/licenses/by/4.0.

CC BY NC SA: The CC BY-NC-SA license allows users to copy, to create extracts, abstracts and new works from the Article, to alter and revise the Article, provided this is not done for commercial purposes, and that the user gives appropriate credit (with a link to the formal publication through the relevant DOI), provides a link to the license, indicates if changes were made and the licensor is not represented as endorsing the use made of the work. Further, any new works must be made available on the same conditions. The full

Permission to adapt Hovey, J. L.; Dardona, M.; Allen, M. J.; Dittrich, T. M. *Sep. Purif. Technol.* **2021**, *258*, 118061–118068 for Chapter 2:

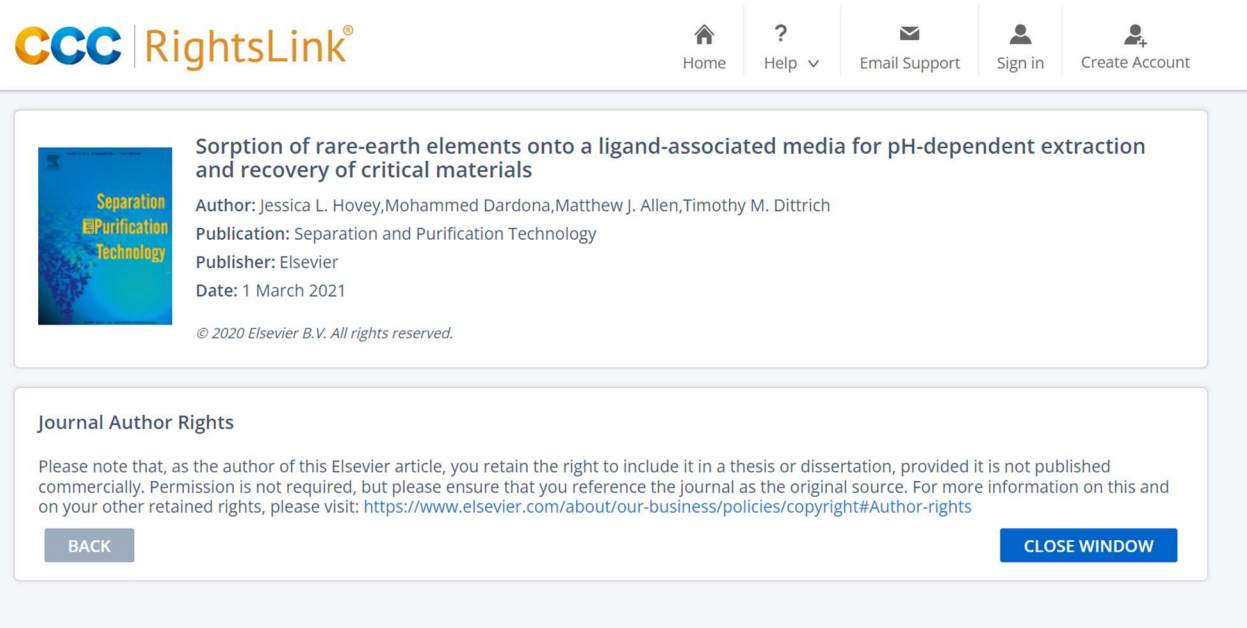

Permission to adapt Corbin, B. A.; Hovey, J. L.; Thapa, B.; Schlegel, H.B.; Allen, M. J. J. *Organomet. Chem.* **2017**, *857*, 88–93 for Chapter 4:

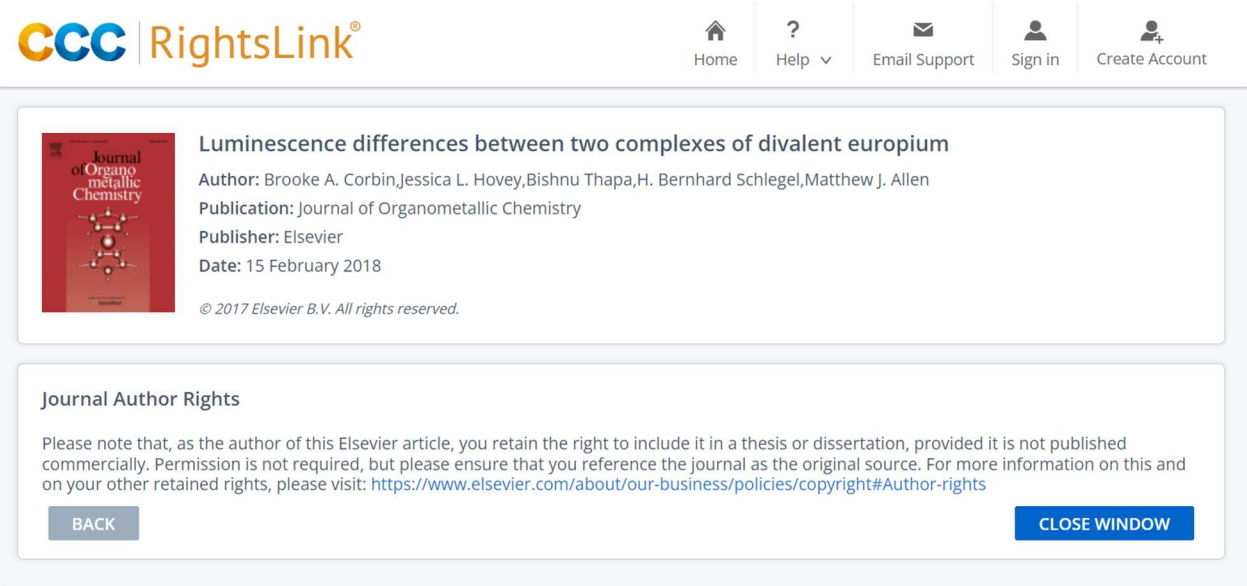

REFERENCES

1. Gutfleisch, O.; Willard, M. A.; Brück, E.; Chen, C. H.; Sankar, S. G.; Liu, J. P. *Adv. Mater.* **2011**, *23*, 821.

2. Humphries, M. *Rare Earth Elements: The Global Supply Chain*, Congressional Research Service, **2012**.

3. Bogart, J. A.; Lippincott, C. A.; Carroll, P. J.; Schelter, E. J. *Angew. Chem., Int. Ed.* **2015**, *54*, 8222.

4. Fröhlich, P.; Lorenz, T.; Martin, G.; Brett, B.; Bertau, M. *Angew. Chem. Int. Ed.* **2017**, *56*, 2544.

5. Tan, Q.; Deng, C.; Li, J. *Sci. Rep.* **2016**, *6*, 19961.

6. Bandara HMD, Field KD, Emmert MH. Rare earth recovery from end-of-life motors employing green chemistry design principles. *Green Chem.* **2016**, *18*, 753.

7. Krishnamurthy, N.; Gupta, C. K. *Extractive Metallurgy of Rare Earths*, Second Edition. CRC Press, **2016**.

8. Kitagawa, J.; Uemura, R. *Sci. Rep.* **2017**, *7*, 8039.

9. Zhuo, Y.; Tehrani, A. M.; Oliynyk, A. O.; Duke, A. C.; Brgoch, J. *Nat. Commun.* **2018**, *9*, 4377.

10. Ebin, B.; Petranikova, M.; Ekberg, C. *J. Mater. Cycles Waste Manag.* **2018**, *20*, 2018.

11. Cheisson, T.; Schelter, E. J. *Science*. **2019**, *363*, 489.

12. Nelson, J. J. M.; Schelter, E. J. *Inorg. Chem.* **2019**, *58*, 979.

13. Amato, A.; Becci, A.; Birloaga, I.; De Michelis, I.; Ferella, F.; Innocenzi, V.; Ippolito, N. M.; Pillar Jimenez Gomez, C.; Vegliò, F.; Beolchini, F. *Renew. Sustain. Energy Rev.* **2019**, *106*, 41.

14. de Oliveira, R. P.; Benvenuti, J.; Espinosa, D. C. R. *Renew. Sustain. Energy Rev.* **2021**, *145*, 111090.

15. Brewer, A.; Dror, I.; Berkowitz, B. *Chemosphere*. **2022**, *287*, 132217.

16. Lee, J. C. K.; Wen, Z. *Nat. Sustain.* **2018**, *1*, 598.

17. Yin, X.; Wang, Y.; Bai, X.; Wang, Y.; Chen, L.; Xiao, C.; Diwu, J.; Du, S.; Chai, Z.; Albrecht-Schmitt, T. E.; Wang, S. *Nat. Commun.* **2017**, *8*, 14438.

18. Kronholm, B.; Anderson, C. G.; Taylor, P. R. *JOM*. **2013**, *65*, 1321.

19. Greenwood, N. N.; Earnshaw, A. *Chemistry of the Elements*, Second Edition. Elsevier Butterworth-Heinemann, **1997**.

20. Grimes, T. S.; Nash, K. L. *J. Solution Chem.* **2014**, *43*, 298.

21. Cheremisina, O.; Sergeev, V.; Ponomareva, M.; Ilina, A.; Fedorov, A. *Metals.* **2020**, *10*, 687.

22. Ansari, S. A.; Mohapatra, P. K. *J. Chromatogr. A*. **2017**, *1499*, 1.

23. Kurysheva, V. V.; Ivanova, E. V.; Prohorova, P. E. *Chim. Techno Acta*. **2016**, *3*, 97.

24. Wehbie, M.; Arrachart, G.; Arrambide Cruz, C.; Karamé, I.; Ghannam, L.; Pellet-Rostaing, S. *Sep. Purif. Technol.* **2017**, *187*, 311.

25. Xie, F.; Zhang, T. A.; Dreisinger, D.; Doyle, F. *Miner. Eng.* **2014**, *56*, 10.

26. Zolfonoun, E.; Yousefi, S. R. *J. Braz. Chem. Soc.* **2016**, *27*, 2348.

27. Zhang, J.; Wang, X.; Dong, Y.; Xu, Z.; Li, G. *At. Spectrosc.* **2016**, *37*, 1.

28. Wang, Z.; Brown, A. T.; Tan, K.; Chabal, Y. J.; Balkus, K. J. Jr. *J. Am. Chem. Soc.* **2018**, *140*, 14735.

29. Hovey, J. L.; Dardona, M,; Allen, M. J.; Dittrich, T. M. *Sep. Purif. Technol.* **2021**, *258*, 118061.

30. Zhang, Y.; Zhong, C.; Zhang, Q.; Chen, B.; He, M.; Hu, B. *RSC Adv.* **2015**, *5*, 5996.

31. Chen, S.; Yan, J.; Li, J.; Lu, D. *At. Spectrosc.* **2017**, *38*, 86.

32. Elsaidi, S. K.; Sinnwell, M. A.; Devaraj, A.; Droubay, T. C.; Nie, Z.; Murugesan, V.; McGrail, B. P.; Thallapally, P. K. *J. Mater. Chem. A*. **2018**, *6*, 18438.

33. Tay, P. K. R.; Manjula-Basavanna, A.; Joshi, N. S. *Green Chem.* **2018**, *20*, 3512.

34. Osman, Y.; Gebreil, A.; Mowafy, A. M.; Anan, T. I.; Hamed, S. M. *World J. Microbiol. Biotechnol.* **2019**, *35*, 93.

35. Park D, Middleton A, Smith R, Deblonde G, Laudal D, Theaker N, Hsu-Kim H, Jiao Y. A biosorption-based approach for selective extraction of rare earth elements from coal byproducts. *Sep. Purif. Technol.* 2020;241:116726.

36. Dong, Z.; Mattocks, J. A.; Deblonde, G. J-P.; Hu, D.; Jiao, Y.; Cotruvo, J. A. Jr.; Park, D. M. *ACS Cent. Sci.* **2021**, *7*, 1798.

37. Chen, L.; Wu, Y.; Dong, H.; Meng, M.; Li, C.; Yan, Y.; Chen, J. *Sep. Purif. Technol.* **2018**, *197*, 70.

38. Giese, E. C. *World J. Microbiol. Biotechnol.* **2020**, *36*, 52.

39. Florek, J.; Giret, S.; Juère, E.; Larivière, D.; Kleitz, F. *Dalton Trans.* **2016**, *45*, 14832.

40. Hu, Y.; Florek, J.; Larivière, D.; Fontaine, F-G.; Kleitz, F. *Chem. Rec.* **2018**, *18*, 1261.

41. Parr, R. G.; Pearson, R. G. *J. Am. Chem. Soc.* **1983**, *105*, 7512.

42. Perry, E. P.; Gysi, A. P. *Geofluids*. **2018**, 1.

43. Juère, E.; Florek, J.; Larivière, D.; Kim, K.; Kleitz, F. *New J. Chem.* **2016**, *40*, 4325.

44. Whitty-Léveillé, L.; Aumaitre, C.; Morin, J-F.; Reynier, N.; Larivière, D. *Sep. Purif. Technol*. **2019**, *228*, 115709.

45. Shusterman, J.; Mason, H.; Bruchet, A.; Zavarin, M.; Kersting, A. B.; Nitsche, H. *Dalton Trans.* **2014**, *43*, 16649.

46. Arrambide, C.; Arrachart, G.; Berthalon, S.; Wehbie, M.; Pellet-Rostaing, S. *React. Funct. Polym.* **2019**, *142*, 147.

47. Yang, Y.; Alexandratos, S. D. *Ind. Eng. Chem. Res.* **2009**, *48*, 6173.

48. Waqar, F.; Jan, S.; Mohammad, H.; Hakim, M.; Alam, S.; Yawar, W. *J. Chin. Chem. Soc.* **2009**, *56*, 335.

49. Xu, Y.; Kim, S-Y.; Ito, T.; Nakazawa, K.; Funaki, Y.; Tada, T.; Hitomi, K.; Ishii, K. *J. Chromatogr. A*. **2012**, *1263*, 28.

50. Suneesh, A. S.; Syamala, K. V.; Venkatesan, K. A.; Antony, M. P.; Vasudeva Rao, P. R. *Sep. Sci. Technol.* **2015**, *50*, 1213.

51. Bai, R.; Yang, F.; Zhang, Y.; Zhao, Z.; Liao, Q.; Chen, P.; Zhao, P.; Guo, W.; Cai, C. *Carbohydr. Polym.* **2018**, *190*, 255.

52. Li, J.; Gong, A.; Li, F.; Qiu, L.; Zhang, W.; Gao, G.; Liu, Y.; Li, J. *RSC Adv.* **2018**, *8*, 39149.

53. Li, F.; Gong, A.; Qiu, L.; Zhang, W.; Li, J.; Liu, Z. *Chem. Eng. J.* **2019**, *361*, 1098.

54. Ogata, T.; Narita, H.; Tanaka, M.. *Hydrometallurgy*. **2016**, *163*, 156.

55. Ogata, T.; Narita, H.; Tanaka, M. *Hydrometallurgy*. **2015**, *155*, 105.

56. Ogata, T.; Narita, H.; Tanaka, M.; Hoshino, M.; Kon, Y.; Watanabe, Y. *Sep. Purif. Technol.* **2016**, *159*, 157.

57. Turanov, A. N.; Karandashev, V. K.; Sukhinina, N. S.; Masalov, V. M.; Zhokhov, A. A.; Emelchenko, G. A. *RSC Adv.* **2015**, *5*, 529.

58. Xu, Y.; Wei, Y.; Liu, R.; Usuda, S.; Ishii, K.; Yamazaki, H. *J. Nucl. Sci. Technol.* **2011**, *48*, 1223.

59. Liu, Z.; Liu, Y.; Gong, A. *Des. Monomers Polym.* **2019**, *22*, 1.

60. Li, J.; Gong, A.; Qiu, L.; Zhang, W.; Shi, G.; Li, X.; Li, J.; Gao, G.; Bai, Y. *J. Chromatogr. A*. **2020**, *1627*, 461393.

61. Momen, M. A.; Healy, M. R.; Tsouris, C.; Jansone-Popova, S.; DePaoli, D. W.; Moyer, B. A. *Ind. Eng. Chem. Res.* **2019**, *58*, 20081.

62. Flores, R.; Momen, M. A.; Healy, M. R.; Jansone-Popova, S.; Lyon, K. L.; Reinhart, B.; Cheshire, M. C.; Moyer, B. A.; Bryantsev, V. S. *Solvent Extr. Ion Exch.* **2021**.

63. Selvan, B. R.; Dasthaiah, K.; Suneesh, A. S.; Venkatesan, K. A.; Antony, M. P.; Gardas, R. L. *Radiochim. Acta*. **2017**, *105*, 275.

64. Ogata, T.; Narita, H.; Tanaka, M. *Chem. Lett.* **2014**, *43*, 1414.

65. Mondal, S.; Ghar, A.; Satpati, A. K.; Sinharoy, P.; Singh, D. K.; Sharma, J. N.; Sreenivas, T.; Kain, V. *Hydrometallurgy*. **2019**, *185*, 93.

66. Pereao, O.; Laatikainen, K.; Bode-Aluko, C.; Kochnev, I.; Fatoba, O.; Nechaev, A. N.; Petrik, L. *Sep. Purif. Technol.* **2020**, *233*, 116059.

67. Losev, V.; Buyko, O.; Metelitsa, S.; Borodina, E.; Kuzmin, N.; Shimanskiy, A. *Sep. Sci. Technol.* **2020**, *56*, 1510.

68. Cui, H.; Feng, X.; Shi, J.; Liu, W.; Yan, N.; Rao, G.; Wang, W. *Sep. Purif. Technol.* **2020**, *234*, 116096.

69. Ogata, T.; Narita, H.; Tanaka, M. *Hydrometallurgy*. **2015**, *152*, 178.

70. Van Nguyen, N.; Iizuka, A.; Shibata, E.; Nakamura, T. *Hydrometallurgy*. **2016**, *165*, 51.

71. Zheng, X.; Wang, C.; Dai, J.; Shi, W.; Yan, Y. *J. Mater. Chem. A*. **2015**, *3*, 10327.

72. Tong, S.; Zhao, S.; Zhou, W.; Li, R.; Jia, Q. *Micrchim. Acta.* **2011**, *174*, 257.

73. Florek, J.; Chalifour, F.; Bilodeau, F.; Larivière, D.; Kleitz, F. *Adv. Funct. Mater.* **2014**, *24*, 2668.

74. Perreault, L. L.; Giret, S.; Gagnon, M.; Florek, J.; Larivière, D.; Kleitz, F. *ACS Appl. Mater. Interfaces*. **2017**, *9*, 12003.

75. Hu, Y.; Drouin, E.; Larivière, D.; Kleitz, F.; Fontaine, F-G. *ACS Appl. Mater. Interfaces*. **2017**, *9*, 38584.

76. Hu, Y.; Castro, L. C. M.; Drouin, E.; Florek, J.; Kählig, H.; Larivière, D.; Kleitz, F.; Fontaine, F-G. *ACS Appl. Mater. Interfaces*. **2019**, *11*, 23681.

77. Florek, J.; Mushtaq, A.; Larivière, D.; Cantin, G.; Fontaine, F-G.; Kleitz, F. *RSC Advances*. **2015**, *5*, 103782.

78. Florek, J.; Larivière, D.; Kählig, H.; Fiorilli, S. L.; Onida, B.; Fontaine, F-G.; Kleitz, F. *ACS Appl. Mater. Interfaces*. **2020**, *12*, 57003.

79. Ramzan, M.; Kifle, D.; Wibetoe, G. *Sep. Sci. Technol.* **2016**, *51*, 494.

80. Hoshi, H.; Wei, Y.; Kumagai, M.; Asakura, H.; Uchiyama, G. *J. Nucl. Sci. Technol.* **2014**, *39*, 874.

81. Zhu, X.; Alexandratos, S. D. *Chem. Eng. Sci.* **2015**, *127*, 126.

82. Lee, Y-R.; Yu, K.; Ravi, S.; Ahn, W-S. *ACS Appl. Mater. Interfaces*. **2018**, *10*, 23918.

[83] Shu Q, Khayambashi A, Wang X, Wei Y. Studies on adsorption of rare earth elements from nitric acid solution with bis(2-ethylhexyl)phosphoric acid impregnated polymeric adsorbent. *Adsorp. Sci. Technol.* 2018;36(3–4):1049.

84. Knutson, H-K.; Max-Hansen, M.; Jönsson, C.; Borg, N.; Nilsson, B. *J. Chromatogr. A.* **2014**, *1348*, 47.

85. Saipriya, G.; Kumaresan, R.; Nayak, P. K.; Venkatesan, K. A.; Kumar, T.; Antony, M. P. *Radiochim. Acta*. **2015**, *104*, 1.

86. Saipriya, K.; Kumaresan, R.; Nayak, P. K.; Venkatesan, K. A.; Kumar, T.; Antony, M. P. *Radiochim. Acta*. **2016**, *104*, 781.

87. Zhang, W.; Yu, S.; Zhang, S.; Zhou, J.; Ning, S.; Wang, X.; Wei, Y. *Hydrometallurgy*. **2019**, *185*, 117.

88. Kifle, D.; Wibetoe, G.; Frøseth, M.; Bigelius, J. *Solvent Extr. Ion Exch.* **2013**, *31*, 668.

89. Šebeseta, F.; Kameník, J. *J. Radioanal. Nucl. Chem.* **2010**, *283*, 845.

90. Chen, Y.; Zhu, B.; Wu, D.; Wang, Q.; Yang, Y.; Ye, W.; Guo, J. *Chem. Eng. J*. **2012**, *181–182*, 387.

91. Yan, P.; He, M.; Chen, B.; Hu, B. *Spectrochim. Acta B*. **2017**, *136*, 73.

92. Shu, Q.; Khayambashi, A.; Zou, Q.; Wang, X.; Wei, Y.; He, L.; Tang, F. *J. Radioanal. Nucl. Chem*. **2017**, *313*, 29.

93. Raju, C. S. K.; Lück, D.; Scharf, H.; Jakubowski, N.; Panne, U. *J. Anal. At. Spectrom.* **2010**, *25*, 1573.

94. Cui, H.; Chen, J.; Li, H.; Zou, D.; Liu, Y.; Deng, Y. *AIChE J.* **2016**, *62*, 2479.

95. Ishihara, R.; Asai, S.; Otosaka, S.; Yamada, S.; Hirota, H.; Miyoshi, K.; Umeno, D.; Saito, K. *Solvent Extr. Ion Exch.* **2012**, *30*, 171.

96. Yadav, K. K.; Singh, D. K.; Anitha, M.; Varshney, L.; Singh, H. *Sep. Purif. Technol.* **2013**, *118*, 350.

97. Lee, G. S.; Uchikoshi, M.; Mimura, K.; Isshiki, M. *Sep. Purif. Technol.* **2009**, *67*, 79.

98. Turanov, A. N.; Karandashev, V. K. *Cent. Eur. J. Chem.* **2009**, *7*, 54.

99. Lee, G. S.; Uchikoshi, M.; Mimura, K.; Isshiki, M. *Sep. Purif. Technol.* **2010**, *71*, 186.

100. Kumar, B. N.; Radhika, S.; Kantam, M. L.; Reddy, B. R. *J. Chem Technol. Biotechnol.* **2011**, *86*, 562.

101. Basualto, C.; Gaete, J.; Molina, L.; Valenzuela, F.; Yañez, C.; Marco, J. F. *Sci. Technol. Adv. Mater.* **2015**, *16*, 035010.

102. Molina, L.; Gaete, J.; Alfaro, I.; Ide, V.; Valenzuela, F.; Parada, J.; Basualto, C. *J. Mol. Liq*. **2019**, *275*, 178.

103. Kim, J-G. *Curr. Nanosci.* **2014**, *10*, 11.

104. Zhang, L.; Wu, D.; Zhu, B.; Yang, Y.; Wang, L. *J. Chem. Eng. Data*. **2011**, *56*, 2280.

105. Wu, D.; Sun, Y.; Wang, Q. *J. Hazard. Mater.* **2013**, *260*, 409.

106. Qiu, S.; Zhao, Z.; Sun, X. *J. Chem. Eng. Data*. **2017**, *62*, 469.

107. Bae, J-S.; Lee, J-Y.; Kim, J-S.; Han, C. *Sep. Sci. Technol.* **2013**, *48*, 1682.

108. Li, C-F.; Wang, X-C.; Li, Y-L.; Chu, Z-Y.; Guo, J-H.; Li, X-H. *J. Anal. At. Spectrom.* **2015**, *30*, 895.

109. Kim, H.; Lee, J.; Jung, H. *J. Porous Mater*. **2019**, *26*, 931.

110. Ruiqin, L.; Yuezhou, W.; Tozawa, D.; Yuanlai, X.; Usuda, S.; Yamazaki, H.; Ishii, K.; Sano, Y.; Koma, Y. *Nucl. Sci. Tech.* **2011**, *22*, 18.

111. İnan, S.; Tel, H.; Sert, Ş.; Çetinkaya, B.; Sengül, S.; Özkan, B.; Altaş, Y. *Hydrometallurgy*. **2018**, *181*, 156.

112. Zhang, W.; Ye, G.; Chen, J. *J. Radioanal. Nucl. Chem.* **2013**, *295*, 1667.

113. Habib, M.; Hafid, M.; Abdelkader, T.; Caroline, B.; Anne, B. *Sep. Purif. Technol.* **2019**, *209*, 359.

114. Nazari, A. M.; McNeice, J.; Ghahreman, A. *J. Ind. Eng. Chem.* **2018**, *59*, 388.

115. Safiulina, A. M.; Ivanets, D. V.; Kudryavtsev, E. M.; Baulin, D. V.; Baulin, V. E.; Tsivadze, A. Y. *Russ. J. Inorg. Chem.* **2019**; *64*, 536.

116. Zhu, X.; Alexandratos, S. D. *React. Funct. Polym.* **2014**, *81*, 77.

117. Alexandratos, S. D.; Zhu, X. *New J. Chem.* **2015**, *39*, 5366.

118. Alexandratos, S. D.; Zhu, X. *Materials.* **2017**, *10*, 968.

119. Alexandratos, S. D.; Zhu, X. *Vib. Spectrosc.* **2018**, *95*, 80.

120. Reddy, B. R.; Kumar, B. N.; Radhika, S. *Solvent Extr. Ion Exch.* **2009**, *27*, 695.

121. Yantasee, W.; Fryxell, G. E.; Addleman, R. S.; Wiacek, R. J.; Koonsiripaiboon, V.; Pattamakomsan, K.; Sukwarotwat, V.; Xu, J.; Raymond, K. N. *J. Hazard. Mater.* **2009**, *168*, 1233.

122. Park, H-J.; Tavlarides, L. L. *Ind. Eng. Chem. Res.* **2010**, *49*, 12567.

123. Abderrahim, O.; Ferrah, N.; Didi, M. A.; Villemin, D. *J. Radioanal. Nucl. Chem.* **2011**, *290*, 267.

124. Turanov, A. N.; Karandashev, V. K.; Masalov, V. M.; Zhokhov, A. A.; Emelchenko, G. A. *J. Colloid Interface Sci.* **2013**, *405*, 183.

125. Moloney, M. P.; Causse, J.; Loubat, C.; Grandjean, A. *Eur. J. Inorg. Chem.* **2014**, *13*, 2268.

126. Kumar, B. N.; Radhika, S.; Reddy, B. R. *Chem. Eng. J.* **2010**, *160*, 138.

127. Liu, E.; Chen, L.; Dai, J.; Wang, Y.; Li, C.; Yan, Y. *J. Mol. Liq.* **2019**, *277*, 786.

128. Zhang, W.; Avdibegović, D.; Koivula, R.; Hatanpää, T.; Hietala, S.; Regadío, M.; Binnemans, K.; Harjula, R. *J. Mater. Chem. A.* **2017**, *5*, 23805.

129. Ravi, S.; Lee, Y-R.; Yu, K.; Ahn, J-W.; Ahn, W-S. *Micropor. Mesopor. Mat.* **2018**, *258*, 62.

130. Callura, J. C.; Perkins, K. M.; Noack, C. W.; Washburn, N. R.; Dzombak, D. A.; Karamalidis, A. K. *Green Chem.* **2018**, *20*, 1515.

131. Page, M. J.; Soldenhoff, K.; Ogden, M. D. *Hydrometallurgy*. **2017**, *169*, 275.

132. Seisenbaeva, G. A.; Melnyk, I. V.; Hedin, N.; Chen, Y.; Eriksson, P.; Trzop, E.; Zub, Y. L.; Kessler, V. G. *RSC Adv.* **2015**, *5*, 24575.

133. Smith, R. C.; Taggart, R. K.; Hower, J. C.; Wiesner, M. R.; Hsu-Kim, H. *Environ. Sci. Technol.* **2019**, *53*, 4490.

134. Zhao, Z.; Qiu, Z.; Yang, J.; Lu, S.; Cao, L.; Zhang, W.; Xu, Y. *Hydrometallurgy*. **2017**, *167*, 183.

135. Głowińska, A.; Trochimczuk, A. W. *Molecules*. **2020**, *25*, 4236.

136. De Jesus, K.; Rodriguez, R.; Baek, D. L.; Fox, R. V.; Pashikanti, S.; Sharma, K. *J. Mol. Liq.* **2021**; *333*, 116006.

137. Artiushenko, O.; Ávila, E. P.; Nazarkovsky, M.; Zaitsev, V. *Sep. Purif. Technol.* **2020**, *231*, 115934.

138. Dave, S. R.; Kaur, H.; Menon, S. K. *React. Funct. Polym.* **2010**, *70*, 692.

139. Ning, S.; Zou, Q.; Wang, X.; Liu, R.; Wei, Y. *Sci. China Chem.* **2016**, *59*, 862.

140. Dolatyari, L.; Yaftian, M. R.; Rostamnia, S. *J. Taiwan Inst. Chem. Eng.* **2016**, *60*, 174.

141. Roosen, J.; Spooren, J.; Binnemans, K. *J. Mater. Chem. A*. **2014**, *2*, 19415.

142. Legaria, E. P.; Samouhos, M.; Kessler, V. G.; Seisenbaeva, G. A. *Inorg. Chem.* **2017**, *56*, 13938.

143. Galhoum, A. A.; Mahfouz, M. G.; Abdel-Rehem, S. T.; Gomaa, N. A.; Atia, A. A.; Vincent, T.; Guibal, E. *Cellulose*. **2015**, *22*, 2589.

144. Yang, Y.; Alexandratos, S. D. *Inorganica Chim. Acta.* **2012**, *391*, 130.

145. Liu, E.; Zheng, X.; Xu, X.; Zhang, F.; Liu, E.; Wang, Y,; Li, C.; Yan, Y. *New J. Chem.* **2017**, *41*, 7739.

146. Ashour, R. M.; Samouhos, M.; Legaria, E. P.; Svärd, M.; Högblom, J.; Forsberg, K.; Palmlöf, M.; Kessler, V.G.; Seisenbaeva, G. A.; Rasmuson, Å. C. *ACS Sustainable Chem. Eng.* **2018**, *6*, 6889.

147. Noack, C. W.; Perkins, K. M.; Callura, J. C.; Washburn, N. R.; Dzombak, D. A.; Karamalidis, A. K. *ACS Sustainable Chem. Eng.* **2016**, *4*, 6115.

148. Callura, J. C.; Perkins, K. M.; Noack, C. W.; Washburn, N. R.; Dzombak, D. A.; Karamalidis, A. K. *Green Chem.* **2018**, *20*, 1515.

149. Callura, J. C.; Perkins, K. M.; Baltrus, J. P.; Washburn, N. R.; Dzombak, D. A.; Karamalidis, A. K. *J. Colloid Interface Sci.* **2019**, *557*, 465.

150. Legaria, E. P.; Topel, S. D.; Kessler, V. G.; Seisenbaeva, G. A. *Dalton Trans.* **2015**, *44*, 1273.

151. Fryxell, G. E.; Chouyyok, W.; Rutledge, R. D. *Inorg. Chem. Commun.* **2011**, *14*, 971.

152. Zhang, H.; McDowell, R. G.; Martin, L. R.; Qiang, Y. *ACS Appl. Mater. Interfaces*. **2016**, *8*, 9523.

153. Almeida, Sd. N.; Toma, H. E. *Hydrometallurgy*. **2016**, *161*, 22.

154. Matsuda, M.; Ohto, K. *MATEC Web of Conferences*. **2021**, *333*, 04005.

155. Barrak, H.; Ahmedi, R.; Chevallier, P.; M'nif, A.; Laroche, G.; Hamzaoui, A. H. *Sep. Purif. Technol.* **2019**, *222*, 145.

156. Roosen, J.; Binnemans, K. *J. Mater. Chem. A*. **2014**, *2*, 1530.

157. Dupont, D.; Luyten, J.; Bloemen, M.; Verbiest, T.; Binnemans, K. *Ind. Eng. Chem. Res.* **2014**, *53*, 15222.

158. Dupont, D.; Brullot, W.; Bloemen, M.; Verbiest, T.; Binnemans, K. *ACS Appl. Mater. Interfaces*. **2014**, *6*, 4980.

159. Roosen, J.; Roosendael, S. V.; Borra, C. R.; Gerven, T. V.; Mullens, S.; Binnemans, K. *Green Chem.* **2016**, *18*, 2005.

160. Babu, C. M.; Binnemans, K.; Roosen, J. *Ind. Eng. Chem. Res.* **2018**, *57*, 1487.

161. Topel, S. D.; Legaria, E. P.; Tiseanu, C.; Rocha, J.; Nedelec, J-M.; Kessler, V. G.; Seisenbaeva, G. A. *J. Nanopart. Res.* **2014**, *16*, 2783.

162. Legaria, E. P.; Rocha, J.; Tai, C-W.; Kessler, V. G.; Seisenbaeva, G. A. *Sci. Rep.* **2017**, *7*, 43740.

163. Oshita, K.; Sabarudin, A.; Takayanagi, T.; Oshima, M.; Motomizu, S. *Talanta.* **2009**, *79*, 1031.

164. Legaria, E. P.; Saldan, I.; Svedlindh, P.; Wetterskog, E.; Gunnarsson, K.; Kessler, V. G.; Seisenbaeva, G. A. *Dalton Trans.* **2018**, *47*, 1312.

165. Karadaş, C.; Kara, D. *Water Air Soil Pollut*. **2014**, *225*, 1972.

166. Karadaş, C.; Kara, D.; Fisher, A. *Anal. Chim. Acta.* **2011**, *689*, 184.

167. Karadaş, C.; Kara, D. *Water Air Soil Pollut*. **2014**, *225*, 2192.

168. Watanabe, S.; Suzuki, H.; Goto, I.; Kofuji, H.; Matsumura, T. *J. Ion Exchange*. **2018**, *29*, 31.

169. Li, F.; Yang, Z.; Weng, H.; Chen, G.; Lin, M.; Zhao, C. *Chem. Eng. J.* **2018**, *332*, 340.

170. Ramasamy, D. L.; Repo, E.; Srivastava, V.; Sillanpää, M. *Water Res.* **2017**, *114*, 264.

171. Ramasamy, D. L.; Puhakka, V.; Repo, E.; Khan, S.; Sillanpää, M. *Chem. Eng. J.* **2017**, *324*, 104.

172. Ramasamy, D. L.; Wojtuś, A.; Repo, E.; Kalliola, S.; Srivastava, V.; Sillanpää, M. *Chem. Eng. J.* **2017**, *330*, 1370.

173. Ramasamy, D. L.; Puhakka, V.; Iftekhar, S.; Wojtuś, A.; Repo, E.; Hammouda, S. B.; Iakovleva, E.; Sillanpää, M. *J. Hazard. Mater.* **2018**, *348*, 84.

174. Awual, M. D.; Kobayashi, T.; Miyazaki, Y.; Motokawa, R.; Shiwaku, H.; Suzuki, S.; Okamoto, Y.; Yaita, T. *J. Hazard. Mater.* 2013;252–253:313.

175. Awual, M. R.; Kobayashi, T.; Shiwaku, H.; Miyazaki, Y.; Motokawa, R.; Suzuki, S.; Okamoto, Y.; Yaita, T. *Chem. Eng. J.* **2013**, *225*, 558.

176. Awual, M. D.; Yaita, T.; Shiwaku, H. *Chem. Eng. J.* **2013**, *228*, 327.

177. Awual, M. R.; Alharthi, N. H.; Okamoto, Y.; Karim, M. R.; Halim, M. E.; Hasan, M. M.; Rahman, M. M.; Islam, M. M.; Khaleque, M. A.; Sheikh, M. C. *Chem. Eng. J.* **2017**, *320*, 427.

178. Awual, M. R.; Hasan, M. M.; Shahat, A.; Naushad, M.; Shiwaku, H.; Yaita, T. *Chem. Eng. J.* **2015**, *265*, 210.

179. Hamza, M. F.; Abdel-Rahman, A. A-H.; Guibal, E. *J. Chem. Technol. Biotechnol.* **2018**, *93*, 1790.

180. Yang, Y.; Alexandratos, S. D. *Inorg. Chem.* **2010**, *49*, 1008.

181. Yang, Y.; Alexandratos, S. D. *Inorganica Chim. Acta.* **2010**, *363*, 3448.

182. Alexandratos, S. D.; Zhu, X. *J. Appl. Polym. Sci.* **2013**, *127*, 1758.

183. Shimada, A.; Sulakova, J.; Yang, Y.; Alexandratos, S.; Nash, K. L. *Solvent Extr. Ion Exch.* **2014**, *32*, 27.

184. Ding, J.; Tang, S.; Chen, X.; Ding, M.; Kang, J.; Wu, R.; Fu, Z.; Jin, Y.; Li, L.; Feng, X.; Wang, R.; Xia, C. *Chem. Eng. J.* **2018**, *344*, 594.

185. Ma, J.; Wang, Z.; Shi, Y.; Li, Q. *RSC Adv.* **2014**, *4*, 41597.

186. Zhao, Z.; Baba, Y.; Yoshida, W.; Kubota, F.; Goto, M. *J. Chem. Technol. Biotechnol.* **2016**, *91*, 2779.

187. Tadjarodi, A.; Jalalat, V.; Zare-Dorabei, R. *Mater. Res. Bull*. **2015**, *61*, 113.

188. Zare-Dorabei, R.; Jalalat, V.; Tadjarodi, A. *New J. Chem.* **2016**, *40*, 5128.

189. Dashtian, K.; Zare-Dorabei, R. *J. Colloid Interface Sci.* **2017**, *494*, 114.

190. Shiri-Yekta, Z.; Yaftian, M. R.; Nilchi, A. *Korean J. Chem. Eng.* **2013**, *30,* 1644.

191. Kavosi, A.; Faridbod, F.; Ganjali, M. R. *Int. J. Environ. Res*. **2015**, *9*, 247.

192. Srivastava, B.; Barman, M. K.; Chatterjee, M.; Roy, D.; Mandal, B. *J. Chromatogr. A*. **2016**, *1451*, 1.

193. Tu, Z.; Hu, Z.; Chang, X.; Zhang, L.; He, Q.; Shi, J.; Gao, R. *Talanta*. **2010**, *80*, 1205.

194. Deepika, P.; Sabharwal, K. N.; Srinivasan, T. G.; Basudeva Rao, P. R. *Nucl. Technol*. **2012**, *179*, 407.

195. Li, J.; Yang, X.; Bai, C.; Tian, Y.; Li, B.; Zhang, S.; Yang, X.; Ding, S.; Xia, C.; Tan, X.; Ma, L.; Li, S. *J. Colloid Interface Sci.* **2015**, *437*, 211.

196. Johnson, B. E.; Santschi, P. H.; Chuang, C-Y.; Otosaka, S.; Addleman, R. S.; Douglas, M.; Rutledge, R. D.; Chouyyok, W.; Davidson, J. D.; Fryxell, G. E.; Schwantes, J. M. *Environ. Sci. Technol.* **2012**, *46*, 11251.

197. Li, D.; Chang, X.; Hu, Z.; Wang, Q.; Li, R.; Chai, X. *Talanta*. **2011**, *83*, 1742.

198. Wang, Q.; Chang, X.; Hu, Z.; Li, D.; Li, R.; Chai, X. *Microchim. Acta*. **2011**, *172*, 395.

199. Zhao, Y.; Li, J.; Zhang, S.; Wang, X. *RSC Adv.* **2014**, *4*, 32710.

200. Berijani, S.; Ganjali, M. R.; Sereshti, H.; Norouzi, P. *Intern. J. Environ. Anal. Chem.* **2012**, *92*, 355.

201. Ashour, R. M.; Abdel-Magied, A. F.; Abdel-khalek, A. A.; Helaly, O. S.; Ali, M. M. *J. Environ. Chem. Eng.* **2016**, *4*, 3114.

202. Guerra, D. L.; Viana, R. R.; Airoldi, C. *Desalination*. **2010**, *260*, 161.

203. Metwally, E.; Elkholy, S. S.; Salem, H. A. M.; Elsabee, M. Z. *Carbohydr. Polym.* **2009**, *76*, 622.

204. Galhoum, A. A.; Mafhouz, M. G.; Abdel-Rehem, S. T.; Gomaa, N. A.; Atia, A. A.; Vincent, T.; Guibal, E. *Nanomaterials*. **2015**, *5*, 154.

205. Zhao, K.; Cheng, G.; Wei, J.; Zhou, J.; Zhang, J.; Chen, L. *Macromol. Symp.* **2010**, *297*, 126.

206. Jing, T.; Xia, H.; Niu, J.; Zhou, Y.; Dai, Q.; Hao, Q.; Zhou, Y.; Mei, S. *Biosens. Bioelectron.* **2011**, *26*, 4450.

207. Zambrzycka, E.; Roszko, D.; Leśniewska, B.; Wilczewska, A. Z.; Godlewska-Żyłkiewicz, B. *Spectrochim. Acta B*. **2011**, *66*, 508.

208. Bunina, Z. Y.; Bryleva, K.; Yurchenko, O.; Belikov, K. *Adsorp. Sci. Technol.* **2017**, *35*, 545.

209. Alizadeh, T.; Amjadi, S. *Talanta*. **2013**, *106*, 431.

210. Bunina, Z.; Bryleva, K.; Belikov, K. *ACS Omega*. 2021, *6*, 3336.

211. Zheng, X.; Zhang, Y.; Zhang, F.; Li, Z.; Yan, Y. *J. Hazard. Mater.* **2018**, *353*, 496.

212. Gao, B.; Zhang, Y.; Xu, Y. *Hydrometallurgy*. **2014**, *150*, 83.

213. Kim, H.; Kim, Y.; Chang, J. Y. *J. Polym. Sci. A Polym. Chem.* **2012**, *50*, 4990.

214. Zdunek, J.; Benito-Peña, E.; Linares, A.; Falcimaigne-Cordin, A.; Orellana, G.; Haupt, K.; Moreno-Bondi, M. C. *Chem. Eur. J.* **2013**, *19*, 10209.

215. Liu, J.; Yang, X.; Cheng, X.; Peng, Y.; Chen, H. *Anal. Methods*. **2013**, *5*, 1811.

216. Jiajia, G.; Jibao, C.; Qingde, S. *J. Rare Earths*. **2009**, *27*, 22.

217. Liu. Y.; Qiu, J.; Jiang, Y.; Liu, Z.; Meng, M.; Ni, L.; Qin, C.; Peng, J. *Micropor. Mesopor. Mat.* **2016**, *234*, 176.

218. Zheng, X.; Zhang, F.; Liu, E.; Xu, X.; Yan, Y. *ACS Appl. Mater. Interfaces*. **2017**, *9*, 730.

219. Liu, E.; Xu, X.; Zheng, X.; Zhang, F.; Liu, E.; Li, C. *Sep. Purif. Technol.* **2017**, *189*, 288.

220. Wang, J.; Wei, J.; Li, J. *Chem. Eng. J.* **2016**, *293*, 24.

221. Yussoff, M. M.; Mostapa, N. R. N.; Sarkar, M. S.; Biswas, T. K.; Rahman, M. L.; Arshad, S. E.; Sarjadi. M. S.; Kulkarni, A. D. *J. Rare Earths*. **2017**, *35*, 177.

222. Iftekhar, S.; Srivastava, V.; Hammouda, S. B.; Sillanpää, M. *Carbohydr. Polym.* **2018**, *194*, 274.

223. Zheng, X.; Liu, E.; Zhang, F.; Dai, J.; Yan, Y.; Li, C. *Cellulose*. **2017**, *24*, 977.

224. Dolak, İ.; Keçili, R.; Hür, D.; Ersöz, A.; Say, R. *Ind. Eng. Chem. Res.* **2015**, *54*, 5328.

225. Lai, X.; Hu, Y.; Fu, Y.; Wang, L.; Xiong, J. *J. Inorg. Organomet. Polym.* **2012**, *22*, 112.

226. Manoochehri, M.; Khalesi, P. *World Appl. Sci. J.* **2012**, *19*, 215.

227. Branger, C.; Meouche, W.; Margaillan, A. *React. Funct. Polym.* **2013**, *73*, 859.

228. Hu, Y.; Pan, J.; Zhang, K.; Lian, H.; Li, G. *Trends Anal. Chem.* **2013**, *43*, 37.

229. Whitcombe, M. J.; Kirsch, N.; Nicholls, I. A. *J. Mol. Recognit.* **2014**, *27*, 297.

230. Fu, J.; Chen, L.; Li, J.; Zhang, Z. *J. Mater. Chem. A*. **2015**, *3*, 13598.

231. Wilfong, W. C.; Kail, B. W.; Bank, T. L.; Howard, B. H.; Gray, M. L. *ACS Appl. Mater. Interfaces*. **2017**, *9*, 18283.

232. Wehbi, M.; Bourgeois, D.; Améduri, B. *Polym. Chem.* **2019**, *10,* 4173.

233. Jumadilov, T. K.; Kondaurov, R. G.; Kozhabekov, S. S.; Tolegen, G. A.; Eskalieva, G. K.; Khakimzhanov, S. A. *J. Chem. Technol. Metall.* **2018**, *53*, 88.

234. Watanabe, T.; Saito-Kokubu, Y.; Murakami, H.; Iwatsuki, T. *Limnology*. **2018**, *19*, 21.

235. Kim, J-G. *Arch. Metall. Mater.* **2015**, *60*, 1529.

236. Laurino, J. P.; Mustacato, J.; Huba, Z. J. *Minerals*. **2019**, *9*, 477.

237. Lahiji, M. N.; Keshtkar, A. R.; Moosavian, M. A. *Part. Sci. Technol.* **2016**, *36*, 340.

238. Ebrahimi, M.; Zamani, H. A. *Anal. Lett.* **2009**, *42*, 1041.

239. Zamani, H. A. *Anal. Lett.* **2009**, *42*, 615.

240. Naddaf, E.; Zamani, H. A. *Anal. Lett.* **2009**, *42*, 2838.

241. Nekoei, M.; Zamani, H. A.; Mohammadhossieni, M. *Anal. Lett.* **2009**, *42*, 284.

242. Zamani, H. A.; Nekoei, M.; Mohammadhosseini, M.; Ganjali, M. R. *Mater. Sci. Eng. C*. **2010**, *30*, 480.

243. Zamani, H. A.; Rohani, M.; Zangenh-Asadabadi, A.; Zabihi, M. S.; Ganjali, M. R.; Salavati-Niasari, M. *Mater. Sci. Eng. C*. **2010**, *30*, 917.

244. Zamani, H. A.; Mohammadhosseini, M.; Nekoei, M.; Ganjali, M. R. Determination of erbium ions in water samples by a PVC membrane erbium-ion selective electrode. *Sensor Lett.* **2010**, *8*, 303.

245. Zamani, H. A.; Zabihi, M. S.; Rohani, M.; Zangeneh-Asadabadi, A.; Ganjali, M. R.; Faridbod, F.; Meghdadi, S. *Mater. Sci. Eng. C*. **2011**, *31*, 409.

246. Zamani, H. A.; Arvinfar, A.; Rahimi, F.; Imani, A.; Ganjali, M. R.; Meghdadi, S. *Mater. Sci. Eng. C*. **2011**, *31*, 307.

247. Zamani, H. A.; Kamjoo, R.; Mohammadhosseini, M.; Zaferoni, M.; Rafati, Z.; Ganjali, M. R.; Faridbod, F.; Meghdadi, S. *Mater. Sci. Eng. C*. **2012**, *32*, 447.

248. Manfredi, C.; Mozzillo, R.; Volino, S.; Trifuoggi, M.; Giarra, A.; Gargiulo, V.; Alfé, M. O*Appl. Surf. Sci.* **2020**, *505*, 144264.

249. Manousi, N.; Gomez-Gomez, B.; Madrid, Y.; Deliyanni, E. A.; Zachariadis, G. A. *Microchem. J.* **2020**, *152*, 104428.

250. Hanuman, V. V.; Chakrapani, G.. *J. Indian Chem. Soc.* **2013**, *90*, 1919.

251. Mahanta, P. L.; Chakrapani, G.; Radhamani, R. *At. Spectrosc.* **2010**, *31*, 21.

252. Chen, S.; Liu, C.; Lu, D.; Zhu, L. *At. Spectrosc.* **2009**, *30*, 20.

252. Chen, S.; Zhu, S.; Lu, D. *Microchem. J.* **2013**, *110*, 89.

254. Chen, S.; He, Y.; Lu, D.; Guo, X. *At. Spectrosc.* **2013**, *34*, 73.

255. Su, S.; Chen, B.; He, M.; Hu, B.; Xiao, Z. *Talanta*. **2014**, *119*, 458.

256. Müller, T.; Friedrich, B. *J. Power Sources*. **2006**, *158*, 1498.

257. Xu, C.; Kynický, J.; Smith, M. P.; Kopriva, A.; Brtnický, M.; Urubek, T.; Yang, Y.; Zhao, Z.; He, C.; Song, W. *Nat. Commun.* **2017**, *8,* 14598.

258. U.S. Geological Survey, 2019, Mineral Commodity Summaries 2019, U.S. Global Survey, p. 133.

259. Erickson, B. *Chem. Eng. News* **2018**, 28.

260. Franus, W.; Wiatros-Motyka, M. W.; Wdowin, M. *Environ. Sci. Pollut. Res.* **2015**, *22,* 9464.

261. Cole, B. E.; Cheisson, T.; Higgins, R. F.; Nakamaru-Ogiso, E.; Manor, B. C.; Carroll, P. J.; Schelter, E. J. *Inorg. Chem.* **2020**, *59,* 172.

262. Ellis, R. J.; Brigham, D. M.; Delmau, L.; Ivanov, A. S.; Williams, N. J.; Nguyen Vo, M.; Reinhart, B.; Moyer, B. A.; Bryantsev, V. S. *Inorg. Chem.* **2017**, *56*, 1152.

263. Fang, H.; Cole, B. E.; Bogart, J. A.; Cheisson, T.; Manor, B. C.; Carroll, P. J.; Schelter, E. J. *Angew. Chem.* **2017**, *56*, 13450.

264. Higgins, R. F.; Cheisson, T.; Cole, B. E.; Manor, B. C.; Carroll, P. J.; Schelter, E. J. *Angew. Chem.* **2020**, *132,* 1867.

265. Huang, C.; Wang, Y.; Huang, B.; Dong, Y.; Sun, X. *Miner. Eng.* **2019**, *130,* 142.

266. Boyd, R.; Jin, L.; Nockemann, P.; Robertson, P. K. J.; Stella, L.; Ruhela, R.; Seddon, K. R.; Nimal Gunaratne, H. Q. *Green Chem.* **2019**, *21,* 2583.

267. Khodakarami, M.; Alagha, L.; *Sep. Purif. Technol.* **2020**, *232*, 115952.

268. Makanyire, T.; Sanchez-Segado, S.; Jha, A. *Adv. Manuf.* **2016**, *4,* 33.

269. Araucz, K.; Aurich, A.; Kołodyńska, D. *Chemosphere* **2020**, *251*, 126331.

270. Anastopoulos, I.; Bhatnagar, A.; Lima, E. C. *J. Mol. Liq.* **2016**, *221,* 954.

271. Zhang, W.; Hietala, S.; Kriachtchev, L.; Hatanpää, T.; Doshi, B.; Koivula, R. *ACS Appl. Mater. Interfaces*. **2018**, *10,* 22083.

272. Dardona, M.; Dittrich, T. M. Investigating the potential for recovering REEs from coal fly ash and power plant wastewater with an engineered sorbent. In *World Environmental and Water Resources Congress 2019: Emerging and Innovative Technologies and International Perspectives* (2019) (pp. 45-51). Reston, VA: American Society of Civil Engineers.

273. Helm, L.; Morrow, J. R.; Bond, C. J.; Carniato, F.; Botta, M.; Braun, M.; Baranyai, Z.; Pujales-Paradela, R.; Regueiro-Figueroa, M.; Esteban-Gómez, D.; Platas-Iglesias, C.; Scholl, T. J. Gadolinium-based contrast agents, in: V.C Pierre, M.J. Allen (Eds.), Contrast Agents for MRI: Experimental Methods, Royal Society of Chemistry, London, 2018, pp. 121–242.

274. Tóth, É.; Burai, L.; Merbach, A. E. *Coord. Chem. Rev.* **2001**, *2016–2017*, 363.

275. Hermann, P.; Kotek, J.; Kubíček, V.; Lukeš, I. *Dalton Trans.* **2008**, *23*, 3027.

276. Burkett, C. M.; Edmiston P. L. *J. Non-Cryst. Solids*. **2005**, *351,* 3174.

277. Edmiston, P. L.; Underwood, L. A. *Sep. Purif. Technol.* **2009**, *66,* 532.

278. Burkett, C. M.; Underwood, L. A.; Volzer, R. S.; Baughman, J. A.; Edmiston, P. L. *Chem. Mater.* **2008**, *20,* 1312.

279. Boukhalfa, H.; Peterson, D. S.; Gonzales, E. R.; Tulley-Cordova, C. L.; Tarimala, S.; Ware, S. D. *React. Funct. Polym.* **2017**, *113,* 31.

280. Nishihama, S.; Sakaguchi, N.; Hirai, T.; Komasawa, I. *Hydrometallurgy*. **2002**, *64,* 35.

281. Bligh, S. W. A.; Chowdhury, A. H. M. S.; Kennedy, D.; Luchinat, C.; Parigi, G. *Magn. Reson. Med.* **1999**, *41* ,767.

282. Byegård, J.; Skarnemark, G.; Skålberg, M.; *J. Radioanal. Nucl. Chem.* **1999**, *241,* 281.

283. Bauer, D.; Diamond, D.; Li, J.; Sandalow, D.; Telleen, P.; Wanner, B. Executive Summary. Critical Materials Strategy, U.S. Department of Energy, 2010, p. 8.

284. Schlögel, R.; Jones, W. *J. Chem. Soc. Dalton Trans.* **1984**, 1283.

285. Ruston, L. L.; Robertson, G. M.; Pikramenou, Z. *Chem. Asian J.* **2010**, *5*, 571.

286. Laurent, S.; Vander Elst, L,; Copoix, F.; Muller, R. N. *Investig. Radiol.* **2001**, *36*, 115.

287. Jasanada, F.; Nepveu, F. *Tetrahedron Lett.* **1992**, *33*, 5745.

288. Rinehart, J. D.; Fang, M.; Evans, W. J.; Long, J. R. *Nat. Chem.* **2011**, *3*, 538.

289. Labouille, S.; Nief, F.; Le Goff, X.-F.; Maron, L.; Kindra, D. R.; Houghton, H. L.; Ziller, J. W.; Evans, W. J. *Organometallics*. **2012**, *31*, 5196.

290. MacDonald, M. R.; Bates, J. E.; Ziller, J. W.; Furche, F.; Evans, W. J. *J. Am. Chem. Soc.* **2013**, *135*, 9857.

291. Soderholm, L.; Antonio, M. R.; Skanthakumar, S.; C.W. Williams, C. W. *J. Am. Chem. Soc.* **2002**, *124*, 7290.

292. Plečnik, C. E.; Liu, S.; Shore, S. G. *Acc. Chem. Res.* **2003**, *36*, 499.

293. Molander, G. A.; Czakó, B.; St. Jean Jr. D. J. *J. Org. Chem.* **2006**, *71*, 1172.

294. Raehm, L.; Mehndi, A.; Wickleder, C.; Reyé, C.; Corriu, R. J. P. *J. Am. Chem. Soc.* **2007**, *129*, 12636.

295. Nicolaou, K. C.; Ellery, S. P.; Chen, J. S. *Angew. Chem. Int. Ed.* **2009**, *48*, 7140.

296. Nomoto, A.; Kojo, Y.; Shiino, G.; Tomisaka, Y.; Mitani, I.; Tatsumi, M.; Ogawa, A. *Tetrahedron Lett.* **2010**, *51*, 6580.

297. Rao, C. N.; Hoz, S. *J. Org. Chem.* **2012**, *77,* 9199.

298. Starynowicz, P. *Polyhedron*. **2013**, *50,* 283.

299. Ekanger, L. A.; Ali, M. M.; Allen, M. J. *Chem. Commun.* **2014**, *50*, 14835.

300. Kuda-Wedagedara, A. N. W.; Wang, C.; Martin, P. D.; Allen, M. J. *J. Am. Chem. Soc.* **2015**, *137*, 4960.

301. Ekanger, L. A.; Polin, L. A.; Shen, Y.; Haacke, E. M.; Martin, P. D.; Allen, M. J. *Angew. Chem. Int. Ed.* **2015**, *54*, 14398.

302. Bartlett, P. N.; Champion, M. J. D.; Light, M. E.; Levason, W.; Reid, G.; Richardson, P. W. *Dalton Trans.* **2015**, *44*, 2953.

303. Terraschke, H.; Wickleder, C. *Chem. Rev.* **2015**, *115,* 11352.

304. Chciuk, T. V.; Anderson, Jr., W. R.; Flowers, II, R. A. *J. Am. Chem. Soc.* 2016, *138*, 8738.

305. Deacon, G. B.; Junk, P. C.; Werner, D. *Chem. Eur. J.* **2016**, *22,* 160.

306. Basal, L. A.; Yan, Y.; Shen, Y.; Haacke, E. M.; Mehrmohammadi, M.; Allen, M. J. *ACS Omega* **2017**, *2,* 800.

307. Ekanger, L.A.; Basal, L. A.; Allen, M. J. *Chem. Eur. J.* **2017**, *23*, 1145.

308. Klementyeva, S. V.; Gritsan, N. P.; Khusniyarov, M. M.; Witt, A.; Dmitriev, A. A.; Suturina, E. A.; Hill, N. D. D.; Roemmele, T. L.; Gamer, M. T.; Boeré, R. T.; Roesky, P. W.; Zibarev, A. V.; Konchenko, S. N. *Chem. Eur. J.* **2017**, *23*, 1278.

309. Xémard, M.; Jaoul, A.; Cordier, M.; Molton, F.; Cador, O.; Le Guennic, B.; Duboc, C.; Maury, O.; Clavaguéra, C.; Nocton, G. *Angew. Chem. Int. Ed.* **2017**, *56*, 4266.

310. Ekanger, L. A.; Mills, D. R.; Ali, M. M.; Polin, L. A.; Shen, Y.; Haacke, E. M.; Allen, M. J. *Inorg. Chem.* **2016**, *55,* 9981.

311. Ekanger, L. A.; Polin, L. A.; Shen, Y.; Haacke, E. M.; Allen, M. J. *Contrast Media Mol. Imaging* **2016**, *11,* 299.

312. Lenora, C. U.; Carniato, F.; Shen, Y.; Latif, Z.; Haacke, E. M.; Martin, P. D.; Botta, M.; Allen, M. J. *Chem. Eur. J.* **2017**, *23*, 15404.

313. Regueiro-Figueroa, M.; Barriada, J. L.; Pallier, A.; Esteban-Gómez, D.; de Blas, A.; Rodríguez-Blas, T.; Tóth, É.; Platas-Iglesias, C. *Inorg. Chem.* **2015**, *54*, 4940.

314. Tomisaka, Y.; Nomoto, A.; Ogawa, A. *Tetrahedron Lett.* **2009**, *50*, 584.

315. Maity, S.; Prasad, E. *J. Photochem. Photobiol., A* **2014**, *274*, 64.

316. Pust, P.; Weiler, V.; Hecht, C.; Tücks, A.; Wochnik, A. S.; Henß, A.-K.; Wiechert, D.; Scheu, C.; Schmidt, P. J.; Schnick, W. *Nat. Mater.* **2014**, *13,* 891.

317. Qin, X.; Liu, X.; Huang, W.; Bettinelli, M.; Liu, X. *Chem. Rev.* **2017**, *117*, 4488.

318. Jiang, J.; Higashiyama, N.; Machida, K.-i.; Adachi, G.-y. *Coord. Chem. Rev.* **1998**, *170*, 1.

319. Sabbatini, N.; Ciano, M.; Dellonte, S.; Bonazzi, A.; Bolletta, F.; Balzani, V. *J. Phys. Chem.* **1984***, 88,* 1534.

320. Adachi, G.-y.; Higashiyama, N. *Nippon Kagaku Kaishi* **1993**, *5,* 418.

321. Fieser, M. E.; MacDonald, M. R.; Krull, B. T.; Bates, J. E.; Ziller, J. W.; Furche, F.; Evans, W.; J. *J. Am. Chem. Soc.* **2015**, *137,* 369.

322. Fieser, M. E.; Johnson, C. W.; Bates, J. E.; Ziller, J. W.; Furche, F.; Evans, W. J. *Organometallics,* **2015***, 34*, 4387.

323. Christoffers, J.; Starynowicz, P. *Polyhedron* **2008**, *27,* 2688.

324. Dolg, M.; Stoll, H.; Savin, A.; Preuss, H. *Theor. Chim. Acta* **1989**, *75*, 173.

325. Harder, S.; Naglav, D.; Ruspic, C.; Wickleder, C.; Adlung, M.; Hermes, W.; Eul, M.; Pöttgen, R.; Rego, D. B.; Poineau, F.; Czerwinski, K. R.; Herber, R. H.; Nowik, I. *Chem. Eur. J.* **2013**, *19*, 12272.

326. Kühling, M.; Wickleder, C.; Ferguson, M. J.; Hrib, C. G.; McDonald, R.; Suta, M.; Hilfert, L.; Takats, J.; Edelmann, F. T. *New J. Chem.* **2015**, *39,* 7617.

327. Kelly, R. P.; Bell, T. D. M.; Cox, R. P.; Daniels, D. P.; Deacon, G. B.; Jaroschik, F.; Junk, P. C.; Le Goff, X. F.; Lemercier, G.; Martinez, A.; Wang, J.; Werner, D. *Organometallics* **2015**, *34*, 5624.

328. Goodwin, C. A. P.; Chilton, N. F.; Natrajan, L. S.; Boulon, M. -E.; Ziller, J. W.; Evans, W. J.; Mills, D. P. *Inorg. Chem.* **2017**, *56,* 5959.

329. Dorenbos, P. *J. Phys.: Condens. Matter* **2003**, *15,* 575.

330. Smith, P. H.; Barr, M. E.; Brainard, J. R.; Ford, D. K.; Freiser, H.; Muralidharan, S.; Reilly, S. D.; Ryan, R. R.; Silks, III, L. A.; Yu, W. -h. *J. Org. Chem.* **1993**, *58,* 7939.

331. Redko, M. Y.; Huang, R.; Dye, J. L.; Jackson, J. E. *Synthesis.* 2006, *5*, 759.

332. Frisch, M. J.; Trucks, G. W.; Schlegel, H. B.; Scuseria, G. E.; Robb, M. A.; Cheeseman, J. R.; Scalmani, G.; Barone, V.; Petersson, G. A.; Nakatsuji, H.; Li, X.; Caricato, M.; Marenich, A.V.; Bloino, J.; Janesko, B. G.; Gomperts, R.; Mennucci, B.; Hratchian, H. P.; Ortiz, J. V.; Izmaylov, A. F.; Sonnenberg, J. L.; Williams-Young, D.; Ding, F.; Lipparini, F.; Egidi, F.; Goings, J.; Peng, B.; Petrone, A.; Henderson, T.; Ranasinghe, D.; Zakrzewski, V. G.; Gao, J.; Rega, N.; Zheng, G.; Liang, W.; Hada, M.; Ehara, M.; Toyota, K.; Fukuda, R.; Hasegawa, J.; Ishida, M.; Nakajima, T.; Honda, Y.; Kitao, O.; Nakai, H.; Vreven, T.; Throssell, K.; Montgomery, Jr., J. A.; Peralta, J. E.; Ogliaro, F.; Bearpark, M. J.; Heyd, J. J.; Brothers, E. N.; Kudin, K. N.; Staroverov, V. N.; Keith, T. A.; Kobayashi, R.; Normand, J.; Raghavachari, K.; Rendell, A. P.; Burant, J. C.; Iyengar, S. S.; Tomasi, J.; Cossi, M.; Millam, J. M.; Klene, M.; Adamo, C.; Cammi, R.; Ochterski, J. W.; Martin,

R. L.; Morokuma, K.; Farkas, O.; Foresman, J. B.; Fox, D. J. Gaussian 09, Revision E.01, Gaussian, Inc., Wallingford CT, 2016.

333. Becke, A. D. *J. Chem. Phys.* **1993**, *98*, 5648.

334. Perdew, J. P. *Phys. Rev. B*. **1986**, *33*, 8822.

335. Perdew, J. P.; Burke, K.; Wang, Y. *Phys. Rev. B*. **1996**, *54*, 16533.

336. Cao, X.; Dolg, M. *J. Chem. Phys.* **2001**, *115,* 7348.

337. Cao, X.; Dolg, M. *J. Mol. Struct.* **2002**, *581*, 139.

338. Harding, L. B.; Goddard, III, W. A. *J. Chem. Phys.* **1977**, *67*, 2377.

339. Seeger, R.; Pople, J. A. *J. Chem. Phys.* **1977**, *66*, 3045.

340. Bauernschmitt, R.; Ahlrichs, R.; *J. Chem. Phys.* **1996**, *104*, 9047.

341. Marenich, A. V.; Cramer, C. J.; Truhlar, D. G. *J. Phys. Chem. B.* **2009**, *113*, 6378.

342. Stratmann, R. E.; Scuseria, G. E.; Frisch, M. J. *J. Chem. Phys.* **1998**, *109*, 8218.

343. Furche, F.; Ahlrichs, R. *J. Chem. Phys.* **2002**, *117*, 7433.

344. Scalmani, G.; Frisch, M. J.; Mennucci, B.; Tomasi, J.; Cammi, R.; Barone, V. *J. Chem. Phys.* **2006**, *124*, 094107.

345. Improta, R.; Barone, V.; Scalmani, G.; Frisch, M. J. *J. Chem. Phys.* **2006**, *125*, 054103.

346. Improta, R.; Scalmani, G.; Frisch, M.; Barone, V. *J. Chem. Phys.* **2007**, *127*, 74504.

347. Martin, R. L. *J. Chem. Phys.* **2003**, *118*, 4775.

348. Dennington, T. K. R.; Milliam, J. Gaussview, Version 5 ed., Semichem Inc., Shawnee Mission, KS 2009.

349. Wang, D.; Zhao, C.; Phillips, D. L. *Organometallics.* **2004**, *23,* 1953.

350. Yin, H.; Carroll, P. J.; Manor, B. C.; Anna, J. M.; Schelter, E. J. *J. Am. Chem. Soc.* **2016**, *138,* 5984.

ABSTRACT

LANTHANIDE COORDINATION CHEMISTRY IN RARE-EARTH ELEMENT EXTRACTION AND PHOTOCATALYSIS

by

JESSICA LYNN HOVEY

August 2022

Advisor: Dr. Matthew J. Allen

Major: Chemistry (Inorganic)

Degree: Doctor of Philosophy

This thesis outlines projects pertaining to the extraction, enrichment, and use of rare-earth elements in the trivalent and divalent states through the modification of coordination chemistry. Modulating the coordination environment can impact the selectivity of rare-earth elements in solid-liquid enrichment through the adjustment of donor atoms, denticity and pK_a values as detailed in **Chapter 1**. Changes in coordination environment, such as to the identity of donor atoms, can lead to major differences in properties such as luminescence. The studies reported in this thesis contribute to the body of knowledge surrounding the use of coordination chemistry for both the solid–liquid extraction of rare-earth elements and the luminescence properties of divalent europium.

Chapter 2 describes the analysis of a multidentate, pH-dependent solid-phase media for rare-earth element extraction. Separation experiments showed selectivity for the mid and heavy rare-earth elements and attachment of the ligand to the solid phase had similar thermodynamic affinities to trends in unmodified ligands. The pH-dependent nature of the ligand was characterized, and efficiency was retained for at least six cycles of reuse. The solid-phase media retained the selectivity for mid and heavy rare-earth elements from fly ash leachate, even in competition with much higher concentrations of competing ions. The results of this study expand

the body of research surrounding solid–liquid extraction of rare-earth elements towards creating an organic solvent-free method of extraction.

Chapter 3 focused on the interactions between the noncovalently attached ligand and resin in the solid-phase media described in **Chapter 2**. By adjusting the length of the hydrophobic group that interacts with the hydrophobic resin, we found that the ligand featuring the butyl hydrophobic groups showed less loading onto the resin than the ligand featuring the hexyl hydrophobic groups. We also determined that the ligand featuring butyl groups showed less wash off at pH 5.5 than the ligand with hexyl groups, suggesting that longer hydrophobic groups lead to less wash off and therefore more efficient solid-phase media than solid-phase media with shorter hydrophobic groups. This study outlines preliminary results towards the rational design of reusable noncovalently attached solid-phase media for the enrichment of rare-earth elements.

Chapter 4 aimed to distinguish the experimental luminescent differences between two divalent europium cryptates using computational analyses. Crystal structures were optimized in methanol and time-dependent density functional theory calculations were used to calculate excitation and emission spectra of both complexes. Natural-transition orbitals revealed that similar orbitals were involved in the excitation and emission of both complexes. Therefore, the bright yellow luminescence observed experimentally with the octaaza-cryptate was attributed to a greater splitting of the 5d orbitals of the octaaza-cryptate relative to the 2.2.2-cryptate. This study provided foundational knowledge for the calculation of emission spectra for solvated divalent europium complexes.

This thesis outlines the general ligand design for rare-earth elements taking into consideration the charge density of the metal, ligand donor identity, ligand denticity, and the range of pK_a values on the ligand. **Chapter 5** discusses how these reports are expected to provide tools for the rational design of ligands for rare-earth element enrichment and modulation of photophysical properties of low-valent rare-earth element complexes using coordination chemistry.

AUTOBIOGRAPHICAL STATEMENT

My name is Jessica Lynn Hovey, and I was born to Todd Eric Hovey and Penny Lynn Walsh. After graduated high school Magna Cum Laude at Stevenson High School in Livonia, MI, in 2012, I started at Oakland University in Rochester, MI, to pursue a bachelor's degree in chemistry. During my time at Oakland University, I studied in the laboratories of Dr. Roman Dembinski and Dr. Evan Trivedi where I garnered an appreciation for organic and inorganic synthesis. I held several leadership roles at Oakland University including Volunteer Coordinator, Vice President, and President of the Oakland University Chapter of the American Chemical Society. I was given the opportunity to research with Dr. Juan Luis Vivero-Escoto as an NSF NanoSURE summer intern at the University of North Carolina at Charlotte. I graduated Cum Laude from Oakland University with a Bachelor's of Science in Chemistry from the Honor's College and was awarded Chemistry Departmental Honors and also obtained a minor in French Language in 2016.

I was accepted to the Graduate Chemistry Program at Wayne State University in Detroit, MI, in 2016 and joined Dr. Matthew Allen's laboratory where I pursued synthetic inorganic chemistry. I am proud to have met and collaborated with numerous skilled scientists during my time at Wayne State who all taught me the invaluable skill of communication in the scientific community. I obtained several teaching and poster awards, which I attribute to the hard work I spent improving my communication skills in both learning and teaching.

Outside of the lab, we experienced an unprecedented pandemic that affected not only the progress of research, but the wedding that myself and my husband, Jacob Darrow, had planned. We were married in 2020, and I could not have asked for a better life partner or past five years in graduate school. I give a heartfelt thank you to everyone involved in my studies, and I am incredibly proud at the accomplishments that I have achieved thus far. I cannot wait to see what's next!